MicroCantilever (MC) based nanomechanical sensor for detection of molecular

interactions

by

Kyungho Kang

A dissertation submitted to the graduate faculty

in partial fulfillment of the requirements for the degree of

DOCTOR OF PHILOSOPHY

Major: Mechanical Engineering

Program of Study Committee:
Pranav Shrotriya, Major Professor
Abhijit Chandra
Balaji Narasimhan
Marit Nilsen-Hamilton
Sriram Sundararajan

Iowa State University

Ames, Iowa

2011

DEDICATION

This dissertation is dedicated to my parents back home.

TABLE OF CONTENTS

v

LIST OF TABLES

LIST OF FIGURES

ABSTRACT

Specific aims of this study are to investigate the mechanism governing surface stress generation associated with chemical or molecular binding on functionalized microcantilevers. Formation of affinity complexes on cantilever surfaces leads to charge redistribution, configurational change and steric hindrance between neighboring molecules resulting in surface stress change and measureable cantilever deformation. A novel interferometry technique employing two adjacent micromachined cantilevers (a sensing/reference pair) was utilized to measure the cantilever deformation. The sensing principle is that binding/reaction of specific chemical or biological species on the sensing cantilever transduces to mechanical deformation. The differential bending of the sensing cantilever respect to the reference cantilever ensures that measured response is insensitive to environmental disturbances. As a proof of principle for the measurement technique, surface stress changes associated with: self-assembly of alkanethiol, hybridization of ssDNA, and the formation of cocaine-aptamer complexes were measured. Dissociation constant (K_d) for each molecular reaction was utilized to estimate the surface coverage of affinity complexes. In the cases of DNA hybridization and cocaine-aptamer binding, measured surface stress was found to be dependent on the surface coverage of the affinity complexes. In order to achieve a better sensitivity for DNA hybridization, immobilization of receptor molecules was modified to enhance the deformation of underlying surface. Single-stranded DNA (ssDNA) strands with thiol-modification on both 3' and 5' ends were immobilized on the gold surface such that both ends are attached to the gold surface. Immobilization condition was controlled to obtain similar receptor density as single-thiolated DNA strands. Hybridization of double-thiolated

DNA strands leads to an almost two orders of magnitude increase in cantilever deformation. In both DNA hybridization and the conventional mode for cocaine detection, the lowest detectable concentration was determined by binding activity between the ligand and receptor molecules. In order to overcome this limitation for cocaine detection, a novel competition sensing mode that relies on rate of aptamers unbinding from the cantilever due to either diffusion or reaction with cocaine as target ligands in solution was investigated. The rate of unbinding is found to be dependent on the concentration of cocaine molecules. A model based on diffusion-reaction equation was developed to explain the experimental observation. Experimental results indicate that the competition mode reduces the lowest detectable threshold to 200 nM which is comparable to that achieved analytical techniques such as mass spectrometry.

CHAPTER 1. OVERVIEW

A novel surface stress sensor is used for quantitative analysis of nanomechanical response arising from adsorption of small molecules on microcantilevers. The deflection of the microcantilever is indicative of surface stress that can be correlated with the amount of ligands bound to the microcantilever. In detail, the surface of a microcantilever is functionalized with receptor molecules that have high affinity for the ligand. In the surface stress sensor, adsorption of the ligand on the sensitized surface provides differential measurements of deflection between a sensing and reference microcantilevers. An optical interferometry is used to measure cantilever deflection that converts molecular interactions into a measureable quantitative signal with high precision and accuracy.

The sensor's principal applications would be biomedical, forensic and biosecurity areas; portability is of crucial importance in molecular recognition with high specificity and sensitivity. In current state-of-art microcantilever sensors, optical beam deflection method is utilized for the deflection measurement due to its simplistic configuration and convenience as are common in AFM instrumentation. However, the optical deflectometry requires a large optical distance for high-sensitive detection and suffers from the challenges in integration of all components in a single micro device. The sensitivity of interferometric technique, in contrast, is independent of the distance between detectors and the sensing surface of microcantilevers. Therefore, the surface stress sensor may be amenable to integrate all sensor components into a single MEMS device.

One outstanding aspect of the microcantilever sensor is that the differential measurement of microcantilevers (sensing and reference pair) is inherently insensitive to

environmental disturbances such as nonspecific adsorption, changes in pH, ionic strength, and especially the temperature. The use of nucleic acid aptamers as receptor molecules enables regeneration and robust performance of the sensor because of unique features of aptamers such as reversible thermal denaturation, long term stability and easy and straightforward chemical modification.

Ultimate goal of this study is to achieve a mechanism based understanding of the molecular phenomena governing surface stress generation and influence of nanoscale morphology on such mechanisms. The knowledge of biomolecular interactions would lead to instrumentation capable of sensitive and immediate ligand detection and identification. In order to achieve this goal, we utilized a novel microcantilever based nanomechanical sensor capable of sensitive and specific detection of chemical and biological species. These objectives were achieved through successful completion of tasks as follow:

1) Construction of a novel microcantilever based sensor

2) Validation of the sensitivity and specificity of microcantilever based sensors for measurements of surface stress associated with formation of alkanethiol self-assembled monolayers (SAMs), DNA hybridization, and cocaine/aptamer binding in conventional mode.

3) Influence of receptor molecule immobilization on surface deformation.

4) Invention of a novel sensing mechanism that relies on rate of receptor unbinding due to diffusion or reaction with target ligand.

CHAPTER 2. LITERATURE REVIEW

2.1 Conventional techniques for molecular recognitions

Almost all approaches for detection and identification of biological molecules can be broadly classified into two main groups; labeled and label-free methods. Fluorescence resonance energy transfer (FRET) is an example of labeling systems and achieved high resolution for identification in immunoassays (Hanbury, Miller et al. 1996; Aoyagi and Kudo 2005; Ko and Grant 2006), nucleic acid (Tyagi and Kramer 1996; Fang, Liu et al. 1999; Ueberfeld and Walt 2004), and ligand-receptor interactions (Medintz, Clapp et al. 2003; Ye and Schultz 2003; Sandros, Gao et al. 2005). Although labeling techniques have high sensitivity and large dynamic range of spatial resolution, they also have drawbacks. For instance, time required for extensive sample preparation leads to significant delay in identification. It also requires high cost and skilled scientists for labeling processes and detecting systems. Alternative methods to substitute labeling techniques are label-free methods. Rapid and real-time detections are primary advantages of label-free methods.

Gas chromatography-mass spectrometry (GC-MS) and High-performance liquid chromatography (HPLC) may be standard techniques as label-free biosensing platforms for identifying molecules of controlled substances with great specificity and sensitivity. Mass spectrometry is designed to determine the elemental composition and chemical structure of molecules by measuring mass-to-charge ratios. This technique is often combined with the liquid/gas chromatography (HPLC and GC-MS) and is widely used for forensic analysis (Mortier, Maudens et al. 2002; Follador, Yonamine et al. 2004; Lopez, Bermejo et al. 2006; Valente-Campos, Yonamine et al. 2006; Cristoni, Basso et al. 2007; Johansen and Bhatia

2007; Loopez, Bermejo et al. 2007; Barroso, Dias et al. 2008; Gheorghe, van Nuijs et al. 2008; Jagerdeo, Montgornery et al. 2008; Langman, Bjergum et al. 2009).

Enzyme multiplied immunoassay technique (EMIT) and Enzyme-linked immunosorbent assay (ELISA) were developed for the measurement of substances in test samples present at small concentrations, 5 to 20 ng/mL in general (Kergueris, Bourin et al. 1983; Allard and Deutsch 1987; Badcock and Oreilly 1992; Michael E. Burton 1992; Wilson, Tsanaclis et al. 1996; Ullman 1999; Marin, Keith et al. 2009). These two techniques are enzyme immunoassays used for routine analytical determinations in forensic laboratories. EMIT is a homogeneous and liquid phase assay that is designed for rapid measurements of haptens for drug, hormone and metabolite determinations. ELISA is a heterogeneous and a solid phase assay that requires the separation of reagents. This technique is based on measuring the presence of antibody/antigen or immune complex and is used for diagnosing infectious disease and immunoglobulins. In general, EMIT is faster than ELISA but ELISA has a better sensitivity.

Surface plasmon resonance (SPR) and X-ray photoelectron spectroscopy (XPS) are other examples of label-free surface analytical tools. SPR is a sensitive and accurate tool for detection of specific binding of small molecules but not suitable for bulk because the surface plasmon only penetrates a short distance into the external medium (Zhang, Luo et al. 2006; Kim, Lee et al. 2008; Solanki, Prabhakar et al. 2008). XPS technique is used for quantitative and qualitative analysis of surface chemical or molecular binding. Atomic number and the bonding state of elements determine the characterstic peaks in the photoelectron spectrum. It can identify all elements except hydrogen on the examined surface. This is a widely used technique to confirm the existence of organic molecules on a substrate by comparing peaks

of nitrogen and phosphorous. A typical XPS spectrum contains information on both the X-ray-excited photoelectrons and X-ray-excited Auger electrons (Casero, Darder et al. 2003; Lee, Harbers et al. 2007; Liu, Zhang et al. 2009). Many other methods are also proposed for recognition of chemical or biological molecules such as quartz crystal microbalances (QCM) (Janshoff, Galla et al. 2000), nanowire nanosensors (Wang, Chen et al. 2005), and screen printed electrode (SPE) biosensors (Alonso-Lomillo, Yardimci et al. 2009).

2.2 Microcantilever Nanomechanical Sensors

Among those label-free methods, microcantilever based sensors as biosensing platform are being widely investigated for monitoring molecular interactions. These sensors are designed to measure nanomechanical responses through a static deflection or resonance frequency shift of a microcantilever in both ambient and liquid environments. A single microcantilever was used in the early stages of microcantilever based sensors (Berger, Delamarche et al. 1997; Lang, Berger et al. 1998; Moulin, O'Shea et al. 1999; Raiteri, Nelles et al. 1999). One soon realized that using at least two cantilevers (sensing and reference pairs) in parallel could significantly improve the reliability during measurements. The differential reading of sensing cantilever respect to reference cantilever suppresses signals caused by environmental disturbances such as nonspecific adsorption, changes in pH, ionic strength, and temperature change (Lang, Berger et al. 1998).

The most common method of measuring microcantilever deformation is the beam deflection technique (Meyer and Amer 1988; Raiteri, Grattarola et al. 2001; Ziegler 2004). Laser beam is focused at the free end of the microcantilever and reflected into a position-sensitive detector. When the cantilever bends due to adsorption of ligands, the reflected spot

undergoes a proportional displacement. Therefore, a large optical distance between a cantilever and a detector is required to achieve a sensitive measurement. Alternatively, optical interferometry (Martin, Williams et al. 1987; Rugar, Mamin et al. 1989; Schonenberger and Alvarado 1989; Putman, Degrooth et al. 1992) can be used to measure cantilever deflection. A coherent laser beam is split into two or more parts and recombined to form an interference pattern whose intensity is proportional to path length difference between the beams. The sensitivity of measurement does not depend on the optical distance although it demands accurate in alignments of sensing components, matching the polarization, and common mode rejection. However, the possibility of miniaturization of the sensor into a single MEMS device with a high performance in surface stress measurement is a reasonable compensation for those difficulties in the interferometry technique.

The use of cantilevers for sensing elements was attempted late 1960, but easy availability of microfabricated cantilevers for AFM opened a great potential in use of cantilevers as sensing platform (Wilfinge.Rj, Bardell et al. 1968; Heng 1971; Petersen 1979). In 1994, Thundat and his colleagues (Thundat, Warmack et al. 1994) made the seminal observation that Atomic Force Microscope (AFM) cantilevers deflect due to changes in relative humidity and thus opened a myriad of possibilities for the use of AFM cantilevers for chemical and biological sensing. They predicted possibilities of adsorbate detection of the order of picograms and immediately followed up with another study in which they detected mercury adsorption on cantilever from mercury vapor in air with picogram resolution (Thundat, Warmack et al. 1994; Thundat, Wachter et al. 1995). Also, Berger et al. (Berger, Delamarche et al. 1997) measured differential surface stress induced by formation of alkanethiol self-assembled monolayers (SAMs) on gold coated microcantilever. Godin et al.

(Godin, Williams et al. 2004) reported that surface stress development is dependent on the grain size of the gold film and elucidated the transition phases during SAM formation (Godin, Williams et al. 2004). The thickness of the SAM also affects the magnitude of the measurements as well as sensing performance (White, Phares et al. 2008).

Microcantilever based sensors have been successfully utilized for biomolecular recognitions. Fritz et al. (Fritz, Baller et al. 2000) monitored hybridization of single-stranded DNAs (ssDNAs). They measured surface stress of 5 mN/m and actuation force of 300 pN due to single base mismatch between 12-mer and 16-mer oligonucleotides. Moulin et al. (Moulin, O'Shea et al. 1999) conducted surface stress measurements of immunoglobulin G (IgG) and albumin (BSA) and found that the strength of surface stress change is time dependent. They also hypothesized that the direction of cantilever bending is due to molecular interaction. Hydrophobic forces between adsorbed proteins bend the cantilever down to compressive direction, while high mobility of molecules from weak surface-protein interaction may bend cantilever up to tensile direction.

Majumdar and coworkers (Biswal, Raorane et al. 2006; Stachowiak, Yue et al. 2006) reported a series of works on label-free microcantilever sensor for biological detections. Stachowiak et al. (Stachowiak, Yue et al. 2006) investigated the efficiency of DNA hybridization in various ionic strength and dependence on the grafting density as well as the length of the DNA. They found that surface grafting density of ssDNAs can be controlled by changing the DNA chain length and ionic strength. Also, they observed that the density of receptor molecules on gold surface for hybridization is a key parameter and has an exponential relation with generating surface stress changes. Inversely, Biswal et al. (Biswal, Raorane et al. 2006) measured surface stress changes associated with dehybridization of

double-stranded DNA (dsDNA). They observed the response of melting and diffusing dsDNAs away from the cantilever as a function of salt concentration and length of oligonucleotides. They confirmed that increasing salt concentration and oligonucleotide length result in an increase in the melting temperature. They even extended their sensing platform to two-dimensional microcantilever sensor for high-throughput multiplexed chemical and biomolecular analysis. Several cantilevers are fabricated in parallel and each cantilever is functionalized for a specific target molecule. Through this process, they provided that the two-dimensional multiplexed microcantilever sensor can detect many target molecules. With the new sensor platform, they measured surface stress changes in the responses of DNA immobilization on gold surface (Yue, Lin et al. 2004), toluene and water vapor in vapor phase (Lim, Raorane et al. 2006), Prostate specific antigen (PSA) (Yue, Stachowiak et al. 2008) as low as 1 ng/mL which corresponds to 2 mN/m of surface stress change.

More recently, Maraldo et al. (Maraldo, Garcia et al. 2007) performed the prostate cancer detection through prostate cancer biomarker (α-methylacyl-CoA racemase; AMACR) directly in patient urine. They demonstrated the function of microcantilever sensors as a feasible application of cancer detection. There have been many other applications to oligonucleotide hybridization (Hansen, Ji et al. 2001; McKendry, Zhang et al. 2002; Stachowiak, Yue et al. 2006; Zhang, Lang et al. 2006), receptor-ligand (Thaysen, Yalcinkaya et al. 2002; Marie, Thaysen et al. 2003; Savran, Burg et al. 2003; Savran, Knudsen et al. 2004; Mukhopadhyay, Sumbayev et al. 2005), and antigen-antibody interaction (Raiteri, Nelles et al. 1999; Raiteri, Grattarola et al. 2001; Grogan, Raiteri et al. 2002; Dutta, Tipple et al. 2003).

2.3 Operation modes of micro cantilever sensors (Fritz 2008)

Nanomechanical cantilever sensors are generally operated in three basic modes: bimetallic, dynamic and surface stress modes. In bimetallic mode, microcantilevers undergo a static deflection in the response of temperature changes because of different coefficients of thermal expansion between the metallic thin film and the underlying substrate. This mode is widely used for temperature related applications such as thermal actuators (Ramos, Mertens et al. 2007). In dynamic or resonance mode, Attached additional mass on a cantilever lowers its resonance frequency and the consequential frequency shift is detected to measure the mass addition. This mode has been operated in ambient as well as liquid environments (Cleveland, Manne et al. 1993; Humphris, Tamayo et al. 2000; Tamayo, Humphris et al. 2000) and used for detection of mass changes as small as 10^{-17} g (Ilic, Czaplewski et al. 2000; Yang, Ono et al. 2000). However, the cantilever oscillation is damped out in liquid environment and accordingly the sensitivity is significantly diminished. Surface stress mode has been widely used to measure the biomolecular recognitions. When molecules adsorb or bind preferentially to one side of a cantilever, the surface expands (or contract) compared to the other side which leads to bending down (or up) of microcantilever to generate compressive (or tensile) surface stress. Each of these operation modes are schematically represented in Figure 1.

With those basic operating modes, many other modes have been attempted such as cantilever bending due to electric charges (Stephan, Gaulden et al. 2002), magnetic forces (Weizmann, Patolsky et al. 2004) and photothermal spectroscopy that produced heat from the absorption of light (Barnes, Stephenson et al. 1994).
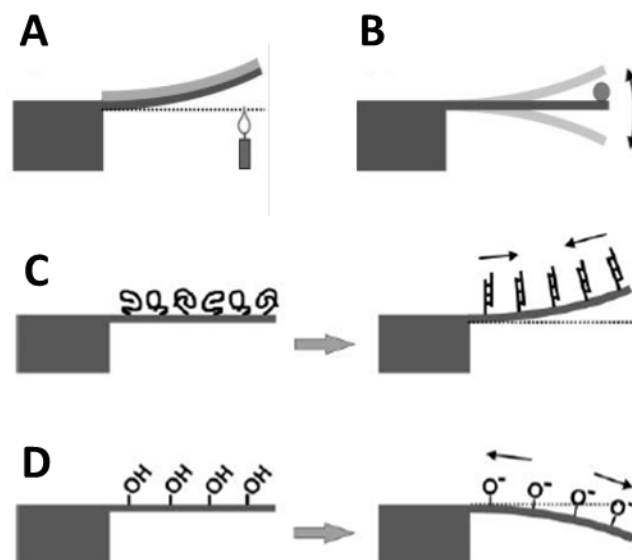
Figure 1 Illustrations of bimetallic mode (A), dynamic mode (B) and surface stress mode (C, D). Tensile surface stress during conformational changes of DNA hybridization (C) Negative surface stress charges and electrostatic repulsion generate compressive surface stress (D) (Fritz 2008)

2.4 Origin of generation of surface stress

Elastic effects of surface chemical reaction have been known for a long time. For instance, adsorbates are used to stabilize surface during crystal growth (Copel, Reuter et al. 1989) and surface stress changes induced by the presence of adsorbed atoms reconstruct the surface due to surface-substrate mismatch and stress-related energy gain (Fiorentini, Methfessel et al. 1993). As adsorbed molecules affect surface stress, residual or applied stress also influences adsorptions (Gsell, Jakob et al. 1998).

Although there have been extensive efforts to elucidate the origin of the biomolecular binding induced surface stress changes, consensus on the underlying mechanisms is still elusive due to complex molecular interactions. Compressive surface stresses are attributed due to an expansion of a cantilever surface influenced by electrostatic repulsion of surface

groups and increasing the number of negative charges on the surface. Alternatively, conformational changes of receptor molecules caused by hybridization or binding that result in formation of ordered structures may relax the repulsive steric interactions between disordered unbound molecules bending the cantilever upward to tensile direction. Therefore, when a surface bound with single-stranded oligonucleotides undergoes hybridization, conformational changes from a single strand to a rod-like double helix may result in initial tensile surface stress changes but as the hybridization proceeds the surface stress development changes sign to compressive stresses due to buildup of charge interactions among neighboring molecules. Conformational changes and electrostatic and hydrophobic forces are dependent on individual ligand/receptor pair, so the transition point and dominant phenomena is difficult to identify (Fritz 2008).

Wu et al. (Wu, Ji et al. 2001) introduced thermodynamic principles to explain the nanomechanical motion of the cantilever during DNA immobilization and hybridization. In addition to the electrostatic repulsive force between neighboring DNA chains, they argued that the origin of cantilever bending is due to a change in configurational entropy and intermolecular energetics induced by specific biomolecular interactions. When immobilized single-stranded DNAs interplay between neighboring chains, the configurational entropy decreases which lead to increase entropic driving force. The configurational entropy of single-stranded DNA is highest in a free solution, but forming double stranded DNAs during DNA hybridization reduces this entropic driving force balanced by the strain energy of bending the cantilever. Therefore, this curvature produces the cantilever bending up to tensile direction (Wu, Ji et al. 2001).

2.5 Aptamers: new approach as a substitute for conventional assays

Aptamers are synthetic oligonucleotides that bind to a designated target ligands and can be implemented as an alternative to antibodies or other bio-mimetic receptors. They are synthesized and characterized by SELEX (Systematic evolution of ligands by exponential enrichment) process in vitro. This method ensures directed evolution of a starting pool of oligonucleotides in response to selection pressure on the population through repeated rounds of selection and amplification. Target-specific aptamers using SELEX technology have been identified for various classes of targets including inorganic and small organic molecules, peptides, proteins, carbohydrates, and antibiotics, as well as complex targets such as mixtures or whole cells and organisms (Klussmann 2006).

In 1990, Tuerk et al. (Tuerk and Gold 1990) first described a new selection and amplification method (SELEX) used for a combinatorial nucleic acid library to select RNA oligonucleotides which have a strong and specific binding with T4 DNA polymerase gp43 as a non-nucleic acid target (Tuerk and Gold 1990). In the same year, Ellington et al. (Ellington and Szostak 1990) isolated RNA molecules with average length of 100 nt from large numbers of random sequence RNA molecules which recognize and bind to six small organic dyes (Cibacron Blue 3GA, Reactive Red 120, Reactive Yellow 86, Reactive Brown 10, Reactive Green 19, and Reactive Blue 4). They named these selected RNA sequences to *aptamers* from the Latin *aptus* meaning "to fit.' In 1992, they showed a successful isolation of a set of ligand-binding ssDNA sequences from a large pool of random sequence DNAs and reported DNA aptamers would be more stable than RNA aptamers because of the greater stability of DNA (Ellington and Szostak 1990; Ellington and Szostak 1992).

Bock and his colleagues (Bock, Griffin et al. 1992) attempted the isolation of single-stranded DNA aptamer to the protease thrombin of the blood coagulation cascade and reported binding affinities in the range 25-200 nM. They also found an aptamer molecule of 96-mer single-stranded DNA that binds human thrombin (Bock, Griffin et al. 1992). An endeavor of aptamer-based biosensor was made in 1998 by Potyrailo et al. (Potyrailo, Conrad et al. 1998). They immobilized a fluorescently labeled anti-thrombin DNA aptamer to a glass surface and detected thrombin in solution by monitoring changes in the evanescent-wave-induced fluorescence anisotropy of the immobilized aptamer. Through this technique, they achieved a sensitivity limit of about 0.7 attomole of thrombin in a 140-pL interrogated volume (Potyrailo, Conrad et al. 1998).

Aptamers as the receptors designed to bind a controlled substance and their main advantages over antibodies for molecular recognition are as follow (Lee, So et al. 2008; Kazunori Ikebukuro 2009):

1) Aptamers have consistently high quality because they are chemically synthesized and purified.

2) Aptamers are selected in vitro whereas antibodies are produced as the induction of an immune response in vivo.

3) Aptamers can be optimized for any conditions but antibodies can only work under physiological conditions.

4) Aptamers are more stable at high temperature and can be regenerated easily after denaturation.

5) Aptamers can be easily labeled whereas labeling the antibodies can result in loss of their affinity to their target molecules.

Therefore, Aptamers possess a number of advantages over antibodies to be useful tools in analytical, diagnostics and therapeutic applications. The most important characteristic of aptamers is its ability to bind their target molecules with high specificity.

2.6 Aptamer-based biosensors

Aptamer-based biosensors (often called aptasensors) utilize three main approaches for transducing the aptamer/ligand binding into a measurable signal: electrochemical, optical emission and colorimetry (Scheller, Wollenberger et al. 2001; Lee, So et al. 2008; Cho, Lee et al. 2009; Liu, Cao et al. 2009).

DNA hybridization has been the basis for development of aptasensors reported by Fan et al. (Fan, Plaxco et al. 2003). They built an electrochemical DNA (E-DNA) sensor and successfully measured the change in electron transfer efficiency as low as 10 pM concentration. The strategy involves a stem-loop oligonucleotide immobilized at a gold electrode. In the absence of target, the stem-loop structure holds the electroactive ferrocene-tag into close proximity of gold surface; thus, enabling rapid electron transfer and efficient redox of the ferrocene label. When hybridized with complementary strands the ferrocene-tag moves away from the surface and a large change occurs in redox currents (Fan, Plaxco et al. 2003). Later, they have applied electronic aptamer-based (E-AB) sensors for detection of thrombin in blood serum (Xiao, Lubin et al. 2005) and cocaine (Baker, Lai et al. 2006). Their idea has inspired many other groups to utilize this strategy for the detection of small and micromolecular analytes (Alonso-Lomillo, Yardimci et al. 2009; Canete, Yang et al. 2009; Cekan, Jonsson et al. 2009; Cheng, Sen et al. 2009; Kim, Kim et al. 2009; Pan, Guo et al.

2009; Torres-Chavolla and Alocilja 2009; Velasco-Garcia and Missailidis 2009; Xiang, Tong et al. 2009).

Another approach for transduction utilizes changes in optical emission for detection of the ligand through fluorescent tags and quantum dots (QDs). Levy and coworkers (Levy, Cater et al. 2005) functionalized QDs with a thrombin-binding aptamer. When a short piece of quencher-labeled DNA was hybridized to the thrombin aptamer on QDs, they observed that 19-fold increase in fluorescence in the presence of 1 µM thrombin (Levy, Cater et al. 2005). Choi et al. (Choi, Chen et al. 2006) claimed that they can detect thrombin concentration as little as ~1 nM through spectroscopic measurements of thrombin using photoluminescence transduction of the QD (Choi, Chen et al. 2006). Because of QDs' superior properties such as greater photostability, higher fluorescent efficiency, longer fluorescent lifetimes, and sharper emission bands compared to traditional organic fluorophores (Levy, Cater et al. 2005; Michalet, Pinaud et al. 2005), aptamer conjugated QDs have been utilized for detection of bacteria (Dwarakanath, Bruno et al. 2004) and various tumor cells (Chu, Marks et al. 2006; Chu, Shieh et al. 2006; Bagalkot, Zhang et al. 2007; Chen, Deng et al. 2008; Ding, Helquist et al. 2008; Levy-Nissenbaum, Radovic-Moreno et al. 2008).

Aptamer-based colorimetric sensors determine the presence of target molecules through change in solution color. They often work with gold nanoparticles (AuNPs) where the color change is due to the cross-linking of DNA on AuNPs or aptamers with target ligands. Since Mirkin's group (Mirkin, Letsinger et al. 1996) first reported AuNPs-DNA conjugates, it has been developed to the ultrasensitive detection of DNA and proteins (Taton, Mirkin et al. 2000; McKenzie, Faulds et al. 2007; Zhang, Song et al. 2007). Mirkin et al.

(Mirkin, Letsinger et al. 1996) presumed that the stability of AuNPs is dependent on salt concentration; however, high concentration of salt induces aggregation of colloids and produces a similar red-to-blue color changes. Alternatively, Li and coworkers (Li and Rothberg 2004; Li and Rothberg 2004; Li and Rothberg 2004) found that thiol-modified DNA used to functionalize AuNPs can be replaced by a non-thiolated short single-stranded DNA. They also reported that shorter DNA strands and higher temperatures provide faster adsorption, but a long or double-stranded DNA is not effectively associated with AuNPs (Li and Rothberg 2004; Li and Rothberg 2004; Li and Rothberg 2004).

2.7 Aptamer-based biosensors for cocaine detection

The U.S. Department of Health and Human Services (HHS) (Services 2008) has established a standard of cocaine metabolite cutoff levels, effective October 2010, to 150 ng/mL and 100 ng/mL for initial screening and confirmatory cutoff levels respectively. Current methods of initial screening and identifying biological samples for drugs of abuse can match the new standard for detection and identification of cocaine metabolite. For instance, enzyme multiplied immunoassay technique (EMIT) (Mead, Niekro et al. 2003; Contreras, Hernandez et al. 2006; Baker and Jenkins 2008) and enzyme-linked immunosorbent assay (ELISA) (Kerrigan and Phillips 2001; Spiehler, Isenschmid et al. 2003; Lopez, Martello et al. 2010) are the two predominant enzyme base immunoassays utilized for screening tests. In both techniques, detection of the controlled substance is based on optical absorbance resulting from enzymatic activity. Gas chromatography coupled with mass spectrometry (GC-MS) (Valente-Campos, Yonamine et al. 2006; Cristoni, Basso et al. 2007; Barroso, Dias et al. 2008) and high performance liquid chromatography (HPLC) (Johansen

and Bhatia 2007; Jagerdeo, Montgornery et al. 2008; Nesmerak, Sticha et al. 2010) can achieve detection levels required for the confirmatory identification of controlled substances. These techniques require extensive sample preparation, a long performance time and/or specialized instrumentation to validate drug presence. The sample often must be sent to the lab, which results in a significant delay in identification (Stojanovic, de Prada et al. 2001; Maurer 2005; Strano-Rossi, Molaioni et al. 2005; Cognard, Bouchonnet et al. 2006; Dixon, Brereton et al. 2006; Kaeferstein, Falk et al. 2006; Contreras, Gonzalez et al. 2007; Johansen and Bhatia 2007; Schaffer, Hill et al. 2007; Walsh, Crouch et al. 2007). Aptamer based biosensors (often called aptasensors) have been investigated as an alternative method to overcome these drawbacks. Sensitivity and detection times of conventional and aptamer based techniques are compared in Figure 2.

Aptamers are synthetic oligonucleotides that recognize and bind to their respective targets. Aptamers are much smaller and stable than their protein (antibody) counterparts, and unlike antibodies, ligand binding is often accompanied by large structural changes in the aptamers that can be utilized for detection of the target ligands (Stojanovic, de Prada et al. 2001). Aptamers have been selected that recognize two drugs of abuse, which are cocaine (Stojanovic, de Prada et al. 2001) and codeine (Win, Klein et al. 2006), and many medicinal drugs and antibiotics including theophylline (Jenison, Gill et al. 1994), tobramycin (Wang and Rando 1995), neomycin (Wallis, Vonahsen et al. 1995), kanamycin (Lato, Boles et al. 1995), dopamine (Mannironi, DiNardo et al. 1997), chloramphenicol (Burke, Hoffman et al. 1997), streptomycin (Wallace and Schroeder 1998) and tetracycline (Berens, Thain et al. 2001). The affinities (Ka) of these aptamers are in the range of 10^5 to 10^7 M^{-1}.
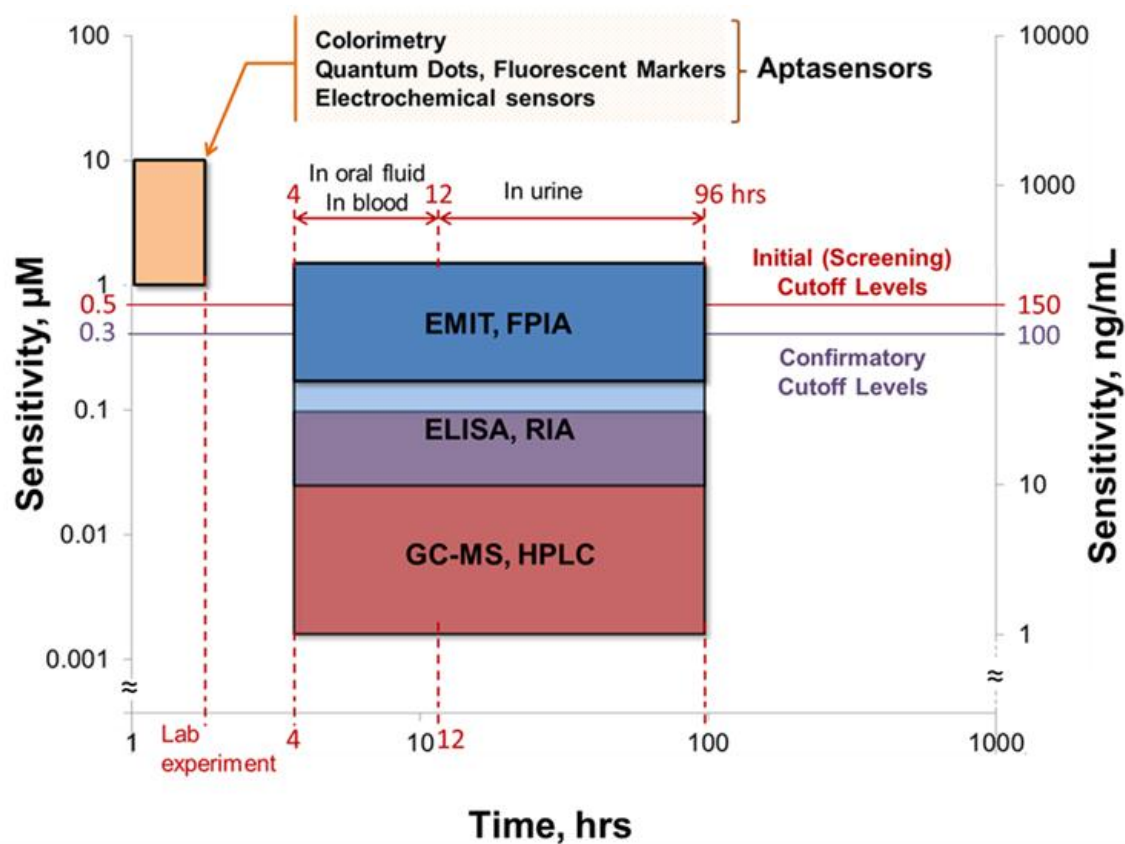
Figure 2 Comparisons of sensitivity and time for conventional and aptamer based sensing techniques (Preston, Huestis et al. 1999; Stojanovic, de Prada et al. 2001; Stojanovic and Landry 2002; Kroener, Musshoff et al. 2003; Verstraete 2004; Baker, Lai et al. 2006; Gareri, Klein et al. 2006; Concheiro, de Castro et al. 2007; Shlyahovsky, Li et al. 2007; White, Phares et al. 2008; Zhang, Wang et al. 2008; Freeman, Li et al. 2009; Li, Zhang et al. 2009; Madru, Chapuis-Hugon et al. 2009)

Aptamers can be selected to have exquisite discrimination between molecules because their specificity can be tuned by the selection conditions. For example, aptamers have been isolated that distinguish between caffeine and theophylline, which differ by only a single methyl group (Jenison, Gill et al. 1994) and that distinguish tyramine and dopamine, which differ by a single hydroxyl group (Mannironi, Scerch et al. 2000). Very little change in the oligonucleotide sequence may be necessary to change the specificity of a nucleic acid.

For example, two RNA aptamers were isolated that differ by only 3 nucleotides in 44 and that respectively specifically recognize only one of the two closely related amino acids, arginine and citrulline (Mannironi, Scerch et al. 2000).
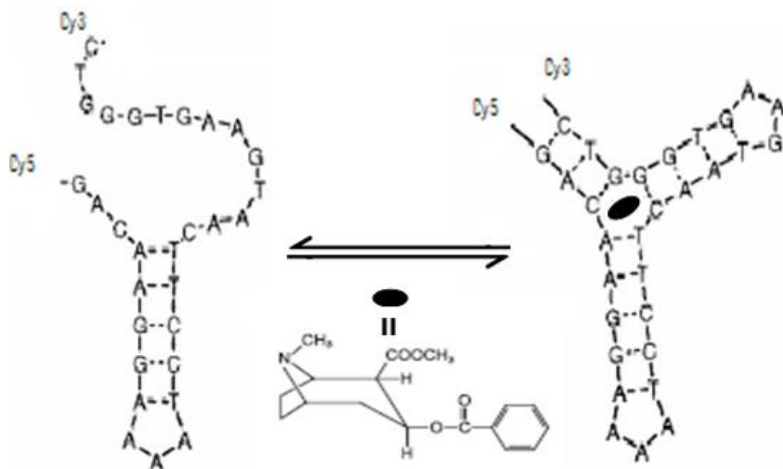
Figure 3 Conformational changes of cocaine aptamer from a tertiary structure (Stojanovic, de Prada et al. 2001)

In 2001, Stojanovic and coworkers (Stojanovic, de Prada et al. 2001)ꞌ reported a DNA based aptamer that undergoes specific binding with cocaine. It was hypothesized that binding of the aptamer with a cocaine molecule results in a change of aptamer structure from an unstructured single stranded DNA to a three way stem. The aptamer was used for cocaine detection through fluorescent and colorimetric sensors and a 10 µM detection limit was reported (Stojanovic, de Prada et al. 2001; Stojanovic and Landry 2002). Baker et al. (Baker, Lai et al. 2006) used the same DNA aptamer in electronic aptamer-based (E-AB) sensors and measured a dissociation constant (K_d) of 90 µM for cocaine/aptamer binding and detection limits of below 10 µM for cocaine molecules.

Freeman et al. (Freeman, Li et al. 2009) conducted QD-based optical sensing as well as electrochemical sensing of cocaine by employing a split cocaine-aptamer and pyrene modification to create supramolecular complexes. They demonstrated as detection limits of 1 μM for FRET-based sensing and 10 μM for the amperometric response of the system respectively. Madru et al. (Madru, Chapuis-Hugon et al. 2009) demonstrated that the anticocaine aptamer-based sorbent can be used for the selective extraction of cocaine from human plasma. They showed close to 90% of extraction recovery with 3.5 μM of the detection limit of cocaine. Shlyahovsky et al. (Shlyahovsky, Li et al. 2007) proposed the amplified analysis of cocaine by an autonomous aptamer-based machine and obtained a detection limit for cocaine of 5 μM for 60 minutes operating time for the machine. Li and Zhang et al. (Zhang, Wang et al. 2008; Li, Zhang et al. 2009) utilized a split aptamer that reassembles into the full tertiary structure in the presence of target. AuNPs then differentiates between these two states through surface-plasmon resonance-based color change. This colorimetry was able to detect as low as 2 μM cocaine solution. In summary, the cocaine aptamer has been used in variety of different platforms to achieve detection threshold between 1 to 10 μM.

Micromechanical cantilever (MC) based sensors have been investigated for detection of chemical and biological species (Thundat, Oden et al. 1997; Sepaniak, Datskos et al. 2002). A MC intended for chemical or biological sensing is normally modified by coating one of the cantilevers with a responsive phase that exhibits high affinity to the targeted ligand. The surface stress change induced due to the binding of ligand on the sensitized surface is resolved for detection. Potential uses of cantilever transducers in biosensors, biomicroelectromechanical systems (Bio-MEMS), proteomics, and genomics are intriguing

trends in advanced biomedical analyses (Fritz, Baller et al. 2000; Hansen, Ji et al. 2001; Wu, Ji et al. 2001; Savran, Knudsen et al. 2004). When antibodies or small DNA fragments were immobilized on one side of a cantilever, the presence of complementary biological species produced cantilever deflections (Hansen, Ji et al. 2001; Wu, Ji et al. 2001). On the basis of the deflection behavior of MCs, even very small mismatches in receptor–ligand complementarity could be detected. A single base pair mismatch was detected by oligonucleotide hybridization experiments performed on a cantilever surface (Fritz, Baller et al. 2000; Hansen, Ji et al. 2001; Wu, Ji et al. 2001).

CHAPTER 3. SENSOR CONFIGURATIONS

3.1 Sensing principle

In majority of the current state of art sensors, molecule absorption induced surface stress change is inferred from the deflection of a single or multiple laser beams reflected from the sensing surface. A large optical path is required between sensitized surface and position sensitive detectors to achieve high sensitivity in surface stress measurement. Deflection of two laser beams reflected each from sensing and reference cantilevers may also be used for differential surface stress measurement but that setup may suffer from the following drawbacks: measured sensitivity is again proportional to the distance between a cantilever and a photodetector; and measured response is determined by subtracting the two signals, which may lead to resolution losses.

We modified Mark-Zehnder interferometer with single-mode fiber optic couplers that transduce molecular interactions into a measureable cantilever deflection. The differential surface stress sensor consists of two adjacent rectangular-tipless AFM cantilevers, a sensing/reference pair, where only the sensing surface is activated for adsorption of chemical or biological molecules. Absorption/adsorption of analyte species on the sensitized surface is expected to induce differential bending of the sensing and reference cantilevers. The microcantilevers and a pair of microlens arrays (MLAs) are arranged in the optical arrangement shown schematically in Figure 4 (B) to measure the differential displacement between sensing and reference cantilevers. In this optical configuration, incident laser beams at points A and C always arrive to points B and D, respectively, regardless of their incident angle. The differential bending of cantilevers produces a change in path length difference.
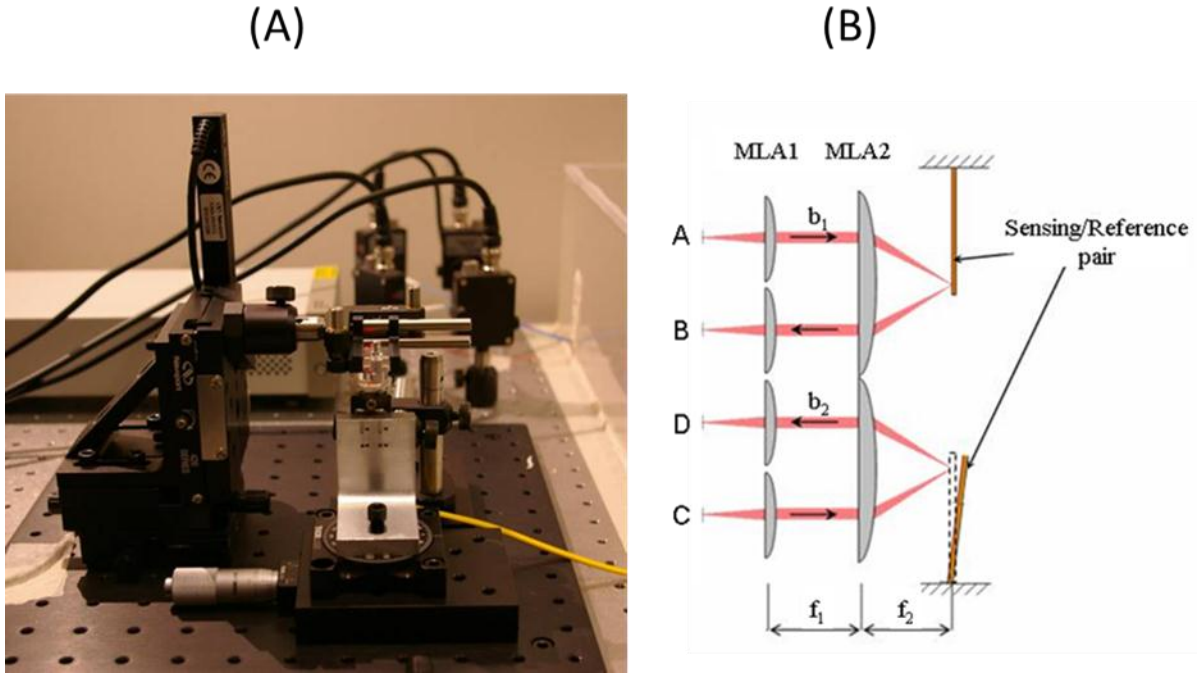
Figure 4 Photograph of experimental setup (A), and schematic image of sensing principle (B).

An optical circuit shown in Figure 5 is utilized for assembling the surface stress sensor. In the system, fiber coupled Fabry-Perot Laser source provided 635 nm wavelength was propagating into microlens array 1 (MLA1) through 3-dB single-mode fiber couplers at 50/50 ratio. MLA1 with a diameter of 240 μm and a pitch of 250 μm collimates incident/refractive beams from off-axis and delivers at precise positions on microlens array 2 (MLA2) as well as receive back to couplers. MLA2, a diameter of 900 μm and a pitch of 1mm, focus the direct beams on the sensitized surface of cantilever pair. Sensing and reference cantilevers are symmetrically positioned about the lens axis on the focal plane of MLA2 and MLA1. The sensing cantilever undergoes submicron-scale bending when specific binding occurred on its functionalized surface.
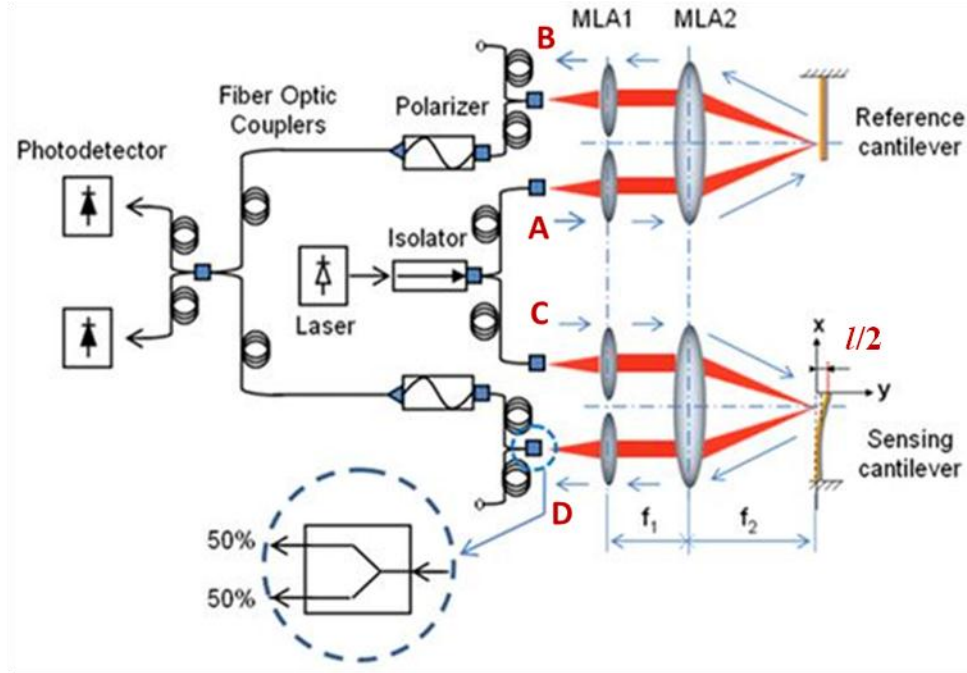
Figure 5 Schematic configuration of MC based nanomechanical sensor

After reflecting from the sensing and reference surfaces, the two beams accumulate a path length difference, *l*, equal to twice the differential displacement between sensing and reference surface. The beams are interfered to measure the path length difference and differential surface stress (Δσ) between the two cantilevers is determined using Stoney's formula (Stoney 1909).

$$\Delta\sigma = \left(\frac{E}{3(1-v)}\right)\left(\frac{t}{L}\right)^2 l \qquad\qquad \textbf{(1)}$$

where E is the Young's modulus and v is the Poisson's ratio; L and t are the effective length and thickness of the cantilever; l is the static deflection of the cantilever beam.

Young's modulus is significantly high among those magnitudes in Equation (1), changing cantilevers to plastic or softer materials would significantly affect the sensitivity on the surface stress measurement. For instance, silicon (E = 170 GPa) and Polyethylene terephthalate (PET, E = 3 GPa) were tested for sensitivity affected on the sensing platform. The numerical calculation showed the surface stress changes of 89.95 mN/m and 1.32 mN/m for silicon and PET respectively at a constant beam deflection of 100 nm.
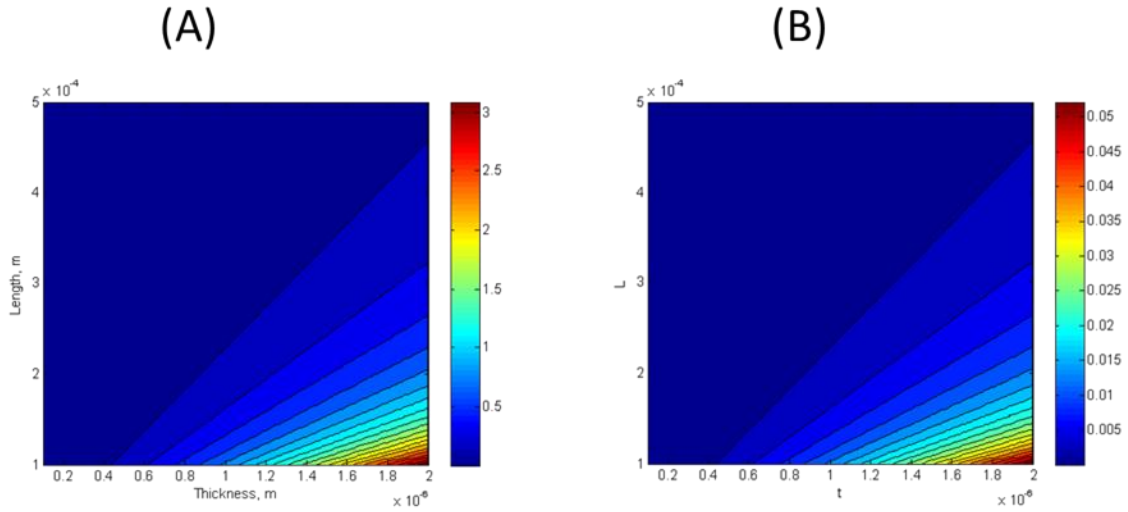
Figure 6 Comparison of surface stress changes when two different materials (Silicon and PET) are used for cantilevers at a constant beam deflection of 100 nm, obtained surface stress changes were 89.95 and 1.32 mN/m respectively.

The polarization plane of the reflected beams was matched by cautiously pulling the fiber optic couplers but not kinking or folding the couplers. An isolator is also applied to block the reflective beam coming back to the laser cavity. Common mode rejection was then utilized to ensure maximum fringe visibility in the interfered beams. An isolation box covered all fiber couplers as well as sensor components to eliminate acoustic and vibrational

noise from the system. Motorized and manual actuators were used to assist in aligning of MLAs with respect to the sensing/reference cantilevers.

Measurements of differential surface stress ensure that detected signal is proportional to specific absorption of analyte species on the sensing cantilever and not on the other. Therefore, the differential surface stress measurement eliminates the influence of environmental disturbances such as nonspecific adsorption, changes in pH, ionic strength, and especially the influence of temperature. Surface stress sensor integrated the interferometer technique ensures that the resolution is independent of optical distance between cantilevers and photodetectors. The sensor is amenable to miniaturize and may facilitate the integration of all components of sensors into a single microfabricated chip.

Intensities of interfered beams may be modeled as two components of interference and the outputs (I_{12}^1 and I_{12}^2) are related to intensity of reflected beams, I_1 and I_2, from sensing and reference cantilevers as:

$$I_{12}^1 = I_1 + I_2 + 2\sqrt{I_1 I_2} \cos\left(\frac{4\pi l}{\lambda} + \phi_0\right), \qquad (2)$$

$$I_{12}^2 = I_1 + I_2 - 2\sqrt{I_1 I_2} \cos\left(\frac{4\pi l}{\lambda} + \phi_0\right), \qquad (3)$$

where ϕ_0 is the phase difference, and λ is the laser's wavelength. The interfered outputs from the two arms are out of phase with each other (180 °). The interfered intensity dependent on $\left(4\pi l/\lambda + \phi_0\right)$ is the most sensitive operating point for the interferometer and is given at quadrature ($\pi/2$, $3\pi/2$, etc.) (Rugar, Mamin et al. 1989).

Two waves generate either a constructive or a destructive interference depending on their relative phase. The stability of the wave is described by coherence, and the degree of

coherence is often expressed as a fringe visibility. The fringe visibility (V) is defined in Equation (4).

$$V = \frac{I_{12}^1 - I_{12}^2}{I_{12}^1 + I_{12}^2}, \ \ (where \ I_{12}^1 \geq I_{12}^1) \tag{4}$$

If the differences between two interfered signals decrease, the fringes become more difficult to observe. When the polarization, which is the orientation of waves, is not parallel, the fringe visibility again decreases. Therefore, coherence and polarization are directly related with the stability as well as sensitivity of the sensor.

When laser light is coupled into an interferometric sensor, the phase or frequency noise is converted into amplitude noise. One needs to wait for 10 minutes at least to stabilize the signals after turning on the laser. Noise is often common in both outputs and appears with the same sign or polarity in both ports whereas the signal may have a different sign for each of the output ports. In common mode rejection, two outputs from the coupler are subtracted each other and emerged into one signal. The beams formed out of phase (180 °) in the output ports balance the output signals from the detectors and add the two outputs to demonstrate the decrease in noise.

3.2 Microcantilever specifications

Microcantilevers are the heart of nanomechanical sensors capable of transducing molecular adsorption into mechanical deformation. Microcantilevers are made of silicon or silicon nitride where a thin gold film (10 - 200 nm) is deposited on one side by evaporating or sputtering in an ultrahigh vacuum (UHV). A thin layer of Cr or Ti (> 10nm) improves the adhesion between a gold layer and a solid silicon substrate. The typical dimensions of

microcantilevers are several hundred μm long, about 10 to 100 μm wide and 0.5 to 1 μm thick. Commercial AFM cantilevers are often used to reduce the sensor costs. Also, multiple cantilever arrays in parallel have been fabricated on a single chip and used for multiple detections of analyte molecules (Baller, Lang et al. 2000). Again, the sensitivity of microcantilever sensors depends on the aspect ratio and elasticity of the cantilevers as shown in Equation (1).

Typical value for Poisson's ratio is about 0.3, and young's modulus is 170 GPa for silicon and 210 GPa or higher for silicon nitride. The spring constant and resonance frequency of the cantilevers need to be measured to determine an accurate thickness. Spring constant and resonant frequency are expressed in Equations (5) and (6) respectively,

$$k_{spring} = \frac{E \cdot w \cdot t^3}{4L^3} \tag{5}$$

$$f_{res} = \frac{1}{2\pi}\sqrt{\frac{k_{spring}}{n \cdot m_{cant}}} \tag{6}$$

where w is the width of a cantilever, m_{cant} is a mass of the cantilever and n (n = 0.24) is a correction factor. A silicon cantilever used for our sensing platform has a normal spring constant of 0.03 N/m and a resonance frequency of about 6 kHz.

We used two different types of microcantilevers: single-cantilever and eight-cantilevers in parallel shown in Figure 7. The nominal dimensions are $500 \times 100 \times 1$ μm and the pitch for the eight-cantilevers is 250 μm. Both cantilevers were coated with 5 nm of titanium and 30 nm of gold film.
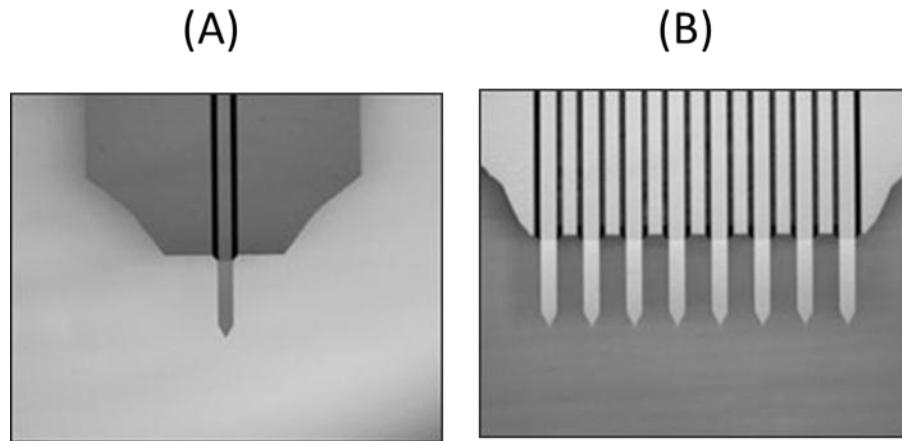
Figure 7 Images of microcantilevers used for microcantilever sensors (Nanoworld 2011)

In general, commercial AFM cantilevers are batch produced with large variation of dimensions and mechanical properties from the manufacture's quote (Sader and White 1993; Sader, Chon et al. 1999). AFM reference cantilever method was utilized to determine the thickness and spring constant of each cantilever for accurate surface stress measurement as shown in Figure 8 (Torii, Sasaki et al. 1996).
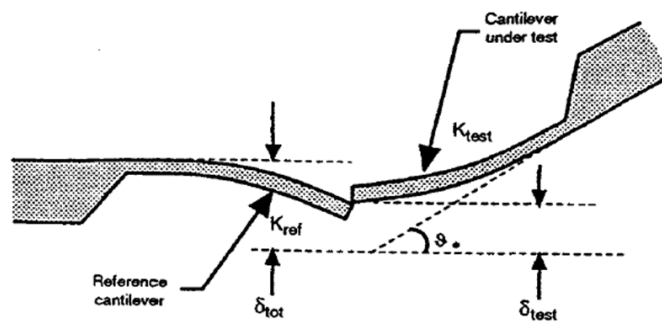
Figure 8 schematic image of the spring constant measurement in AFM contact mode (Tortonese and Kirk 1997)

In brief, a test cantilever mounted on AFM is placed over an infinitely hard sample (sapphire for our test) so that no indentation occurred on the sample but the total cantilever deflection, δ_{tot}, is obtained. Subsequently, the test cantilever is in contact with the free end of a reference cantilever whose specifications and spring constant are known. The deflections obtained through force curves on AFM contact mode are used to calculate the spring constant of the test cantilever in Equation (7).

$$K_{test} = K_{ref} \frac{\delta_{tot}\delta_{test}}{\delta_{test} \cdot cos\theta}$$

(7)

Where, K and δ are normal spring constant and the deflection of a cantilever respectively. The deflection angle, θ, assumed to be zero due to a minute bending of the cantilever. The new spring constant, K_{test} is then manipulated in Equation (5) to calculate accurate thickness of the cantilever.

The thickness of cantilevers used in the microcantilever sensors was between 0.8 to 1.2 μm. Two cantilevers that had similar thickness were selected as a pair of sensing and reference cantilevers. Figure 9 shows a simple estimation of error due to cantilever's geometry. It indicates that when a cantilever has ± 1 percent error on length and thickness, the sensor has 4 percent error in surface stress measurement.
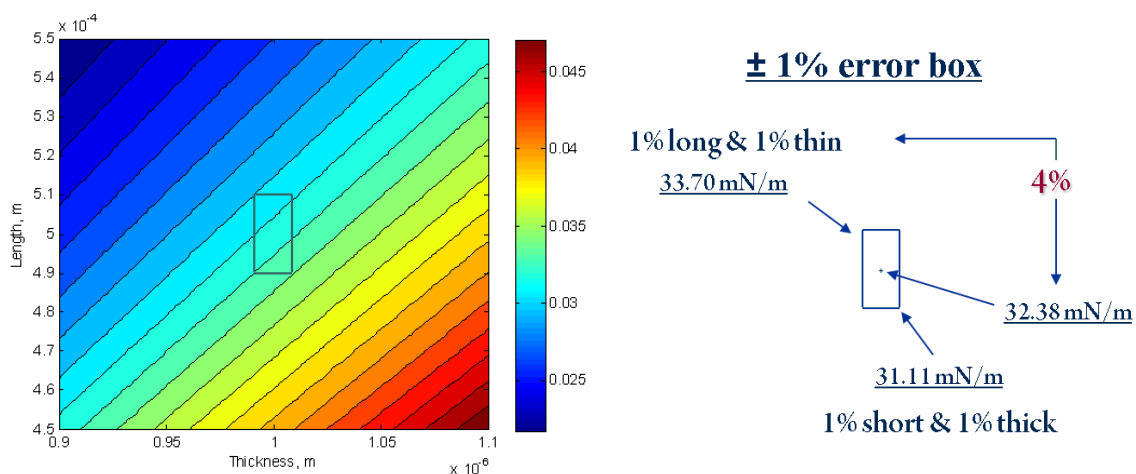
Figure 9 Cantilever error box. It shows the 1 percent error on cantilever geometry results in 4 percent on surface stress measurement
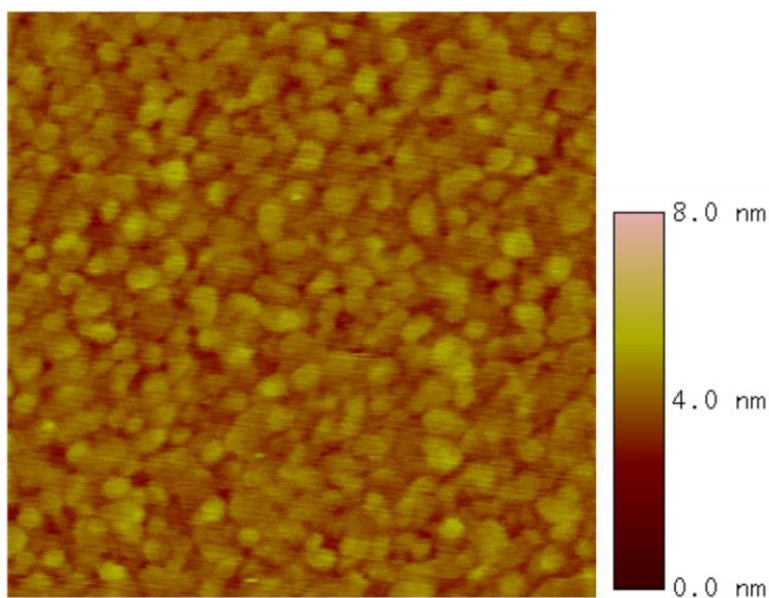
Figure 10 A typical microstructure of gold surface measured by AFM contact mode (750 nm × 750 nm)

Microstructure and surface roughness of the gold film were determined using contact mode atomic force microscope imaging. The grain size was determined to be 40 ± 10 nm

(Figure 10). The mean square roughness of the gold surface was 2.07 ± 0.23 nm for the 750 nm scan size.

3.3 Microcantilever functionalization

Cantilever functionalization is a critical step to ensure a specific adsorption of ligand on the top surface of a cantilever. For sensing applications, one surface has to be selectively functionalized to activate a specific binding while the other surface is passivated from the target ligands. Gold coated cantilevers can easily be functionalized with polymers, organic monolayers, or biomolecules depending on the specific application or analytes to be detected. The chemical immobilization method allows a broad range of biomolecules to be analyzed and has become the cornerstone of biomolecular recognition sensors. Amine, aldehyde and thiol bonds are widely used approaches for immobilizing biomolecules on the sensor surface through a stable bond.

Self-assembled monolayers (SAMs) of organic molecules on a gold surface, particularly thiol linked molecules, undergo low non-specific interactions with various proteins and enzymes. As a result, they are excellent candidates for making monolayer-based protein assay platforms (Ostuni, Chapman et al. 2001; Godin, Williams et al. 2004). Irradiation with UV light results in breaking of the gold-thiol bond. In typical sensing experiments, the energy of a binding reaction (5 to 30 kJ/mole) is weaker than that of thiol/gold bond which is approximately 155 kJ/mole (Emsley 1980; Beijer, Kooijman et al. 1998). Therefore, the energy changes associated with binding, charge interaction, or denaturation of receptor molecules is not expected to exceed the energy barrier required to remove SAM molecules from gold surfaces.

Aptamers are single-stranded RNA (ssDNA) or DNA molecules (mostly 15 to 60 nt) that recognize and bind to their respective targets with high specificity and high affinity (Hermann and Patel 2000). Aptamer molecules can be synthesized with thiol end-groups ensuring immobilization on the cantilever surface through the S-Au bonds. Because aptamers are much smaller than their proteins, affinity complexes of ligand-aptamer is often accompanied large structural changes that can be utilized for detection of target ligands (Stojanovic, de Prada et al. 2001).

In our sensing experiments, the sensing and reference cantilevers were functionalized with respective molecules and the experimental procedures were similar through all sensing experiments. Self-assembly of single-stranded DNAs (ssDNAs), cocaine aptamer, or thiolated cocaine molecules were used as receptor molecules to immobilize on the gold surface of a sensing cantilever. A reference cantilever was coated with controlled DNA strands had the same base lengths as the cocaine aptamer but with their sequence was scrambled. The specific binding of target and receptor molecules would generate the deflection of sensing cantilever. We used microtubes as containers for immobilizing molecules on the cantilevers. Closing cap on the tube prevents contamination and vaporize the solution of target molecules so that the concentration of the molecules would be constant through all incubation procedures

Microcapillary tubes with 187/250 µm inner and outer diameters were employed to functionalize multi-cantilevers. In order to insert and functionalize eight-cantilevers, eight microcapillary tubes are attached in parallel and controlled by a micropositioning stage. Siphonage and capillary force provide solution into the tubes and maintain the solution inside of tubes during the incubation process. By using Multi-cantilevers, we can improve the

signal-to-noise ratio of the sensors, save aligning time, and expand sensors to a multitasking platform. For instance, eight-cantilevers are functionalized with all different receptor molecules and able to detect eight different molecules at one experiment. Likewise, eight same experiments can be done at one experiment.

(A)　　　　　　　(B)
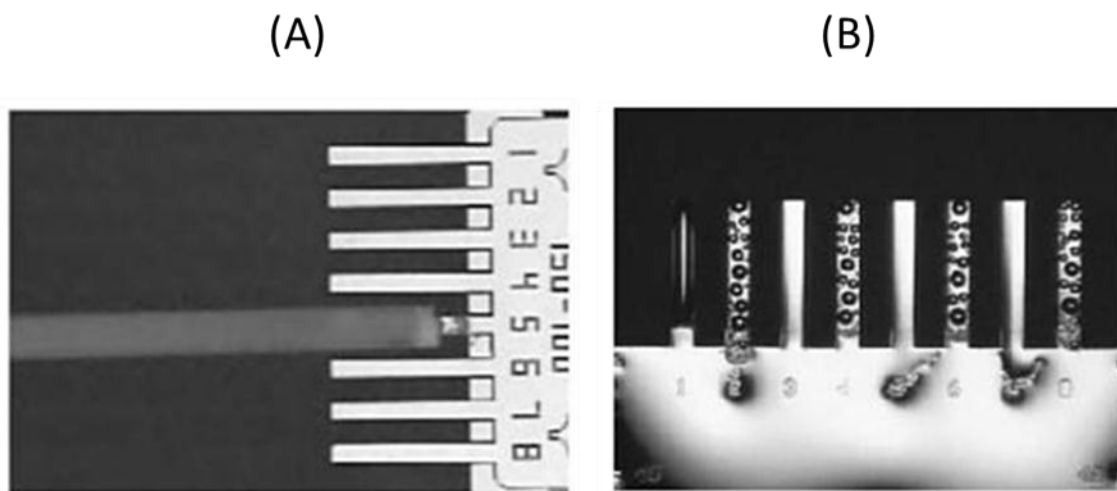
Figure 11 Conceptual images of functionalized multicantilevers (Kambhampati 2004)

CHAPTER 4. EXPERIMENTAL VALIDATION

4.1 Novel differential surface stress sensor for detection of alkanethiol self-assembled monolayers (SAMs)

Modified from conference papers published in MRS 2008 and SPIE 2007

K. Kang, J. Marquardt and P. Shrotriya

4.1.1 Introduction

Microcantilever based sensors are increasingly being investigated to detect the presence of chemical and biological species in both gas and liquid environments. Thundat et al. (Thundat, Warmack et al. 1994) reported the static deflection of microcantilevers due to changes in relative humidity and thermal heating, and thus opened a myriad of possibilities for the use of atomic force microscopy (AFM) cantilever deflection technique for chemical and biological sensing. They predicted possibilities of adsorbate detection of the order of picograms and immediately followed up with another study in which they detected mercury adsorption on cantilever from mercury vapor in air with picogram resolution (Thundat, Warmack et al. 1994; Thundat, Wachter et al. 1995).

Measurements of surface stress changes associated with formation of alkanethiol self-assembled monolayers (SAMs) on a gold surface were utilized to characterize the performance of differential surface stress sensor in ambient condition. Chemisorptions and self-assembly of alkanethiol molecules onto the gold-coated cantilever surface leads to development of compressive surface stress.

Berger et al. (Berger, Delamarche et al. 1997) reported the generation of compressive stresses on the order of 0.1- 0.5 N/m during formation of alkanethiol self-assembled monolayer on the cantilever's surface and also reported that the magnitude of surface stress increased linearly with the carbon chain backbone of the monolayer. Since the first report by Berger et al. (Berger, Delamarche et al. 1997), SAMs have been used as test system for many cantilever based sensing techniques (Ji, Finot et al. 2000; Raiteri, Butt et al. 2000; Stevenson, Mehta et al. 2002; Godin, Williams et al. 2004). This is because they are relatively easy to prepare, form well-ordered close packed films and offers limitless possibilities of variations in chain length, end group and ligand attachments (Ulman 1991). One of the commonly studied SAMs is alkanethiol SAMs ($HS-(CH_2)_{n-1}CH_3$) in which n is the number of carbon atoms in the alkyl chain. Godin et al. (Godin, Williams et al. 2004) have shown that the kinetics of formation of self-assembled monolayers on gold-coated cantilevers and the resulting structure are dependent on the microstructure of the gold film and also the rate at which the SAM reaches the surface.

4.1.2 Experiments

Silicon cantilevers used in the sensor realization are 480 μm long, 80 μm wide, and 1 μm thick with a top side coating of 5nm titanium and 30nm gold film. (Nanoworld, Switzerland). The thickness, microstructure and surface roughness of the gold surface of a sensing/reference cantilever were measured and shown details in Chapter 3.

Liquid octanethiol [$CH_3(CH_2)_7SH$] was selected as alkanethiol solution and purchased from Sigma-Aldrich. All AFM cantilevers were cleaned by immersing for 30 minutes in piranha solution (70% H_2SO_4, and 30% H_2O_2 by volume), rinsed in deionized

water and dried in the gentle N_2 flow. In order to ensure that alkanethiol is only absorbed on the sensing cantilever during the surface stress measurement, alkanethiol SAMs were deposited on the reference cantilever prior to the surface stress measurements.

After cleaning cantilever by piranha solution, one of cantilevers was saved for sensing cantilever and the other cantilever was further treated to use as a reference cantilever. The reference cantilever was prepared by incubating 2 mM octanethiol/ethanol (200 proof) solution for 12 hours to protect formation of SAMs. Formation of a stable SAM on the reference cantilever ensures that alkanethiol molecules are only absorbed on the sensing cantilever during subsequent experiments. It is then removed from the solution and rinsed in anhydrous ethanol for several times (Godin, Tabard-Cossa et al. 2001; Godin, Williams et al. 2004). Because exposing UV causes disulfides or dimers, all procedures were carried out in the dark under a standard fume hood.
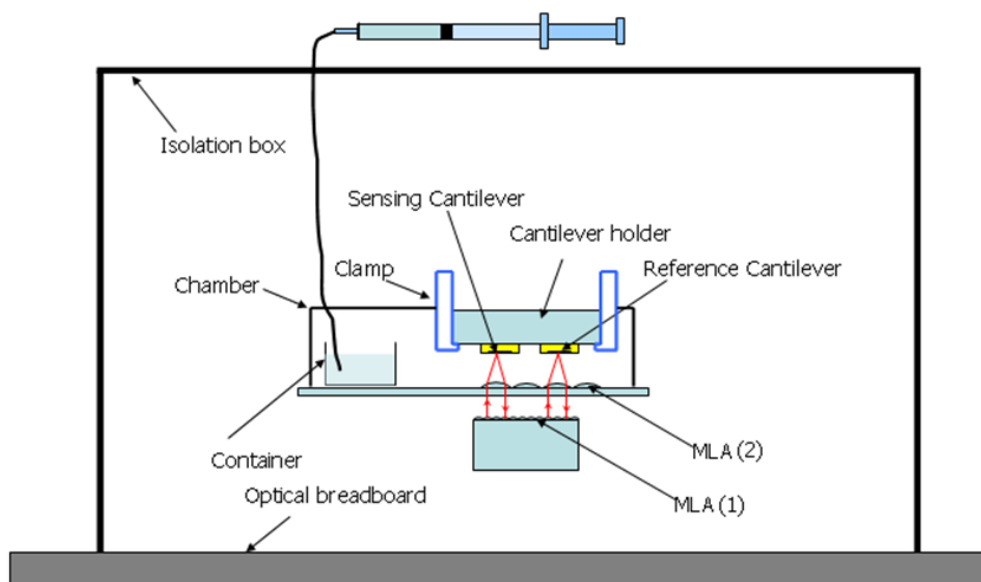
Figure 12 Illustration of experimental setup for alkanethiol self-assembled monolayers (SAMs) in ambient environment.

Surface stress changes associated with formation of alkanethiol SAM were measured in three steps. In the first step, sensing and reference cantilevers were mounted in the sensor and stability of the interferometer was first checked to ensure that measured signal is not affected by drift and ambient noise. In the second step, 20 mL of pure liquid octanethiol was injected into a beaker placed near the two cantilevers. The vapors of alkanethiol solutions were confined near the cantilevers and interferometer was utilized to measure the deflection of sensing cantilever associated with deposition and formation of alkanethiol SAMs. Intensities of the interfered beams as well as back reflection from the first couplers were delivered through photodetectors (D2, D3 and D1, respectively in Figures 4 (B) and 5 and monitored through a data acquisition system. Differential surface stress which is proportional to the cantilever deflection is then calculated by Stoney's Formula with obtained spring constant and geometry of the cantilever.

After the exposure to alkanethiol, both the sensing and reference cantilevers are expected to be fully covered with alkanethiol SAMs; therefore, reintroduction of alkanethiol vapors should not cause further differential bending of the cantilevers. In the last step, sensing and reference cantilevers were again exposed to alkanethiol vapors to ensure that measured surface stress change is associated with only alkanethiol formation.

4.1.3 Results and discussion

Experimental measurements of surface stress induced due to vapor phase deposition of alkanethiol during a typical run are plotted in Figures 13. Intensities of reflected and interfered beams monitored before introduction of alkanethiol vapor are plotted in Figure 13(A). Measured intensities are nearly constant and do not drift with time.
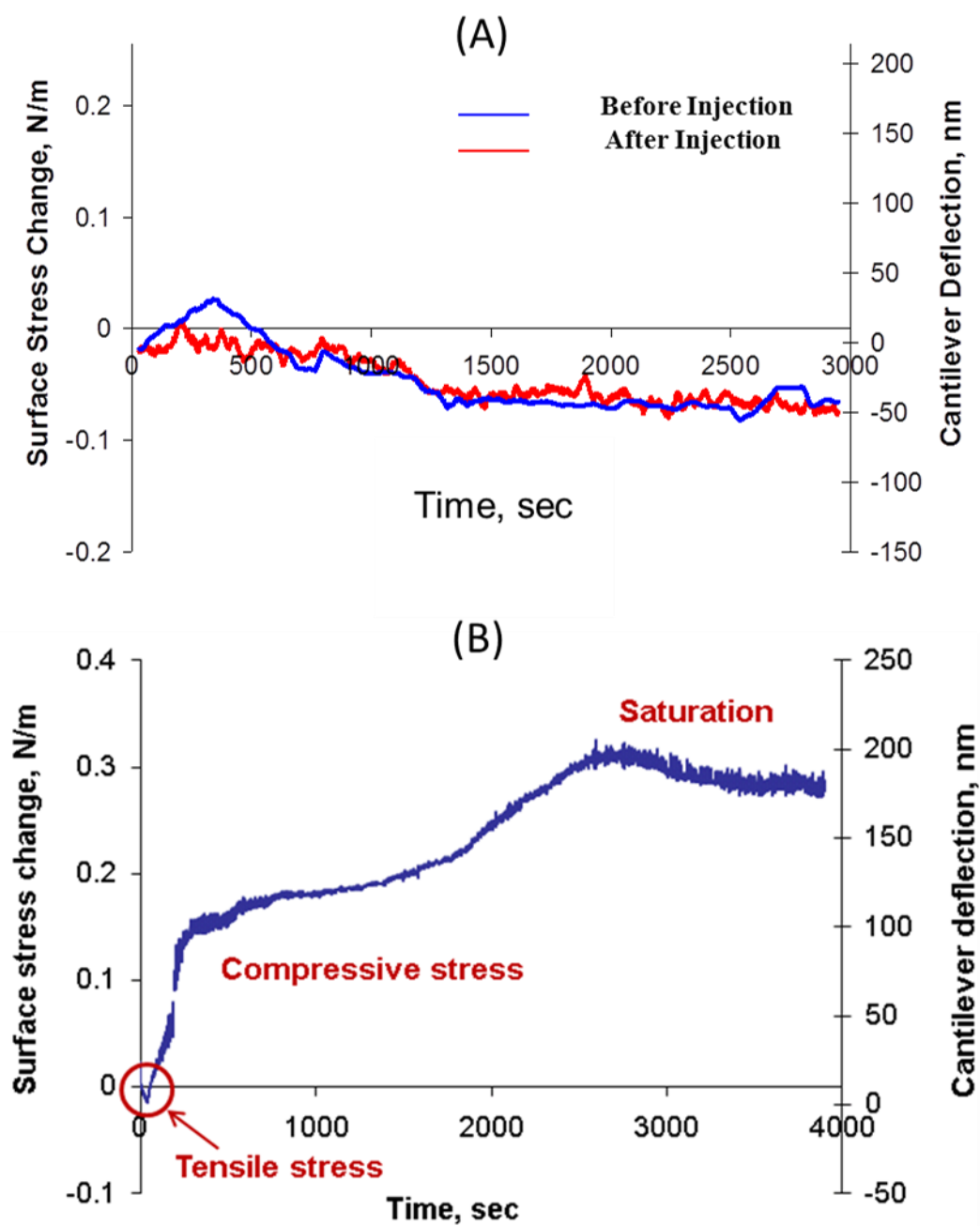
Figure 13 Surface stress change and the corresponding sensing cantilever deflection respect to reference cantilever (A) Intensity of interfered beams before deposition, and Intensity of interfered beams due to alkanethiol exposure after deposition. (B) Different surface stress during deposition.

All intensity measurements display some scatter, and it is most pronounced in the interference signals. The scatter may be the result of thermal noise, environmental vibrations or Fresnel reflections at the junctions between fiber optic cables. We are currently working on improving acoustic noise and vibration isolation of the system. All fiber optic junctions were filled with index matching gel to minimize Fresnel reflections. In the current state, the interference signal displays some noise but the signal to noise ratio is still quite large. Further work is in progress to improve the signal to noise ratio in the interference signal.

After the initial monitoring of interferometer stability, alkanethiol vapor was introduced near the cantilever and differential bending of the cantilevers was monitored to measure the surface stress change associated with formation of alkanethiol SAMs on gold coated reference cantilever. Measured surface stress is plotted as a function of time in Figure 13(B). Surface stress buildup starts after 15 minutes of introducing the solution. Surface stress rapidly builds up and reaches a stable value about 0.29 N/m with the corresponding cantilever deflection of 185 nm.

Godin et al. (Godin, Tabard-Cossa et al. 2001; Godin, Williams et al. 2004) reported that distance of cantilever to the location where alkanethiol droplets are introduced, condition of gold surface like cleanliness and roughness, and grain structure of the gold on the cantilever's surface affects the kinetics and magnitude of surface stress development. Among those conditions, the microstructure of gold film significantly influences the development of the surface stress during the formation of alkanethiol SAMs. They measured surface stress during alkanethiol SAM formation with lager grain sizes of gold and achieved surface stress of 0.51 ± 0.02 N/m and 15.9 ± 0.6 N/m at grain sizes of 90 ± 50 nm and 600 ± 400nm

respectively. The grain size of gold film used for our sensing platform was turned to be 40 ± 10 nm (Figure 10).

Magnitude of surface stress change and kinetics of SAM formation are also influenced by the distance between cantilever and the location where alkanethiol droplets are introduced. During the experiment, octanethiol droplet was introduced at a distance of about 5 mm from the cantilevers. The kinetics of SAM formation observed in the current experiments compare well with other reported measurements for alkanethiol vapor introduced at similar distances (Godin, Tabard-Cossa et al. 2001; Godin, Williams et al. 2004).

After the SAM formation on the sensing cantilever, sensor was again exposed to alkanethiol vapors. Intensity of the interfered beams measured during second exposure of alkanethiol is compared with interfered beams before deposition to check the specificity and plotted in Figure 13(A). As shown in the Figure 13(A), variations of the interfered beam intensities were within the system's normal noise range. A minimal surface stress change during re-introduction of the alkanethiol vapors indicates that both sensing and reference cantilever are covered with alkanethiol SAM. Furthermore, it indicates surface stress change observed during the first introduction is unambiguously associated with SAM formation on sensing cantilever.

4.1.4 Conclusions

A miniature sensor based a pair of microcantilevers, a sensing and reference cantilevers, was developed for differential surface stress measurement associated with formation of alkanethiol SAMs, which is a typical example of detection of chemical species.

High resolution interferometry was utilized to measure the differential surface stress developed due to absorption of chemical species on the sensing cantilever. Surface stress associated with alkanethiol formation on gold surface was measured to characterize the response of the sensor in ambient conditions. Sensitivity of the sensor measurement is not dependent on the distance between the sensing surface and detector; as a result, surface stress sensor is amenable for miniaturization and array of sensors would be easily fabricated on a single MEMS device.

4.2 Differential Surface Stress Sensor for Detection of DNA Hybridization

K. Kang, M. Nilsen-Hamilton, and P. Shrotriya

4.2.1 Introduction

Microcantilever based sensors are increasingly being investigated to detect the presence of chemical and biological species in both gas and liquid environments. Since Thundat et al. (Thundat, Warmack et al. 1994) reported the potential of AFM cantilevers in chemical and biological sensing components, cantilever based sensors have been demonstrated for alkanethiol self-assembled monolayers, proteins, antibodies and antigens, and nucleic acids (DNA/RNA) (Fritz, Baller et al. 2000; Wu, Datar et al. 2001; Godin, Williams et al. 2004; Savran, Knudsen et al. 2004; Bosch, Sanchez et al. 2007)).

Hybridization of single-stranded DNA (ssDNA) molecules with their complements becomes a fundamental platform in biomolecular recognitions. A monolayer of receptor molecules is functionalized on a sensing/reference cantilever. The reference cantilever is then hybridized with complementary molecules prior to an experiment to passivate for additional target ligands. The formation of molecular binding on the cantilever surface generates surface stress and this reaction results in a bending of the cantilever. Surface stress associated with complementary poly T to hybridize with immobilized poly A was investigated to demonstrate the sensor's performance. Dissociation constant (K_d) was obtained by

Isothermal titration calorimetry (ITC) measurements and provided to analyze linearity of the model.

4.2.2 Experiments

In order to achieve sensitive results, high aspect ratio tipless AFM cantilevers with nominal dimensions of 500 μm long, 100 μm wide, and 1 μm thick (Nanoworld, Switzerland) were selected. Cantilevers were coated with 5 nm of titanium and 30 nm of gold film. The thickness and spring constant of each cantilever for accurate surface stress measurements were determined by the AFM reference cantilever method (Chapter 3.2). Cantilevers with similar thickness were selected as a sensing and reference cantilever pair to eliminate the environmental disturbances. Microstructure and surface roughness of the gold film were also determined using contact mode AFM imaging shown in Figure 10. The surface stress change associated with hybridization of a surface immobilized 30 nt polydeoxyriboadenosine [poly A] with its complementary 30 nt polydeoxyribothymidine [poly T] was investigated to demonstrate the sensor performance. Oligonucleotides with the following sequences thiolated poly A: 5'-HS-$(CH_2)_6$-$(A)_{30}$-3' and poly T: $(T)_{30}$ were purchased from Integrated DNA Technologies (Coralville, Iowa) and stored at -20 °C prior to the experiments.

In preparation for the experiments, all cantilevers were cleaned by piranha solution (70% H_2SO_4 and 30% H_2O_2) for 30 minutes and rinsed in de-ionized water and dried in the gentle N_2 flow. Thiol-modified $(dA)_{30}$ was boiled and placed immediately on ice. Only selected portion of thiolated poly A was then reheated till 60 °C to cleave any disulfide bonds and mixed with the binding buffer (50 mM triethylammonium acetate buffer containing 25%

ethanol, pH 7.4) to ensure that the poly A is only immobilized on the gold-coated surfaces. A pair of cantilevers was then immersed into the solution containing 20 μM thiolated $(dA)_{30}$ dissolved into 7.4 pH binding buffer to functionalize cantilevers. After four hours of incubating in thiolated poly A solution, cantilevers were again cleaned and dried by DI water and N_2 stream several times. One of incubated cantilevers was then saved as a sensing cantilever in the refrigerator at 4 °C while the other cantilever was used as a reference cantilever by hybridizing poly T strands adsorbed on reference cantilever. In order to accomplish the hybridization, $(dT)_{30}$ strands were prepared following the same procedure as poly A and equilibrated in the 7.4 pH hybridization buffer. The reference cantilever was incubated for four hours in poly T solution of 20 μM concentration.
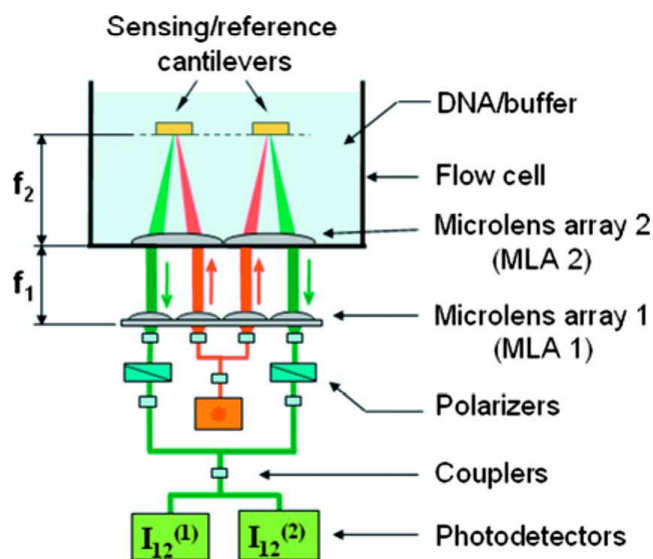
Figure 14 Optical circuit of differential surface stress sensor. MLA1 collimates beams and delivers to MLA2. Bidirectional couplers were used to split the reflected beams and direct one component toward photodetectors to measure the intensities of interfered beams.

Three different experiments were carried out to demonstrate the sensitivity and the specificity of the sensor. In the first experiment, the sensing and reference cantilevers were mounted in the sensor realization shown in Figure 14, and the changes in phase difference between the reflected beams were monitored to determine the differential surface stress development. The two cantilevers were submerged in hybridization buffer and measured the surface stress developments due to hybridization on the sensing cantilever at the final concentration of 0.1 to 1.0 μM of complementary poly T. In the second experiment, only the hybridization buffer alone (No nucleotide) was introduced into the sensor flow cell to determine the influence of environmental effects on sensor performance. A 0.5 μM concentration of noncomplementary 30-mer poly A in hybridization buffer was introduced to measure the surface stress due to nonspecific physisorption of molecules on the cantilever surface or nonspecific binding to receptor molecules.

In the last experiment, influence of temperature on molecular activity while forming base pairing between Adenine and Thymine though hydrogen bonds was investigated. We thawed two different treatments on complementary strands. One was melted at annealing temperature, 60 ºC, and the other was thawed in room temperature but no further treatment. We carried out surface stress measurements during DNA hybridization of ssDNA stands with these two differently treated complementary strands.

Hybridization buffer (20 mL of 20× SSPE (4×), 0.2 M NaCl, 7g SDS (7%), 40 mL Formamide (40%), 0.1 mL NP40 (0.1%), Fill to 100 mL with DEPC H_2O) was initially filled in the flow cell while aligning procedures and exact amount of complementary $(dT)_{30}$ at 7.4 pH was introduced for hybridization to achieve final concentrations.

4.2.3 Results and discussion

After turning on the laser, it requires 10 to 15 minutes for interfered signals to stabilize. Intensity of interfered beams and phase difference were monitored before introducing target molecules to confirm that phase difference (φ) does not drift with time.

A representative profile of surface stress development formed during hybridization reaction is plotted in Figure 15 for injection of 0.1 µM poly T concentration. For this case, largest surface stress change was observed in 5 minutes after injecting complementary target molecules with total volume of 480 µL in the fluid cell. It is important to note that the response time of the cantilever was found to be dependent on the volume of solution in the flow cell. It showed that the surface stress upon DNA hybridization is reliant on the concentration of complementary strands. We also observed that a change of salt concentration in hybridization buffer from 1.0 M to 0.2 mM does not affect the saturation values in surface stress measurements which remained within the normal noise level of ± 3 mN/m.

Following results are consistent with others that surface stress changes induced by DNA hybridization are found to be in the range of 5 to 50 mN/m for oligonucleotides of similar lengths (Fritz, Baller et al. 2000; Alvarez, Carrascosa et al. 2004; Min Yue 2004; Biswal, Raorane et al. 2006). This range is typically 10 to 100 times smaller than surface stress generation during formation of alkanethiol SAMs on gold surfaces.
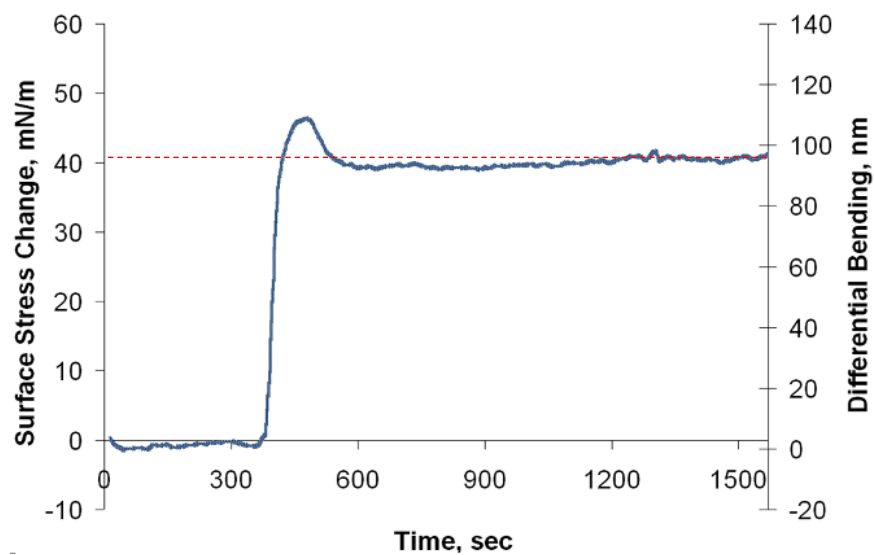
Figure 15 The profile of surface stress development during DNA hybridization at complementary (dT)$_{30}$ at concentration of 0.1 μM
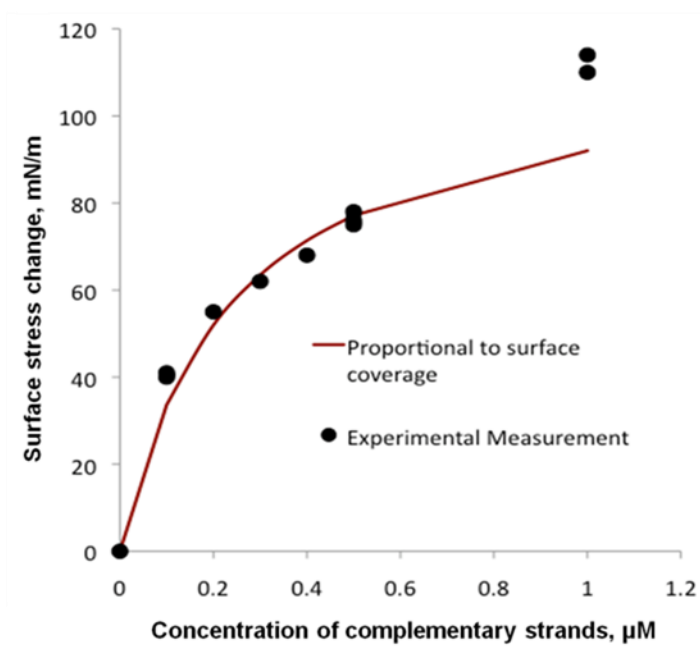
Figure 16 Analytical modeling with experimental data obtained by DNA hybridization of complementary (dT)$_{30}$. Solid red line represents proportion of surface coverage of DNA hybridization.

The equilibrium reaction and the corresponding dissociation constant (K_d) are expressed in Equations (8) through (11).

$$\text{Receptor} + \text{Ligand} \rightleftharpoons \text{Affinity complex}$$

$$\text{Or,} \quad A + B \rightleftharpoons AB \tag{8}$$
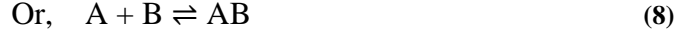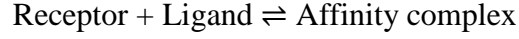
where A and B are concentrations of receptor and ligand, and AB is the concentration of affinity complex of receptor/ligand. The reaction is in equilibrium when the rates of forward and backward reactions are balanced. Therefore, the balance meets when forward reaction ($rate_{\rightarrow}$) is equal to backward rate ($rate_{\leftarrow}$).

$$rate_{\rightarrow} = K_f[A][B] \tag{9}$$

$$rate_{\leftarrow} = K_b[AB] \tag{10}$$

$$K_d = \frac{K_b}{K_f} = \frac{[A][B]}{[AB]} \tag{11}$$

Here, K_d is the dissociation constant and has molar units (M). K_f and K_b are the rate constants for forward and backward reactions respectively. Equation (8) is then developed to Langmuir isotherm (Langmuir 1919). Langmuir isotherm leads to readily derivable expressions for the coverage or adsorption of molecules on a solid surface.

$$\theta = \frac{K_d \cdot \rho}{1 + K_d \cdot \rho} \tag{12}$$

$$\text{or,} \quad \theta = K_d(1 - \theta)\rho \tag{13}$$

where θ is fractional coverage on the surface and ρ is the concentration; K_d is again the dissociation constant. Since surface stress change ($\Delta\sigma$) is greatly dependent on the surface coverage, Equation (13) can be one step further developed.

$$\Delta\sigma = \theta \cdot C = \frac{K_d \cdot \rho}{1 + K_d \cdot \rho} \cdot C$$

(14)

The dissociation constant was measured by ITC (Isothermal Titration Calorimetry) and turned to be 240 nM for hybridization of complementary poly T with immobilized poly A. Surface coverage and measured surface stress would be inputs for identifying mechanism governing surface stress generation. It is a reversible reaction as we derived Equations (8-14), and we used the saturated values for surface stress measurements in equilibrium reaction.
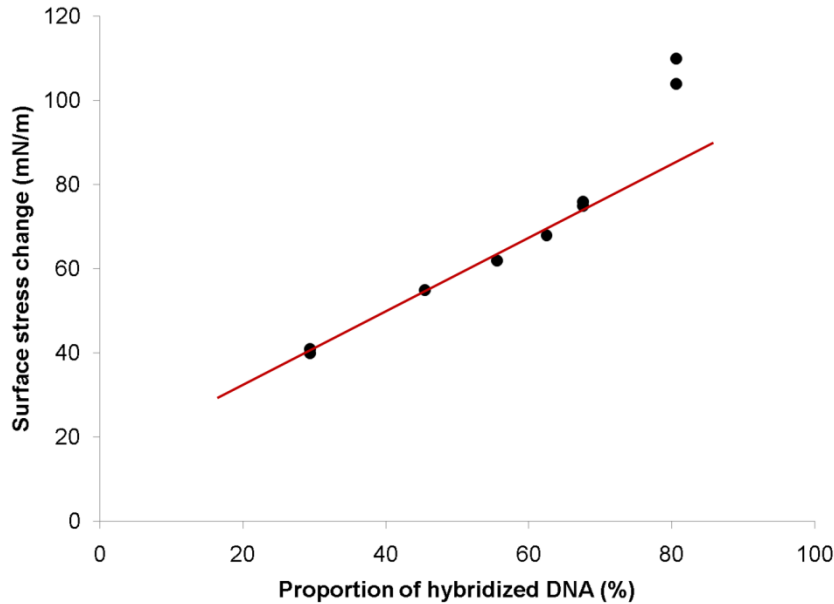
Figure 17 Surface stress changes as a function of normalized separation of complementary poly T to hybridize with immobilized poly A.

Changes in surface stress are significantly influenced by molecular interactions between hybridized chains; consequently, the distance between immobilized or hybridized chains may be a leading contribution for surface stress development. ssDNAs are immobilized on the gold surface as hexagonal closed packing for binding to fraction of

complementary poly T (Hagan, Majumdar et al. 2002). The separation distance for immobilized ssDNAs on gold substrate was turned to be 8 nm (Chapter 5.4).
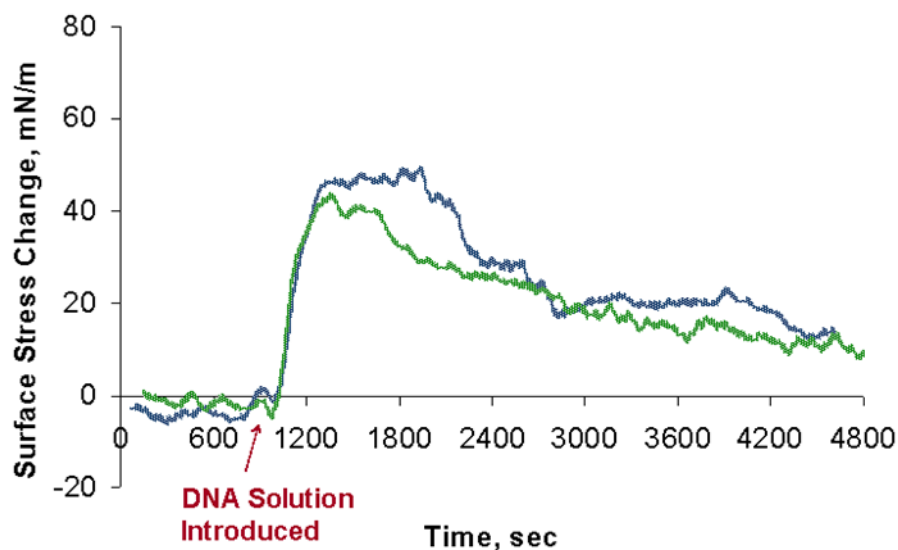
Figure 18 Profiles of surface stress measurements with noncomplementary poly A

Also, experiments with the use of noncomplementary $(dA)_{30}$ were carried out for the analysis of specification in the hybridization buffer. Since complementary strands have been already hybridized with immobilized receptors on sensing and reference cantilevers, no further cantilever deflection is expected after injection of noncomplementary poly A strands. Two results were obtained by introducing 0.5 µM of noncomplementary poly A and shown in Figure 18. The profiles show that surface stresses measurements had peaks to about 45 mN/m but they eventually saturated to the normal noise level after a long period (order of 60-90 minutes). The initial peak and subsequent decay may be due to different rates of physisorption between silicon or gold surface, charge transduction, or reversed-Hoogsteen T·AT triplex formation on the reference cantilever. It could also be sampling interactions

involving reverse Hoogsteen or other configurations between the poly A chains on sensing

cantilever (Uddin, Piunno et al. 1997; Wu, Ji et al. 2001; Cheng, Cuda et al. 2006).
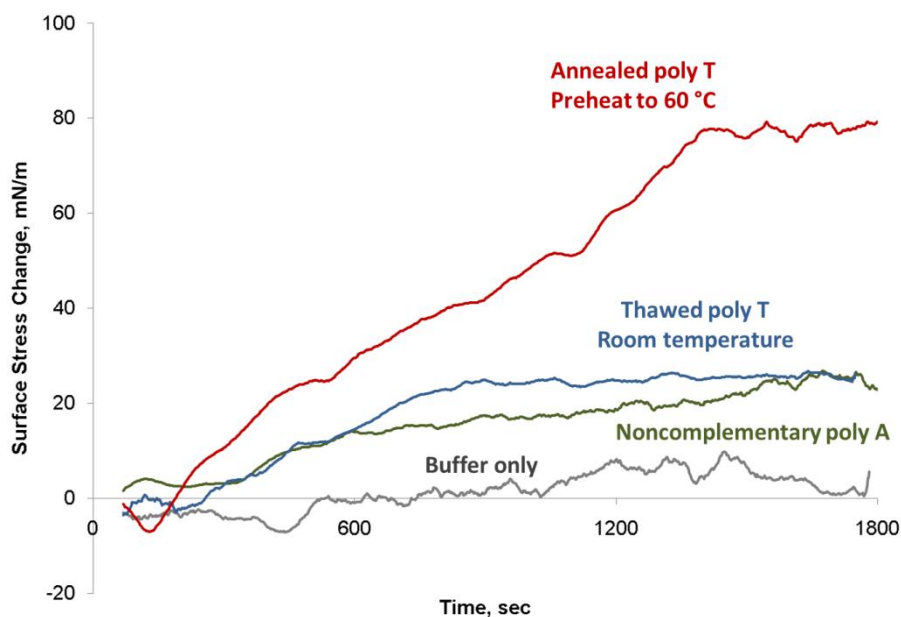
Figure 19 Comparison of surface stress measurements between annealed and non-anneal complementary ssDNAs (30-mer Poly T)

Two different treatments were applied to complementary DNA strands: melting in room temperature without a further treatment and melting at annealing temperature at 60 °C, simply named non-annealed and annealed complementary DNA strands respectively. With an injection of non-annealed complementary DNA strands in a final concentration of 0.5 μM, surface stress change was saturated at 35 mN/m shown in figure 19. It is approximately half compared to that obtained by annealed complementary $(dT)_{30}$. The experimental results show that thawed DNA strands were not able to achieve similar level of binding as the annealed DNA strands. This may be due to stacking or "crystallization" of single stranded DNA in thawed solution. Another interesting observation is that magnitude of the final stress change

observed in "thawed poly T" experiments is comparable to initial peaks observed in noncomplementary experiments discussed above. However, "non-annealed poly T" experiments showed that the final saturation of surface stress measurement was stable for a long duration of time.

4.2.4 Conclusions

A novel differential surface stress sensor is used to measure surface stress changes associated with 30-mer complementary poly T to hybridize with surface immobilized ssDNA receptors (30-mer poly A). Experimental results indicate that surface stress changes develop on exposure to complimentary DNA strands. Varying the poly T concentration from 0.1 to 0.5 μM results in a linear increase of the surface stress changes from 40 to 78 mN/m during DNA hybridization. However, it showed a non-linear behavior when the concentration of complementary poly T is beyond 0.5 μM.

In order to verify the specification of the sensing system, surface stress changes during hybridization of noncomplementary DNA strands were obtained. The results showed a sharp peak, which repeatedly appeared in the experiments with complementary DNA strands, was observed as soon as injection of noncomplementary DNA strands but it decayed and saturated to (nearly) no surface stress value.

Compressive surface stress is hypothesized to occur due to binding of negatively charged complimentary strands and corresponding increase in negative charges on the surface and consequently greater repulsion between the bound surfaces species (Fritz, Baller et al. 2000). The tensile surface stress change during hybridization is attributed to reduction in steric hindrances between single-stranded DNAs (ssDNAs) due to transformation from a

flexible single strand random coil to stiff hybridized double-stranded DNA (Wu, Ji et al. 2001). In the current experiments, the initial tensile stress change may be due to the reduction in steric hindrances but as the hybridization of DNA continues, the Coulombic repulsion between the surface bound chains leads to the development of compressive surface stress.

Surface stress measurements associated with DNA hybridization clearly demonstrate the unique advantages of the differential surface stress sensor. Measurement of differential bending of sensing cantilever with respect to reference cantilever ensures that sensor response is independent of environmental disturbances. Sensitivity of sensor measurement is not dependent on distance between the sensing surface and detector, as a result, surface stress sensor is amenable for miniaturization and array of sensors can be integrated with other systems on a single MEMS device.

4.3 Aptamer Functionalized Microcantilever Sensors for Cocaine Detection

A paper to be submitted to Langmuir

Kyungho Kang, Ashish Sachan, Marit Nilsen-Hamilton, and Pranav Shrotriya

4.3.1 Introduction

A cocaine-specific aptamer was used as a receptor molecule in a microcantilever based surface stress sensor for detection of cocaine molecules. The response of microcantilever for cocaine detection relies on resolving surface stress change associated with formation of affinity complexes between aptamer and cocaine molecules on the sensing surface. A novel interferometric technique was utilized to measure the surface stress induced bending of a sensing cantilever respect to a reference cantilever (Chapter 3). The principle of surface stress measurement is schematically presented in Figure 20. Cocaine aptamer introduced by Stojanovic molecules (Stojanovic, de Prada et al. 2001) is illustrated in Figure 3.
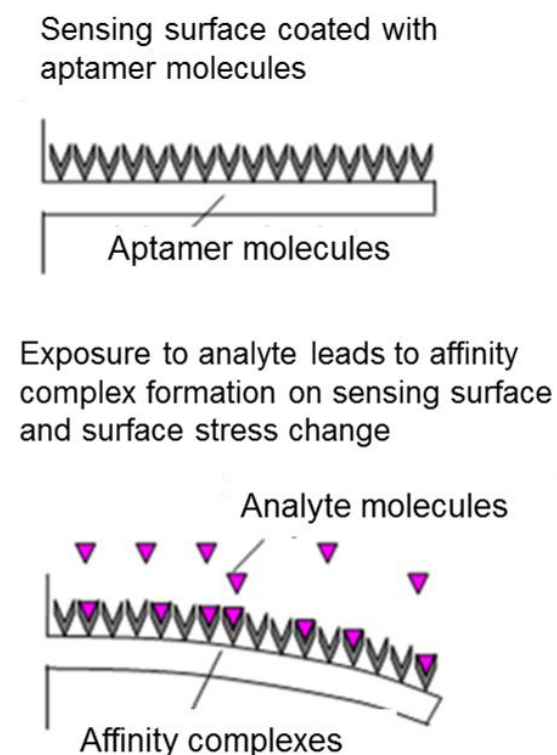
Figure 20 Schematic representation of the sensing strategy for cocaine detection

4.3.2 Experiments

Cocaine aptamers with the sequence of 5'- GAC AAG GAA AAT CCT TCA ATG AAG TGG GTC -3' were purchased from Integrated DNA Technologies (IDT), (Coralville, Iowa). Affinity complexes between aptamers and cocaine as target ligands were measured by isothermal titration calorimetry (ITC) in PBS (20 mM Tris.HCl, pH 7.4, 140 mM NaCl and 5 mM KCl). Cocaine samples dissolved in acetonitrile were purchased from Sigma Aldrich (St. Louis, Missouri). As received, the cocaine samples were diluted in deionized water and vaporized in the vacuumed centrifuge in order to achieve desired concentration of acetonitrile in the solution.

Isothermal titration calorimetry (ITC) experiments were performed using a VP-ITC isothermal titration calorimeter (Microcal, Inc., Northhampton, MA). In each experiment, 600 μM cocaine was titrated using the computer controlled syringe into the sample cell (1.43 mL) containing 20 μM cocaine aptamer at 25 ℃. Both aptamer and cocaine were dissolved in PBS in the presence of various concentrations of acetonitrile. Before each titration the oligonucleotide was heated to 92 °C for 5 minutes in the titration buffer and then cooled to room temperature for 60 minutes. The syringe was set at a stirring speed of 310 rpm. After a 60 seconds initial delay each titration involved an initial 1 μL injection followed by 25 serial injections of 12 μL each at intervals of 300 seconds. The raw data obtained in each experiment was corrected for the effect of titrating cocaine from the syringe the sample cell containing the buffer and various concentrations of acetonitrile but no aptamer. The thermodynamic parameters were calculated using a one-site binding model in the software (Origin 5.0) provided by Microcal (Microcal, Inc).

For surface stress measurements, sensing and reference cantilevers were coated respectively with the cocaine aptamer and a control DNA consisting of the bases as the cocaine aptamer but with their sequence scrambled. Thiol-modified cocaine aptamers and control DNA were purchased from IDT (Coralville, Iowa). Gold-coated microcantilevers with the nominal dimension of 500 μm length, 100 μm width and 1 μm thickness were purchased from Nanoandmore.com (Lady's Island, South Carolina). Microcantilevers were cleaned by the Piranha solution (70% H_2SO_4 and 30% H_2O_2) for 30 minutes, rinsed in deionized water and dried in the gentle N_2 flow. Thiol-modified DNA aptamers were heated till 60 °C to cleave any disulfide bonds and mixed with the saline sodium citrate buffer (20 × SSC), pH 7.4) to obtain a 0.5 μM aptamer solution. Cleaned microcantilevers were immersed

in the aptamer solution for three hours in order to immobilize the thiol-modified DNAs on the gold-coated surface. Functionalized microcantilevers were immersed in 6-mercapto-1-hexanol solution (3 mM concentration) for one hour to displace any adsorbed DNA.

The functionalized sensing and reference cantilevers were mounted in the differential surface stress sensor and exposed to various concentrations of cocaine from 25 to 500 μM in PBS to determine the sensor response as a function of the cocaine concentration. After the sensing experiments, the sensing and reference cantilevers were heated in deionized water at 80 °C to regenerate the aptamer sequence. The regeneration allows the sensing cantilevers to be used a number of times (Baker, Lai et al. 2006) and each cantilevers was used for at least three sensing experiments.

4.3.3 Results and discussion

Isothermal titration calorimetry tests were used to determine the affinity between cocaine molecules and the DNA aptamer. A representative result is plotted in Figure 21. We found that the aptamer's binding affinity is highly sensitive to the presence of acetonitrile, which is the solvent of available cocaine standard solutions (Figure 21 (B)). The dissociation constant (K_d) of the currently available cocaine aptamers was between 11 and 22 μM for very low or minimal acetonitrile concentration as shown in Figure 21 (B), but for concentrations of acetonitrile above 3 μM the dissociation constant rises to greater than 200 μM. This observation probably explains why the aptamer has been reported to have a large range of affinities (Neves, Reinstein et al.; Stojanovic, de Prada et al. 2001; White, Phares et al. 2008).
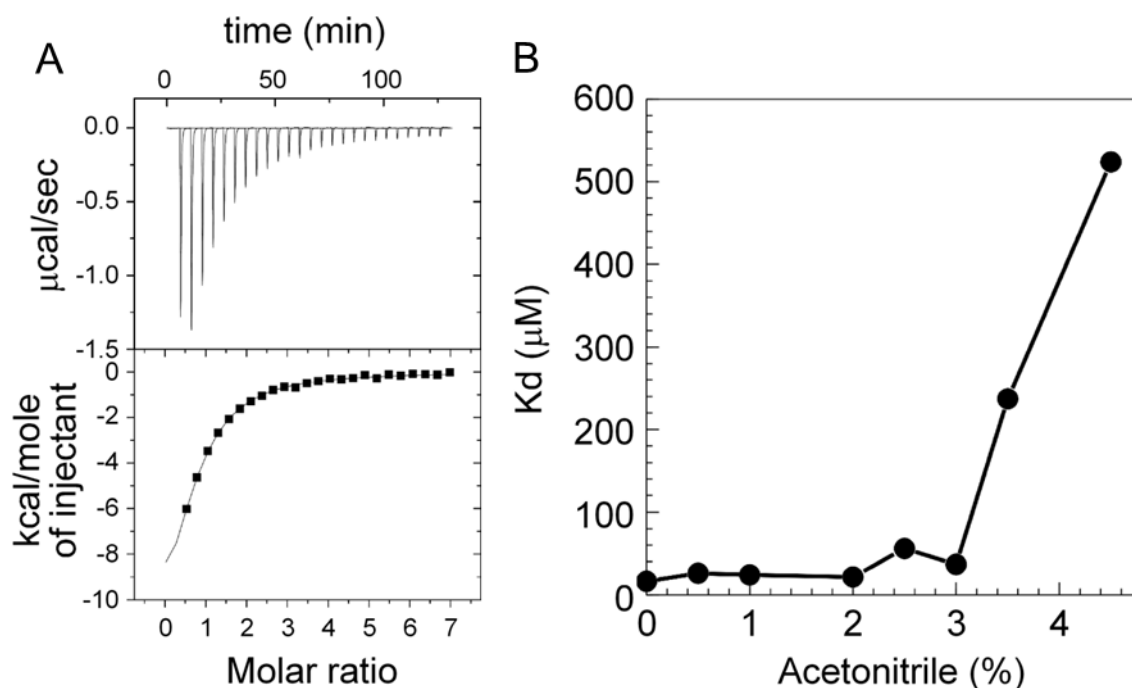
Figure 21 Isothermal titration calorimetry (ITC) was performed to determine the equilibrium constants for the cocaine aptamer: A) Kd of the cocaine aptamer for cocaine in the presence as a function of acetonitrile concentration; B) Representative ITC data shown in this figure gave a Kd = 11 μM

Differential surface stress developed on the functionalized cantilevers was measured as a function of cocaine concentrations in PBS. Sensor response was measured for 10 different cocaine concentrations − 0 μM (pure buffer), 25, 50, 75, 100, 150, 200, 300, 400, 500 μM. At each concentration, the sensing experiments were repeated three times at least to assess the repeatability of the experimental measurement. Two typical experimental observations of surface stress development during direct sensing corresponding to a cocaine concentration of 50 μM and pure buffer are plotted in Figure 22. As shown in the Figure 22, the surface stress starts developing as soon as the cocaine solution is injected in the sensor and saturates to a constant value after a period of approximately 20 minutes. For PBS alone,

there is no surface stress buildup indicating the specificity of sensor response to cocaine solution.
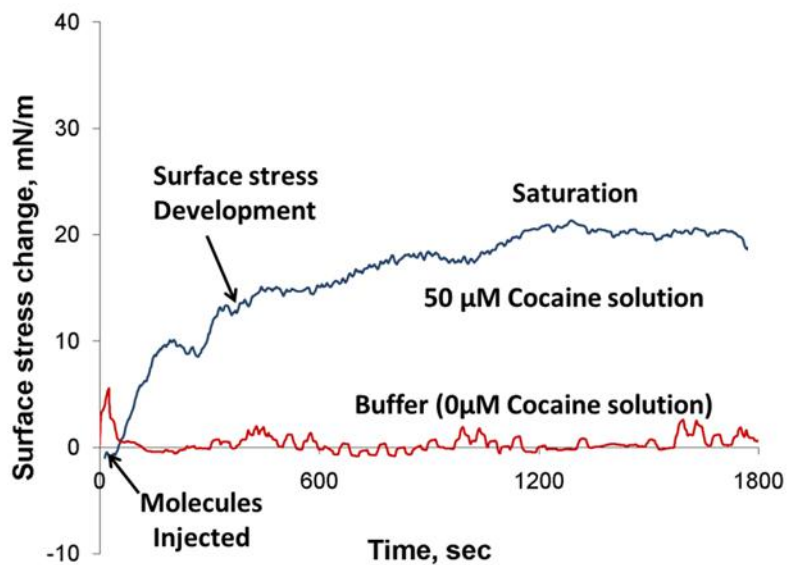
Figure 22 Surface stress developments during direct sensing for 0 and 50 μM cocaine

The saturated surface stress values were recorded for each sensing experiment and are plotted as a function of cocaine concentration in Figure 23, which also shows a Langmuir isotherm fit for the experimental data. Sensitivity of the surface stress measurements was determined to be 25 mN/m based on the surface stress response measured in the absence of cocaine. Based on the sensitivity assumption and fit for the experimental data, the lowest detectable threshold for the cocaine concentration is estimated to be 5 μM.
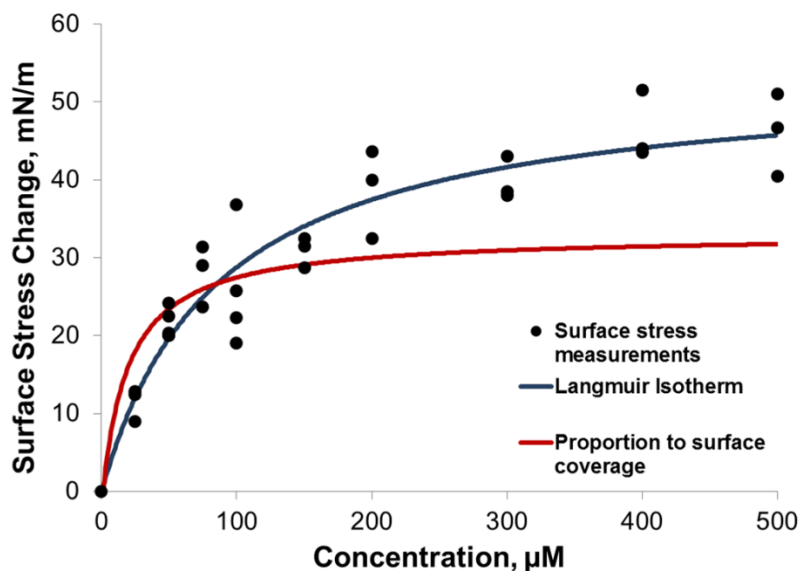
Figure 23 Saturated surface stress values as a function of cocaine concentrations. A curve fitting with Langmuir isotherm along the experimental data is compared with a fit calculated by Kd of 22 μM, which was measured by ITC.

In order to understand the relationship between aptamer-cocaine binding and surface stress development, the dissociation constant measured by ITC was used to estimate the surface coverage of cocaine-aptamer complexes for each cocaine concentration.

$$\theta = \frac{C \cdot K_d}{1 + K_d}$$

(**15**)

Where θ is surface coverage of cocaine aptamer on sensing cantilever, C is the cocaine concentrations. A K_d of 20 μM was utilized to estimate the fraction of initial aptamer molecules that form the cocaine aptamer complexes. Measured surface stress changes (Δσ) were assumed to be directly proportional to coverage of cocaine-aptamer complexes.

$$\Delta\sigma = k \cdot \theta$$

(**16**)

The fit measured surface stress under this assumption is plotted in Figure 23. The proportionality assumption accurately describes the measured surface stress values at cocaine concentrations up to 100 µM (marked as linear regime in the curve) but the measured values continued to increase as the cocaine concentrations increased beyond 100 µM, whereas the predicted values, based on the surface coverage remained nearly constant (indicated as the non-linear regime).
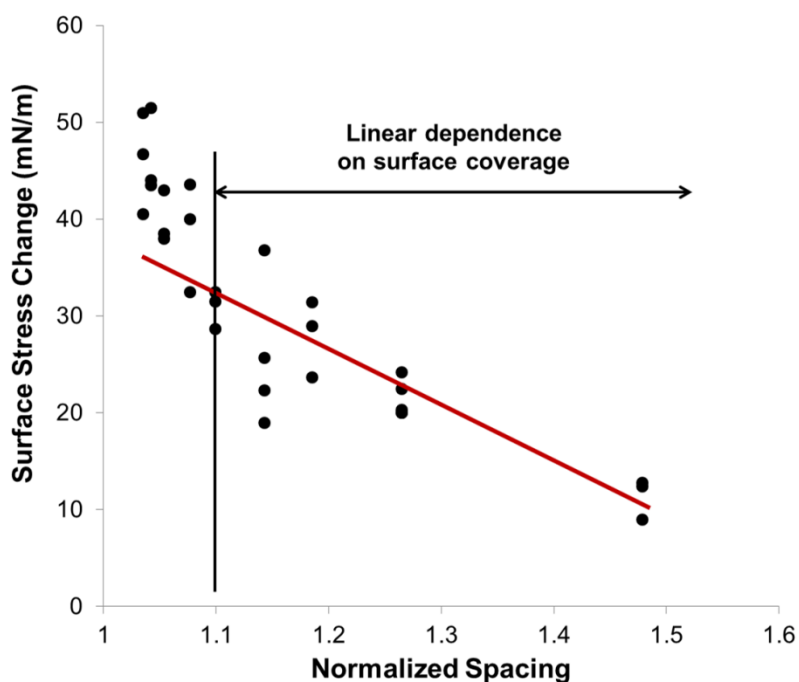
Figure 24 Normalized separation between cocaine-aptamer complexes

The fraction of cocaine/aptamer complex can also be used to estimate the average normalized spacing between cocaine/aptamer complexes on the surface.

$$\frac{a}{a_0} = \frac{1}{\theta}$$

(17)

Where *a* is approximate spacing between aptamer/cocaine complexes, and a_0 is the initial space of cocaine aptamers. The measured surface stress is plotted as a function of the calculated normalized separation between the aptamer-cocaine complexes in Figure 24. As indicated on the plot, the surface stress developed is proportional to coverage of the cocaine-aptamer complexes when the aptamer complexes are spaced at distance larger than 1.1 times the initial separation between the immobilized aptamers. As the cocaine-aptamer complex separation becomes smaller than 1.1 times the immobilized aptamer separation, the developed surface stress is no longer proportion to estimated surface coverage. This transition may be due to the nature of intermolecular repulsion between the cocaine-aptamer complexes. The data presented here can be utilized to estimate the functional form of the interchain repulsion between the cocaine-aptamer complexes and also to determine the mechanism underlying the surface stress generation.

4.3.4 Conclusions

In this study, the existing cocaine aptamer was tested by ITC to determine its affinity for cocaine. From these studies we found that acetonitrile, the common solvent for cocaine standards, causes a significant decrease in affinity of the aptamer for cocaine. By maintaining the acetonitrile concentration below 2 % we realize a 5-fold increase in sensitivity of the aptamer compared with published data and with results from our own studies.

Experimental results presented here have demonstrated a proof-of-concept for cocaine detection with aptamer-functionalized microcantilevers at very low cocaine concentrations. The surface stress generated due to binding of cocaine molecules to the existing cocaine aptamer was determined. As reported above, the binding of cocaine

aptamer/cocaine molecules was found to be dependent on the acetonitrile concentration. Therefore all solutions for the sensing experiments were prepared to ensure that acetonitrile concentration was below 2%. Surface stress changes from 9 to 51 mN/m were measured for the range of cocaine concentrations of 25 μM to 500 μM. The sensor is able to detect cocaine with the lowest detectable concentration down to 5 μM (1.5 μg/mL) at room temperature. The aptamer functionalized cantilever could be regenerated after each sensing experiment and demonstrated not to change in sensitivity and specificity on subsequent experiments. The experimental data also showed that the surface stress generated during the sensing experiments is not directly proportional to the surface coverage of aptamer/cocaine complexes.

CHAPTER 5. DOUBLE-THIOLATED SINGLE-STRANDED DNA FOR HIGHER THRESHOLD SENSITIVITY UPON DNA HYBRIDIZATION

A paper to be submitted to Langmuir

Kyungho Kang, Marit Nilsen-Hamilton, and Pranav Shrotriya

5.1 Abstract

Microcantilever based sensors can be used for quantitative analysis of the nanomechanical response associated with conformational change and the corresponding charge transduction during molecular interaction. A specific binding of complementary 30-mer Thymine (poly T) with surface immobilized single-stranded 30-mer Adenine (poly A) produces a differential bending of a pair of microcantilevers. These microcantilevers transduce these molecular interactions into a quantitative nanomechanical response expressed as surface stress changes. Modifying the immobilization of ssDNA strands from one end attached to both ends attached drives in larger surface deformation during hybridization. This larger deformation leads to reduce sensitivity as low as two orders of magnitude in the detection limit compared with a system operated by single-thiolated ssDNAs with the same experimental procedures.

5.2 Introduction

Microcantilevers functionalized with chemical or biological species transduce specific binding into nanomechanical responses. Due to sensitivity and versatility of microcantilevers, they play an important role in molecular recognitions and have served as

biosensors for detections of DNA, glucose, liposomes, antibody/antigen, proteins, and aptamers (Niemeyer 2007; Waggoner and Craighead 2007).

Berger et al. (Berger, Delamarche et al. 1997) and Godin et al. (Godin, Williams et al. 2004; Godin, Tabard-Cossa et al. 2010) measured quantitative data on surface stress changes during formation of self-assembly of alkanethiol on gold surface. In these reports, they found kinetics of forming self-assembled monolayers on gold and effects of surface coverage and grain size of gold. Particularly, they discovered that surface stress changes during adsorption of alkanethiol on the sensing surface are up to 2-4 orders of magnitude larger than those from intermolecular interactions. They, thus, provided the potential of microcantilever sensors for chemical and biomolecular recognitions (Godin, Tabard-Cossa et al. 2001; Godin, Williams et al. 2004; Godin, Tabard-Cossa et al. 2010). In 2001, Fritz et al. (Fritz, Baller et al. 2000) performed direct translation of DNA hybridization and receptor-ligand binding into nanomechanical response through a microcantilever sensor. They opened a possibility for microcantilever sensors to use of biomolecular recognitions.

There have been many attempts to increase sensitivity of the sensing platform. Mertens et al. (Mertens, Rogero et al. 2008) found when self-assembled monolayer of ssDNAs interacts with complementary ssDNAs, hydration influences significantly on surface stress developments. They controlled humidity and measured the hydration-induced surface stress of ssDNAs and hybridization with the complementary ssDNAs in a humidity chamber. They showed that sensitivity increase of three orders of magnitude compared to the similar size of cantilever can be achieved although it required relatively longer sensing time between 1 to 3 hours.

Weizmann et al. (Weizmann, Patolsky et al. 2004) introduced the magneto-mechanical detection method for single base mismatch between two DNA sequences. ssDNAs functionalized on the gold surface of a cantilever are conjugated with complementary molecules immobilized on magnetic beads. The external magnetic field provided the deflection of the cantilever by the means of amplified magneto-mechanical detection when the biorecognition event is occurred. This method could detect large bending response from extremely diluted biological samples through the preamplified labeling of the magnetic particles.

Pei et al. (Pei, Lu et al. 2010) designed a 3D DNA tetrahedron structure assembled from one vertex (80-nt probe-containing DNA fragments) and three thiol groups (55-nt DNA fragments) conjugated on sensing surface. They argued that the pyramidal DNA structures have a strong affinity with Au surface because the three thiols on the base enhance rigidity and stability of the structure. They reported that a sensor with TSPs (tetrahedron-structured probes)-based platform is able to achieve detection limit of 1 pM when measuring electrochemical signals during hybridization of an avidin-HRP (horseradish peroxidase) with the biotin. Thrombin detection was also carried out in the same experimental setup and achieved the threshold sensitivity as low as 100 pM.

Janice et al. (Marquardt 2008) conducted a microcontact printing of 30-nt poly A on a gold substrate and hybridization of 30-nt poly A with 30-nt poly T. The atomic force microscope (AFM) height measurements showed that the immobilized poly A and hybridized double-stranded DNA (dsDNA) were turned to be 1.68 and 1.59 nm respectively with 95 % confidence. They concluded that complexes affinity of poly A and T does not affect height difference. Although no major difference in height between the single and double-stranded

DNA, complementary DNA strands may build structures lying down rather than vertically standing up (Marquardt 2008).

Cantilevers for alkanethiol self-assembled monolayers (SAMs) and DNA hybridization were predicted to undergo bending down to the direction for compressive stress (in Chapter 2.4). Esplandiu et al. (Erlandsson, McClelland et al. 1988) investigated mechanism governing by SAMs of 1,8-octanedithiol on gold in acidic and alkaline electrolytes. They found that compact monolayers with an upright molecular configuration were formed. Compared with the results of 1-octanethiol SAMs, the dithiol monolayers showed a higher stability as deduced from reduction peak potentials and capacitance values (Erlandsson, McClelland et al. 1988).
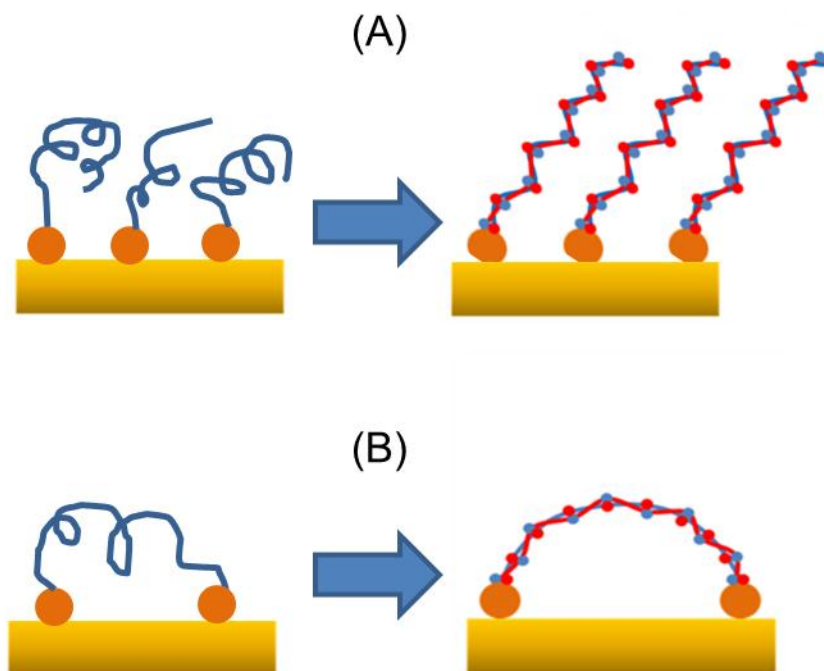
Figure 25 A simplified description of double-thiolated poly A hybridized with the complementary poly T. One end is attached on the gold surface (A), thiols on poly As are immobilized on gold surface through thiol/Au bond (B)

Surface stress induced due to biological binding is driven by changing in intra-molecular interaction during complex formation. This low magnitude of mechanical deformation limits the sensitivity for detection associated with target ligands. In order to overcome this limitation, we investigated the influence of receptor molecules immobilized on sensing surface. We modified the receptor immobilization to ensure that both 5'and 3' ends of a single-stranded DNA (ssDNA) are modified with thiols, and these thiol-modified ssDNAs are immobilized on the sensitized surface of the cantilever. The surface density of receptor molecules was found to be the same with the single-thiolated ssDNA through the fluorescence measurement. The immobilized space is larger enough to prevent intra-molecular reaction between chains. When hybridizing with complementary ssDNAs, the surface immobilized strands undergo twisting and changing in stiffness as well as configurational change from a string to a rod. This change of strings produce higher surface stress in the system and eventually the threshold sensitivity would be lower.

5.3 Experiments

The double-thiolated poly A (The sequence of 5'-/5ThioMC6-D/AAAAA AAAAA AAAAA AAAAA AAAAA AAAAA/3ThioMC3-D/-3') was purchased from Integrated DNA Technologies (Coralvillle, IA) and stored in -20 °C. Cantilevers were cleaned by piranha solution (70% H_2SO_4 and 30% H_2O_2) for 30 minutes and washed by DI water several times. 20 μM double-thiolated poly A in binding buffer (50 mM triethylammonium acetate buffer containing 25% ethanol, pH 7.4) was used to immobilize monolayers of double-thiolated ssDNAs on the gold surface of cantilevers at room temperature for 3 hours. Again cantilevers were cautiously cleaned by DI water and dried in gentle N_2 stream. A sensing

cantilever was further incubated in 3 mM of 6-mercapto-1-hexanol solution for one hour to displace any adsorbed DNA. One cantilever was selected for a reference cantilever and hybridized with complementary target molecules (30-mer poly T as the sequence of 5'-TTTTT TTTTT TTTTT TTTTT TTTTT TTTTT-3') that make insensitive with additional complementary poly T strands.

Grafting density was investigated by fluorescence techniques (Demers, Mirkin et al. 2000). In brief, fluorescein tagged single-thiolated and double-thiolated poly A of 20 μM respectively were functionalized on the gold surfaces in the same binding buffer. After incubating 3 hours, the gold specimen were taken out and rinsed thoroughly with DI water. These single- and double-thiolated poly A strands were again displaced from the surfaces using 12 mM β-mercapthoethanol which found to effectively break the bonds between sulfur and gold. The etching yielded another solution, which was taken to a fluorometer to measure the amount of fluorescence from the DNA present. Surface densities were calculated dividing this amount by the areas of the surfaces into which they were originally attached. The fluorescence was measured using an excitation wavelength of 495 nm and an emission wavelength of 520 nm.

The hybridization experiments were conducted for complementary concentrations of poly T from 2 to 100 nM in pH 7.4 hybridization buffer (20 mL of 20 × SSPE, 0.2 M NaCl, 7g SDS (7%), 40 mL Formamide (40%), 0.1 mL NP40 (0.1%), Fill to 100 mL with DEPC H_2O). After measuring surface stress changes during specific binding of complementary poly T with double-thiolated poly A, the sensor carried out nonspecific binding of poly A on double-thiolated poly A.

5.4 Results

The fluorescence intensity determined the grafting density where single- and double-thiolated poly A anchored on gold surfaces. The grafting densities of single- and double-thiolated poly A on gold surfaces were turned to be the same, in average 1.9×10^{16} molecules/m^2 respectively. Surface coverage as the number of molecules on the sensing surface was calculated and shown in Table 1.

Table 1 Surface coverage of single- and double-thiolated poly A

Surface coverage of Single-thiolated poly A	Surface coverage of Double-thiolated poly A
2.3x10^{16} molecules/m^2	2.7 x10^{16} molecules/m^2
1.7 x10^{16} molecules/m^2	1.0 x10^{16} molecules/m^2
1.7 x10^{16} molecules/m^2	2.0 x10^{16} molecules/m^2

The salt concentration in the buffer was 50 mM and the length of immobilized poly A strands for both experiments was 30 bases respectively. The results of grafting densities agreed with others (in Table 2) and obtained high degree of reliability in the surface coverage measurements.

Table 2 Results of surface coverage with respect to results from other sources

Poly A with single-thiolated	Poly A with double-thiolated	Stachowiak et al. (Stachowiak, Yue et al. 2006)	Castelino et al. (Castelino, Kannan et al. 2005)
0.019 molecules/nm^2	0.019 molecules/nm^2	0.02 molecules/nm^2	0.02 molecules/nm^2

In addition, the distances between molecules were calculated and turned to be 8 nm for both single and double-thiolated poly A by assuming a hexagonal closed pack structure for the attached molecules.

The surface stress measurements were conducted with a single or multiple injections of complementary poly T whose concentrations were randomly selected from 2 to 100 nM. Figure 26 shows typical profiles of surface stress developments during hybridization of complementary and noncomplementary strands. The surface stress change with the final concentration of 10 nM complementary poly T was turned to be 75 mN/m and no surface stress generation with the noncomplementary poly A (1 µM concentration).
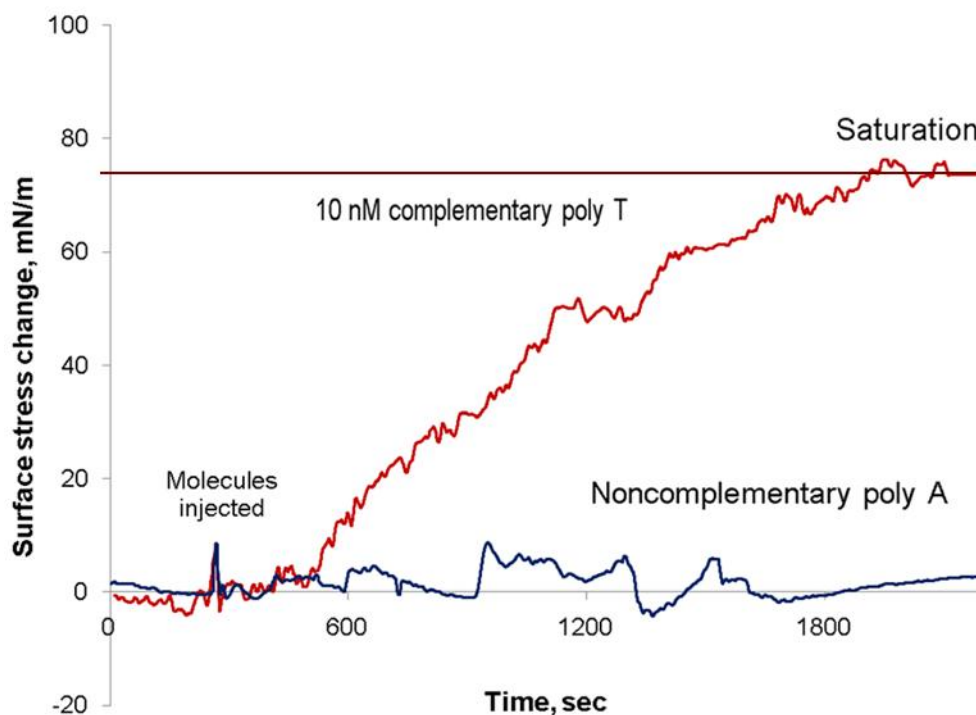
Figure 26 Surface stress developments during injection of 10 nM complementary poly T and noncomplementary poly A on immobilized double-thiol on 30-mer poly A

In Figure 27, changes in surface stress during hybridization of complementary poly T at the concentration from 2 nM to 100 nM with the immobilized double-thiolated poly A were turned to be 30 to 132 mN/m. The experimental results of hybridization of complementary strands with immobilized double- and single-thiolated poly A were compared in Figure 28. Two plots are drawn with the experimental data: one is the fit to Langmuir isotherm and the other is a fit to the proportional to surface coverage calculated by the dissociation constant of 240 nM taken by the result of single-thiolated DNA hybridization. The results show that the double-thiolated immobilization does not agree with the experimental results. It can be said that the binding affinity is different due to modification of receptor molecules from single to double-thiolated for immobilization on the cantilevers. It must affect the binding mechanism while hybridizing ssDNAs to form dsDNAs.
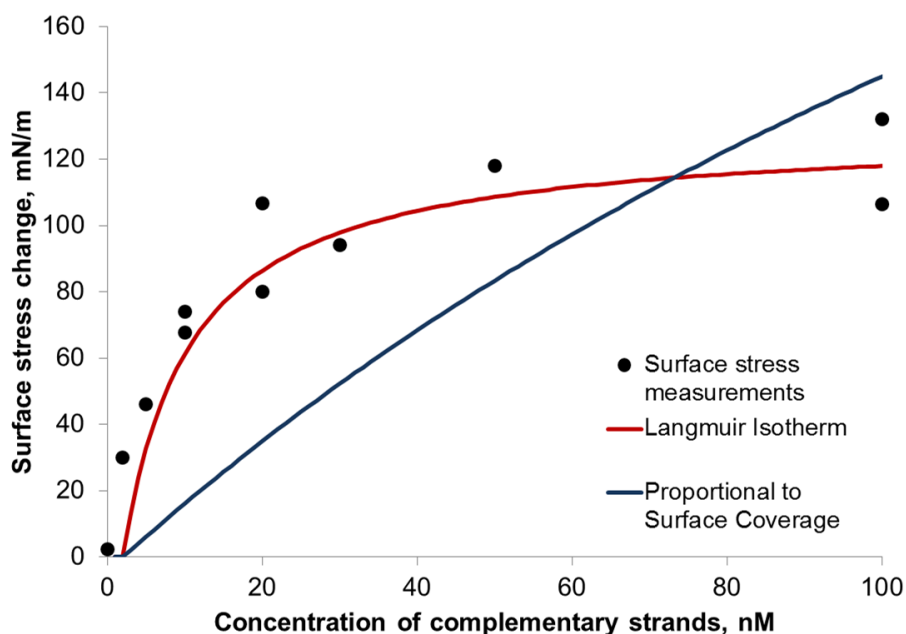
Figure 27 Surface stress changes during hybridization of complementary poly T with double-thiolated ssDNAs

From the statistical details about the radius of gyration followed by a random walk in three dimensions, we are aware of that the total length of poly A or T strands is longer than the end to end distance of the hybridized string. In addition, DNA is a chemically double stranded polymer; thus, when two strands are knotted, they become mechanically thick and rigid. When the repulsive force applies to both ends of a string, these two strands run in opposite directions to each other. Therefore, the dsDNA string tends to stretch out because of increasing in bending and angular potentials during DNA hybridization.
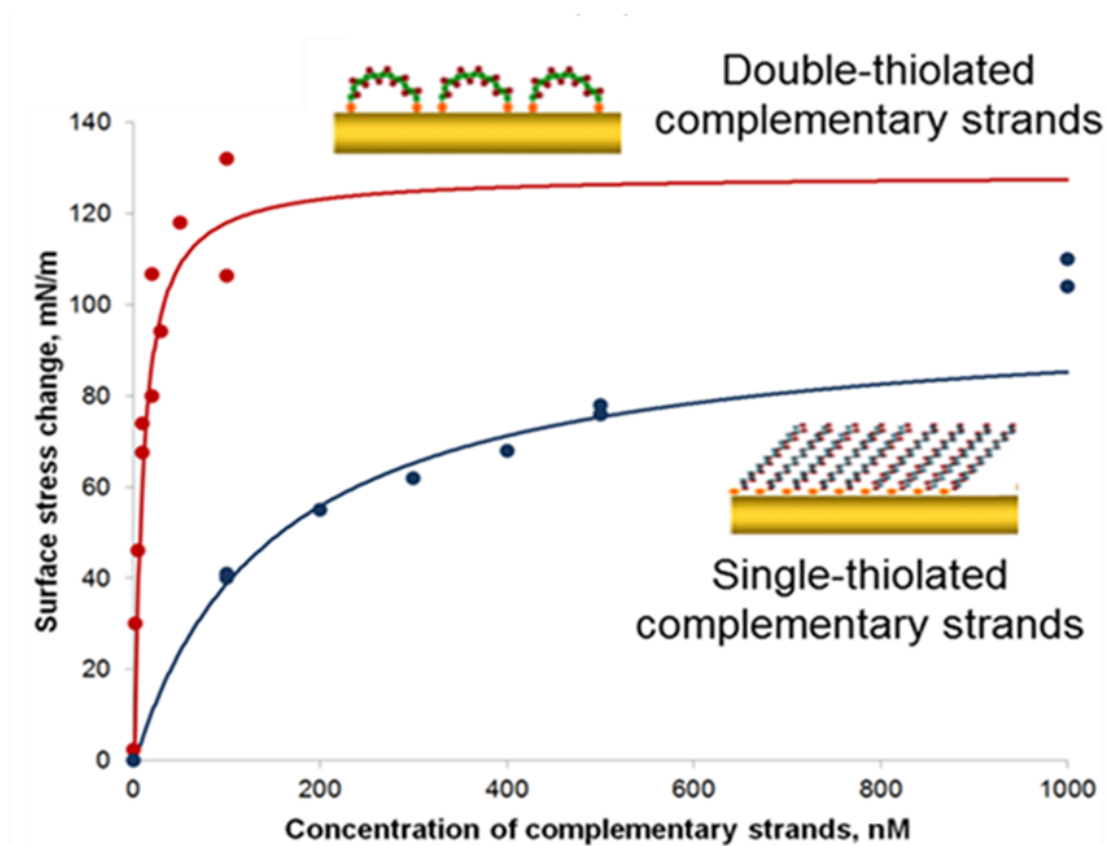
Figure 28 Comparison of surface stress changes during hybridization of complementary strands with immobilized single- and double-thiolated ssDNA strands

5.5 Conclusions

We observed a great potential of double-thiolated DNA immobilization in the field of molecular recognitions. Without any special treatment, sensitivity was significantly improved and reduced threshold of surface stress measurement as low as 500 pM or two orders of magnitude lower than that of the single-thiolated DNA hybridization was recorded. For surface coverage (grafting density), double-thiol poly A had the same surface attachment of single-thiol poly A. Also, AFM height measurements showed that no major difference between ssDNAs and dsDNAs due to hybridization. These showed that double-thiolated molecules contain a different mechanism of surface stress generation which is capable of generating greater values than single thiolated strands. When hybridizing double-thiolated ssDNAs to form dsDNAs on gold surface, the dsDNA strings would leads more stress on the cantilevers and ends up with high surface stress changes.

CHAPTER 6. APTAMER FUNCTIONALIZED MICROCANTILEVER BASED DETECTION OF COCAINE MOLECULES AT ULTRA LOW CONCENTRATION THROUGH COMPETITIVE BINDING

A paper to be submitted to Nano letters

Kyungho Kang, Aaron Kempema, George Kraus Marit Nilsen-Hamilton, and

Pranav Shrotriya

6.1 Abstract

MicroCantilever (MC) based sensors can provide revolutionary sensitivity for forensic detection and identification of controlled substances. We developed a novel "competition" sensing mode based on MC sensors coupled with aptamer-based receptor layers. In the conventional mode of sensing, surface deformation due to binding of ligand on a surface receptor is measured. In the competition mode, the rate of aptamer dissociation from a surface is measured. The rate of aptamer dissociation is determined by diffusion of the aptamer and its reaction with ligands in solution. The competitive sensing mode for cocaine detection resulted in 200 nM detection limit which is about two orders of magnitude of what we obtained in conventional sensing mode.

6.2 Introduction

Aptamers are short single-stranded DNA (ssDNA) or RNA molecules designed to recognize and bind to specific target ligands. Because their specificity can be tuned by the

selection conditions, aptamers can be selected that have exquisite discrimination between molecules. (Jenison, Gill et al. 1994) (Mannironi, Scerch et al. 2000). Very little change in the oligonucleotide sequence may be necessary to change the specificity of a nucleic acid (Mannironi, Scerch et al. 2000). With recognition of the obvious benefits of aptamers in developing microcantilever sensors, many applications have been developed as discussed in a recent review (Mairal, Ozalp et al. 2008). The efficacy of aptamers has been shown on a number of biosensing platforms. Examples include the use of surface plasmon resonance (Win, Klein et al. 2006), electrochemistry (Schlecht, Malave et al. 2007), fluorescence spectrometry (Ozaki, Nishihira et al. 2006), nanotube field-effect transistors (Maehashi, Katsura et al. 2007) and microcantilever technology (Savran, Knudsen et al. 2004).

We have performed conventional direct sensing measurement of cocaine molecules and observed the limitation of the sensitivity, which is dependent on the dissociation constant (K_d). One alternative approach for detection of cocaine molecules is to consider competition between reaction-diffusion. When cocaine as target ligands are introduced in the sensing realm, aptamers bound with thiolated cocaine may accelerate the molecular activity either diffusing away from the binding site into the solution or reacting/binding with cocaine ligands in equilibrium reaction. The conceptual illustration is shown in Figure 29.
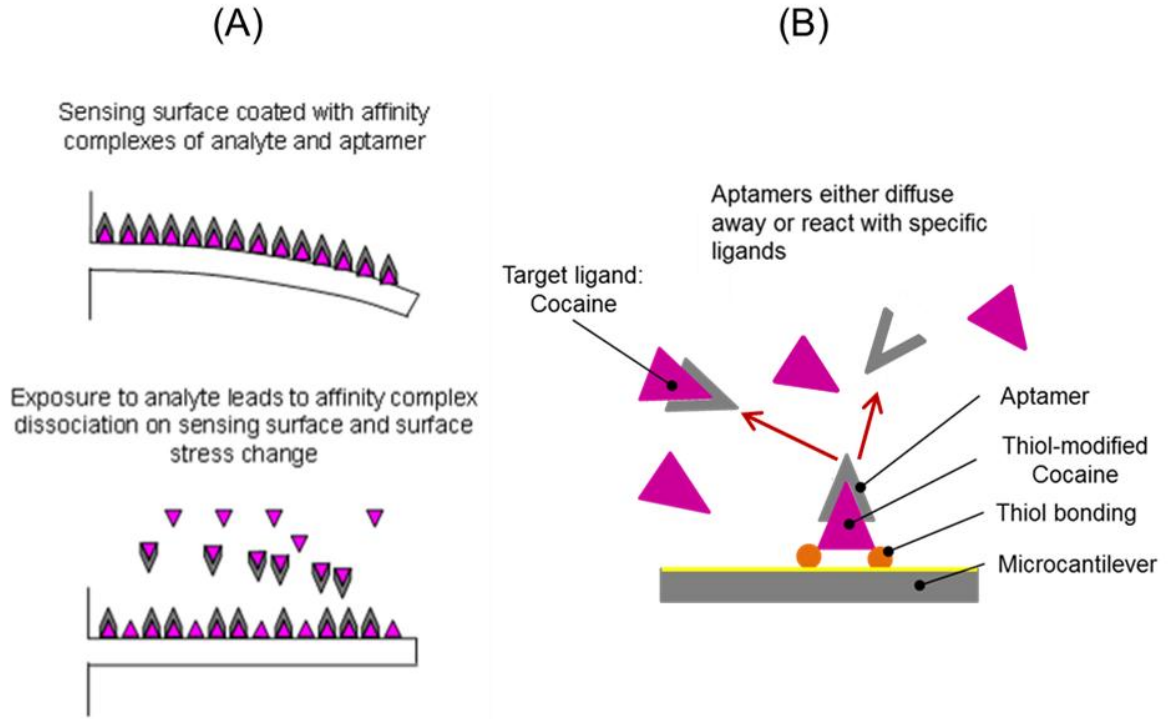
Figure 29 Schematic representation of competitive sensing strategy for cocaine detection and details view of competition between reaction and diffusion of an aptamer

The concept introduced in Figure 29 can be modeled using reaction-diffusion equation of point source in spherical geometry.

$$\dot{C} = D\nabla^2 C - KC = D\left[\frac{1}{r^2}\frac{\partial}{\partial r}r^2\frac{\partial C}{\partial r}\right] - KC$$

(18)

Where, D is a diffusion constant and K is a constant dependent on the cocaine concentration in solution with initial and boundary conditions; $C(r,0) = C_0\delta(r)$, $C(0,t) \rightarrow finite$, and $\lim_{r\rightarrow\infty} C(r,t) = 0$, the general solution of the system is described Equation (19) assuming uniform concentration of cocaine and first order kinetics for cocaine/aptamer binding.

$$C = \frac{1}{D^{3/2}t^{3/2}} e^{-\frac{r^2}{4Dt}} e^{-Kt} \cdot C_0$$

(19)

The rate of aptamer dissociation can be expressed in Equation (20) and differential bending rate is plotted as a function of cocaine concentration in Figure 30.

$$Aptamer\ dissociation\ rate = \frac{\dfrac{e^{-Kt_2}}{t_2^{3/2}} - \dfrac{e^{-Kt_1}}{t_1^{3/2}}}{\dfrac{e^{-Kt_2}}{t_2^{3/2}} + \dfrac{e^{-Kt_1}}{t_1^{3/2}}} \quad ,$$

(20)

$$K = K_f[B]\ and\ [A] \ll [B]$$

Where [A] and [B] are concentration of aptamer and cocaine as target ligands respectively and aptamers are negligibly small amount compared to the amount of cocaine.
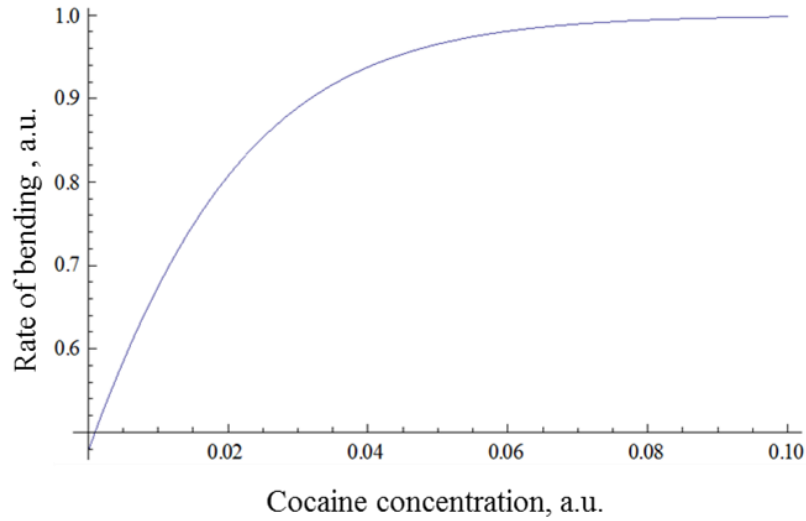
Figure 30 Numerical analysis on diffusion and reaction profile

We utilized an aptamer functionalized microcantilever for cocaine detection has been characterized under a novel "competition" mode that relies on resolving the surface stress changes associated with dissociation of affinity complexes on the sensing surface. Aptamer molecules are much larger than cocaine molecules; therefore, their removal from the sensing surface in the competition sensing mode is expected to give a stress change that is dependent in their surface coverage. The novel competitive mode for microcantilever sensor operation is schematically depicted in Figure 29, and the sensor configuration is presented in Figure 5. The aptamer used for cantilever functionalized has been previously selected to recognize cocaine molecules (Stojanovic, de Prada et al. 2001). In the absence of cocaine the termini of the aptamer are believed to be separated, but in its presence they form a stem and a three-way junction. The extent to which the aptamer changes in structure is a function of the number of bases in its terminal stem (Neves, Reinstein et al. 2010). Surface stress associated with this major structural change was investigated to characterize sensor response to the aptamer-ligand.

6.3 Experiments

In order to implement the competition sensing mode, the experiments were carried out in two steps. First, cocaine/aptamer complexes were immobilized on the surface. The rate of bending during dissociation of affinity complex was then measured in presence of cocaine ligands.

Thiol-modified cocaine molecules were synthesized and immobilized on the microcantilevers. The synthesis began with the known enol ether ester and was generated in

one step via a cycloaddition to N-BOC-pyrrole. The eight-step synthesis of the thiolated cocaine molecule generated a single enantiomer compound shown in Figure 31.
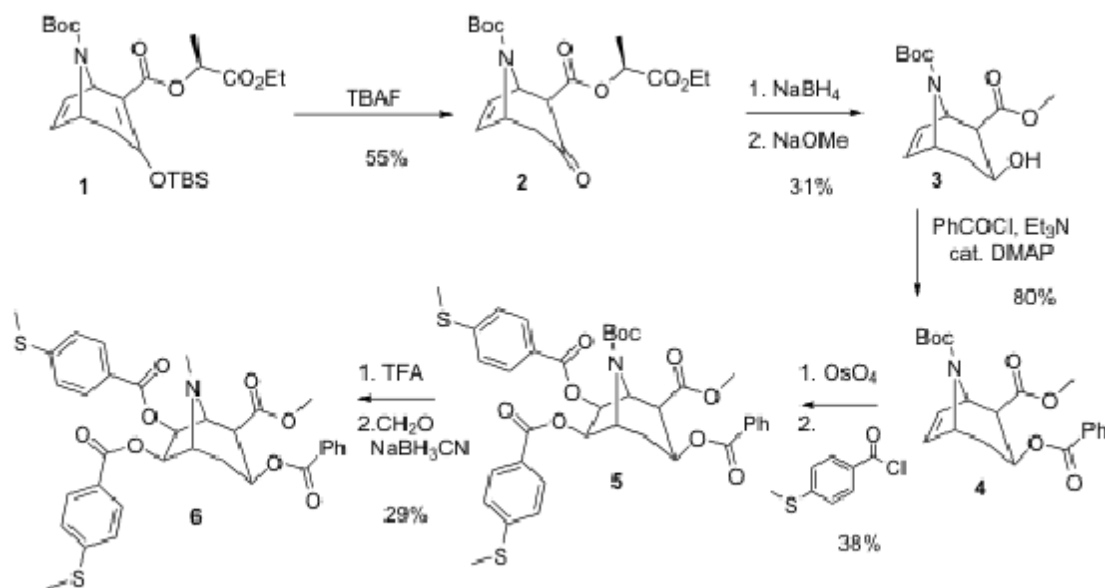
Figure 31 Synthesis producers of thiolated cocaine

Our thiolated cocaine molecule has two points of attachment (via the two sulfur atoms) to the cantilever surface. The site of the connection of the sulfur containing benzoate ester to the cocaine skeleton was designed to best present the key functional groups in the cocaine molecule (methyl ester, benzoate and amine) to the aptamer.

Gold-coated microcantilevers with nominal dimensions of 500 μm length, 100 μm width and 1 μm thickness were purchased from Nanoandmore.com (Lady's Island, South Carolina). Microcantilevers were cleaned by Piranha solution (70 % H_2SO_4 and 30 % H_2O_2), and immersed into 200 μM of thiolated cocaine molecules in ethyl acetate for 15 hours in order to form monolayers of thiolated cocaine on gold surface of the sensing cantilever.

Through this procedures, thiol modified cocaine molecules were tethered onto the gold surface using the sulfur/gold linkage.

DNA cocaine aptamers with the sequence of 5'- GAC AAG GAA AAT CCT TCA ATG AAG TGG GTC -3' and a thiol modified DNA with scrambled sequence were purchased from Integrated DNA Technologies (IDT), (Coralville, Iowa). Aptamer binding affinity for the cocaine was measured by isothermal titration calorimetry (ITC) under the same buffer conditions of monovalent and divalent cations and pH as used for the microcantilever studies in Chapter 4.3.

Contact angle measurements were conducted to validate the surface modification (Smith 1980). The contact angle of gold surface changed from hydrophilic (66.5 °) to hydrophobic (50 °) on exposure to cocaine, which is a hydrophobic molecule, indicating surface modification.

Thiol-cocaine coated microcantilevers were incubated in 400 μM aptamer solution for 30 minutes and monitored incubation time up to 3 hours such that cantilever surface was covered with cocaine/aptamer affinity complexes (as schematically depicted in Figure 29). The reference cantilevers were coated with the scrambled DNA sequence of same length and base composition as the cocaine aptamer so that exposure to cocaine molecules leads to affinity complex dissociation only on the sensing surface. Surface stress during binding and unbinding of aptamers was measured to characterize the attachments and dissociation of aptamers.

The sensing and reference cantilevers were mounted in the surface stress sensor and sensor response was measured for exposure to cocaine solutions of concentration varying from 0 to 100 μM in PBS buffer (pH 7.4, 140 mM NaCl). After the sensing experiment, the

sensing and reference cantilevers were regenerated through heating in deionized water at 80 °C and each cantilever was reused three times for the sensing experiments.

6.4 Results

In the competition sensing mode, the sensing cantilevers were coated with thiolated cocaine molecules and incubated in cocaine-aptamer solution such that exposure to cocaine solution leads to disassociation of cocaine-aptamer complexes on the cantilever surface. Under the competition sensing mode, the final magnitude of the saturated surface stress change is considerably larger than that measured for direct sensing mode (Figure 33) for the same concentration. The surface stress change did not saturate till almost 2 hours after injection of the cocaine solution in the sensor.

The large magnitude of the saturated surface stress change observed during the competition sensing mode indicated that aptamer-cocaine complex dissociation was responsible for the surface stress change as removal of larger aptamer molecules leads to larger deformation of the surface. However, the long time period required to reach the saturation value as well as the constant magnitude of saturated surface stress change irrespective of different cocaine concentrations indicates that the equilibrium is only achieved when significant number of cocaine-aptamer complexes on the cantilever surfaces have undergone dissociation. Dependence of the initial slope of surface stress change on the cocaine concentration indicates that initial rate of disassociation for cocaine-aptamer complexes on the cantilever surface is dependent on concentration of cocaine molecules in solution as predicted by the reaction-diffusion model.
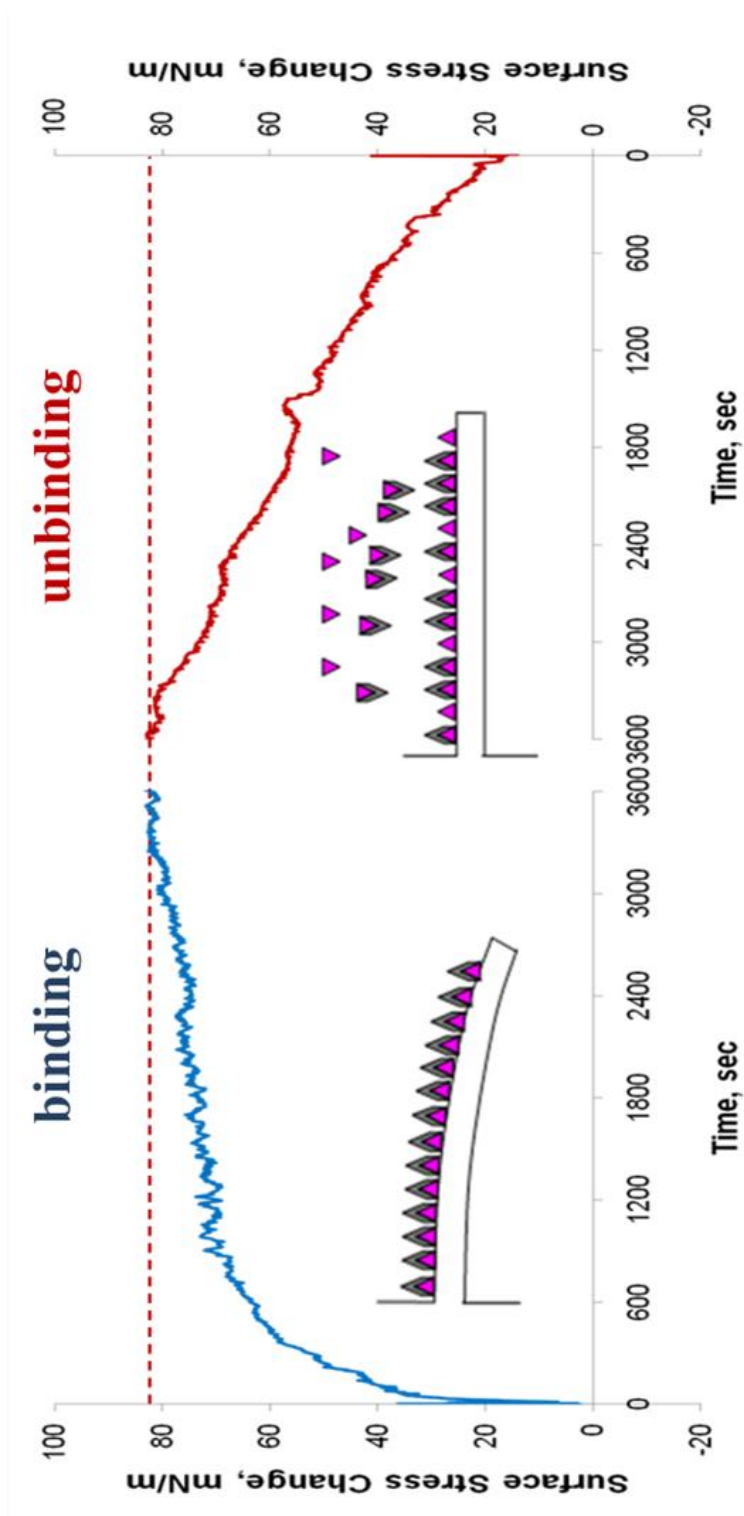
Figure 32 Profiles of surface stress measurements during immobilization of cocaine aptamer on a cantilever and equilibrium reaction after injecting 1 µM cocaine molecules

Figure 32 shows one set of experimental results measured binding and unbinding of aptamers from the cantilever surface. The measured surface stress change corresponding to cocaine concentration of 1 µM was measured under the competition sensing mode. Only the magnitude of the surface stress change is plotted. The binding of aptamers with thiolated cocaine molecules resulted in 83 mN/m of surface stress change and the unbinding was turned to be 65 mN/m in equilibrium states. It shows that the initial bending of a sensing cantilever due to binding of aptamer was recovered approximately 80 percent back during unbinding stage.

It was also interesting to observe that the initial slope of the surface stress change seemed to be dependent on the concentration of cocaine solution introduced into the sensor. Initial slope of the surface stress change during competition sensing mode was measured for seven different cocaine concentrations: 0 (pure buffer), 1, 2, 5, 10, 20, 50 and 100 µM. The normalized slope of the surface stress buildup during the first 20 min after introduction of cocaine is plotted as a function of cocaine concentration for competition sensing mode in Figure 33 (A). Observed values of the normalized slope demonstrate a strong dependence on the concentration in the range from 0 - 10 µM cocaine. Given the sensitivity of surface stress measurements and the experimental results in Figure 33, the lowest detectable cocaine concentration in competition sensing mode is approximated to be 200 nM (equivalent 3 mN/m of surface stress change). To the best of our knowledge, this is the lowest detectable threshold reported for cocaine aptamer based sensing.
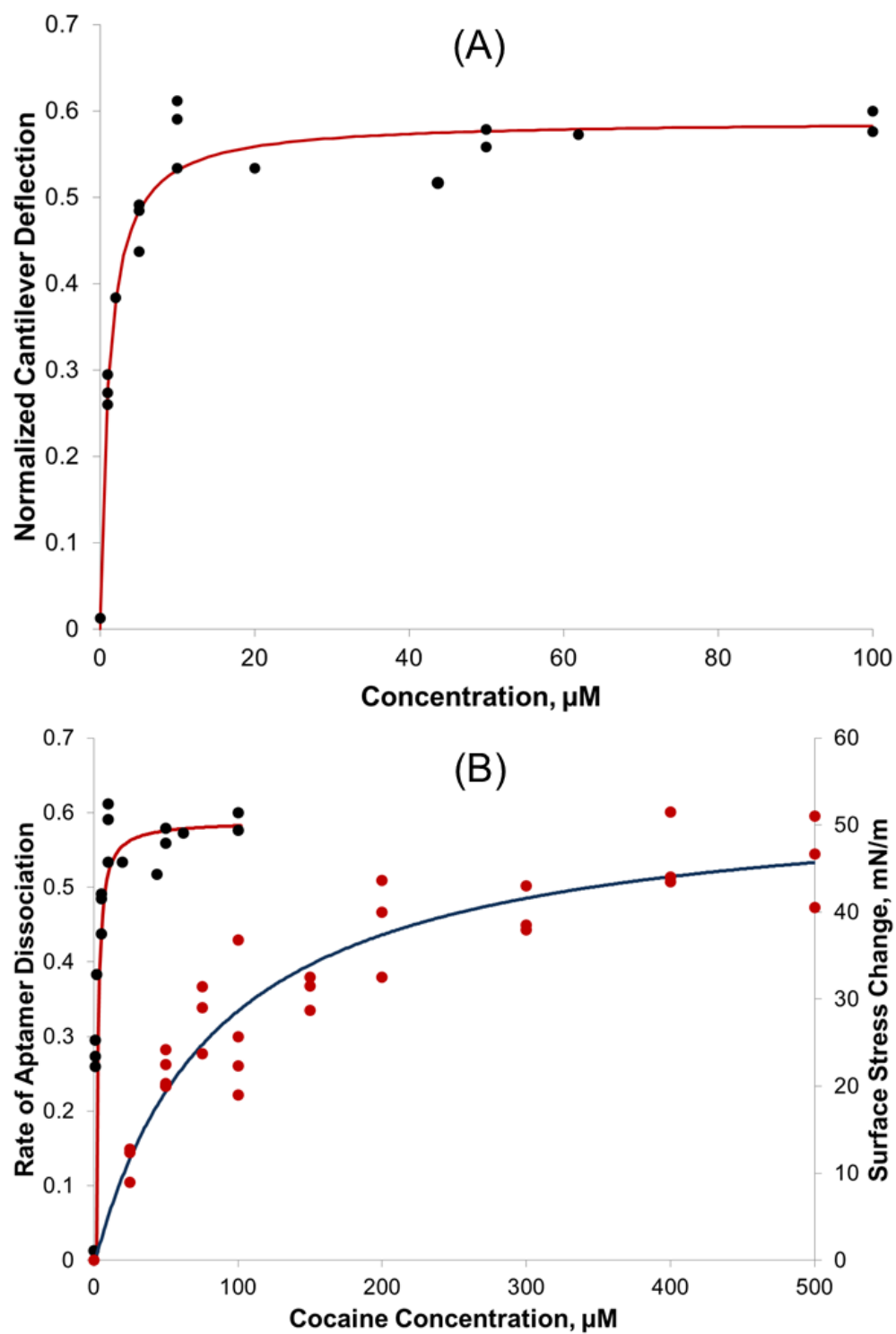
Figure 33 Rate of aptamer dissociation from a surface (A), and comparison of competition and conventional sensing modes for cocaine detection (B)

6.5 Conclusions

Aptamer functionalized microcantilever sensor could combine high sensitivity of microcantilevers and high specificity of aptamers. A sensing approach based on microcantilever functionalized with aptamers provides an invaluable tool for forensic science because of its portability and capability for identification of ligands with high sensitivity and specificity. The contact angle measurement showed that immobilization of thiolated cocaine influence surface modification from hydrophilic to relatively hydrophobic surface. One excellent feature of aptamers as sensor platform is that binding reactions are reversible so that the receptor layers can be recharged for detection and reused in the same sensor many times. Aptamer-functionalized microcantilever used in the novel competition sensing mode have demonstrated threshold sensitivity that match the threshold sensitivities reported for lab-based immunoassays but in significantly shorter time. In addition, the specificity of cocaine detection needs to be tested in biological matrices as well as in real world samples.

CHAPTER 7. CONCLUSIONS

MicroCantilever (MC) based sensors are increasingly being used to detect chemical and biological species in both gas and liquid environments, and these devices could be developed for the use of molecular recognitions. The sensing strategy involves coating one surface of a micromachined cantilever with receptor species that has a high affinity for specific target ligands. The presence of the ligand is detected by resolving the surface stress change associated with absorption/adsorption of receptor molecules immobilized on the sensitized surface. The introduction of cantilevers substantially enriches the portfolio of sensing scenarios that can be used in high performance miniaturized analytical systems.

A miniature sensor consisting of two adjacent micromachined cantilevers (a sensing /reference pair) was utilized for detection of target ligands by measuring the differential surface stress associated with adsorption/absorption of chemical or biological species on the cantilevers. The unique advantages of the surface stress sensor are: 1) differential measurements of surface stress eliminates the influence of environmental disturbances such as nonspecific adsorption, changes in pH, ionic strength, and especially the temperature; and 2) sensitivity of the sensor is independent on the distance between the sensing surface and detectors. Therefore, the sensor is being amenable for miniaturization and enables an array of sensors to be easily fabricated on a single MEMS device.

The performance of the microcantilever sensor was first proved through the surface stress measurements associated with formation of alkanethiol self-assembled monolayers (SAMs) and DNA hybridization in vapor and liquid environments respectively. Whereas, alkanethiol SAM is a typical example of detection of chemical species, and the concept of

self-assembly becomes fundamental for molecular recognitions. We observed that formation of alkanethiol SAMs on gold surface of a sensing cantilever results in highest surface stress changes. The saturated surface stress change was turned to be 0.29 mN/m with an injection of octanethiol $[CH_3(CH_2)_7SH]$ and we also observed the transition point from tensile to compressive stress as Godin reported (Godin, Williams et al. 2004).
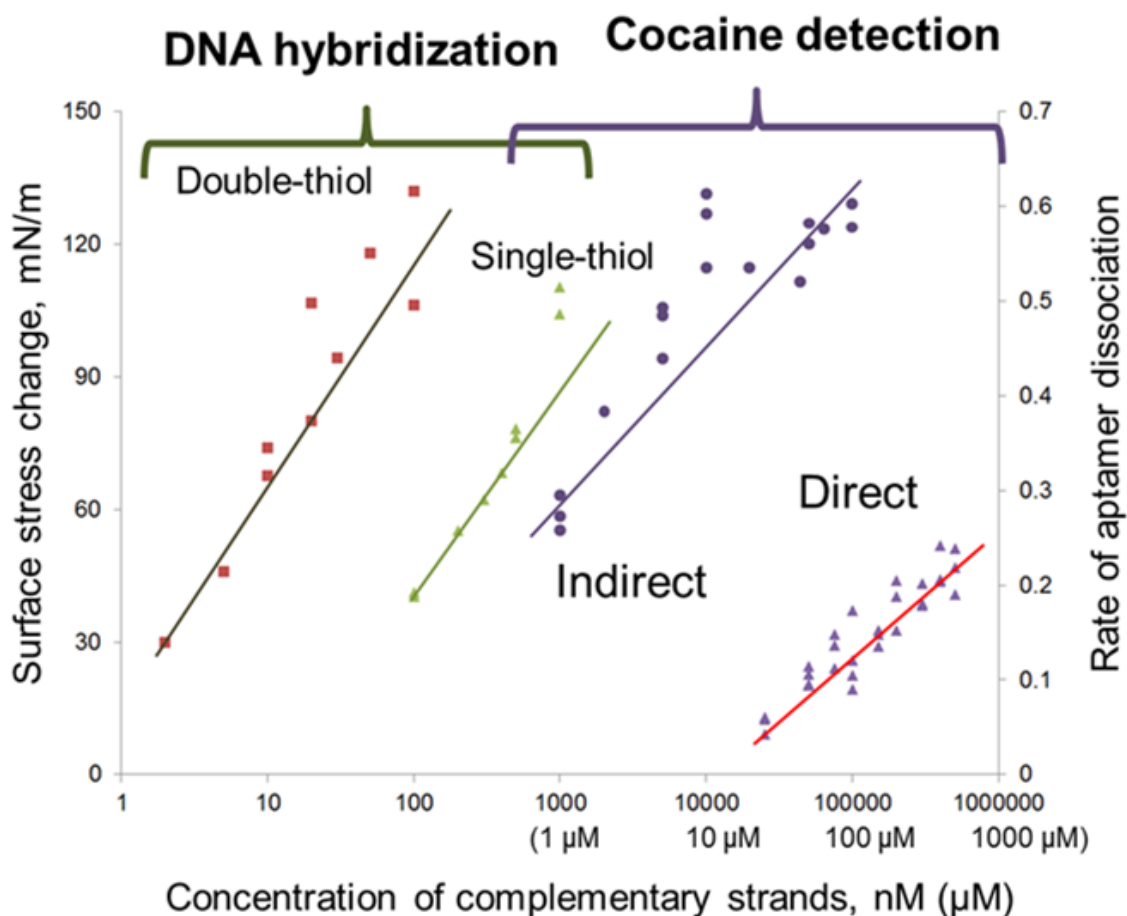

Figure 34 Comparison of experimental results in DNA hybridization and cocaine detection

The response of hybridization of ssDNA receptors (30-mer poly A) with complementary ssDNA strands (30-mer poly T) was measured in liquid environment. The surface stress changes in the concentration of poly T between 0.1 and 1.0 μM were turned to be 40 to 110

mN/m. The binding affinity during formation of dsDNAs through the hybridization was defined by measuring dissociation constant (K_d). We obtained dissociation constant of 240 nM using Isothermal Titration Calorimetry (ITC) and manipulated into Equation (14) derived by equilibrium reaction to find a fit. The curve fitting on surface stress changes based on ITC measurement showed a good reliance on lower concentration of complementary poly T until 0.5 µM, but it becomes nonlinear beyond 0.5 µM. The surface coverage is a dominant element that affects surface stress developments. We also conducted fluorescence measurements to determine surface coverage and average space of single- and double-thiolated DNA strands. The complementary DNA strand is a temperature dependent variable. Surface stress changes resulted in different saturation values when thawing temperature on frozen complementary DNA strands was changed: in room temperature and in annealing temperature at 60 ℃. This might be that ssDNAs are stacked or formed crystallization in thawed solution. On the other hand, thawing molecules at annealing temperature (60 ℃) makes molecules to most active status and affects hybridization efficiency as well.

There have been many attempts to improve stability and sensitivity of the sensor such as adding polarizers and isolator or selecting microcantilevers with a high aspect-ratio. Not only did we consider this mechanical or optical aspect of the sensor, but we also designed a new format of a molecular structure to achieve this goal. First attempt was made by attaching a thiol-group on both ends of single-stranded DNAs (ssDNAs) to achieve mechanically rigid and stable immobilization on the gold surface of a sensing cantilever. While hybridizing with complementary DNA strands, double-thiolated DNA receptors may give rise to more stress on the cantilever due to twisting to form dsDNA strands and repulsive force between molecules. We observed that the activity of hybridization with the double-thiolated poly A

could reduce the sensitivity as low as two orders of magnitude in surface stress changes compared with the measurement of a single-thiolated poly A.

We developed microcantilever sensors with high sensitivity and high specificity for detection and identification of controlled substances. In order to understand the mechanism governing by aptamers associated with controlled substances, the surface stress sensor performed the sensitive and specific identification of cocaine as target ligands. The central hypothesis is that formation of affinity complexes due to the specific absorption of controlled substance molecules on sensitized surfaces would give rise to charge redistribution, configurational change and steric hindrance between neighboring molecules leading to a measurable surface stress change. We have formulated our hypothesis following these reported findings: a) aptamers have highly specific affinity to single target ligands; and b) formation of affinity complexes between surface bound aptamers and target ligands leads to a change in the surface stress state. Thus, the proof-of-concept of our sensing approach is once established, it will become possible to apply this technology for the detection and identification of a variety of drugs of abuse.

The MC sensor response for cocaine detection has been characterized under two different sensing strategies. The first mode is a conventional mode that relies on resolving surface stress change associated with formation of affinity complexes between aptamer and cocaine molecules on the sensing surface. The second mode is a novel "competition" mode that relies on resolving the rate of surface stress changes associated with dissociation of affinity complexes on the sensing surface.

For the conventional sensing mode, thiolated cocaine aptamers were immobilized on the sensing cantilever surface, while the reference cantilever was coated with a control DNA

consisting of the bases as the cocaine aptamer but with their sequence scrambled. The solutions for the sensing experiments were prepared to ensure that acetonitrile concentration is below 2% for all cases, and concentrations of cocaine molecules were varied from 25 μM to 500 μM. Surface stress changes from 9 to 51 mN/m were measured for the range of cocaine concentrations. A given threshold sensitivity of 3 mN/m for surface stress measurements, this sensor is able to detect cocaine with the lowest detectable concentration down to 5 μM in room temperature under the conventional sensing mode.

In the competition sensing mode, the rate of surface stress generated due to dissociation of aptamer/cocaine complexes was measured. A thiol modified cocaine molecule was synthesized and attached on the sensing cantilever. The thiolated cocaine molecule has two points of attachment (via the two sulfur atoms) to the cantilever surface. The site of the connection of the sulfur containing benzoate ester to the cocaine skeleton was designed to best present the key functional groups in the cocaine molecule (methyl ester, benzoate and amine) to the aptamer.

Thiol modified cocaine molecules were tethered onto the gold surface using the sulfur/gold linkage and immersed in a solution of the cocaine aptamers such that the cantilever surface is covered with affinity complexes of cocaine/aptamer. The functionalized cantilevers were then exposed to various concentrations of cocaine molecules that accelerate dissociation of aptamers from the cocaine-aptamer complexes. The experimental results showed that the magnitude was not correlated with the cocaine concentration; however, the rate of bending demonstrated a good correlation with cocaine concentration. More importantly, the rate of bending correlation indicates that the lowest detectable cocaine concentration in competition sensing mode is approximately 200 nM. To the best of our

knowledge, this is the lowest detectable threshold reported for currently known cocaine aptamer based sensing. Aptamer functionalized microcantilevers used in the novel competition sensing mode have demonstrated approximately two orders of magnitude improvement in threshold sensitivity over the conventional sensing mode.

BIBLIOGRAPHY

Allard, K. and D. Deutsch (1987). "Comparison of Gdcs Elisa and Syvas Emit for Qualitatively Determining the Presence of Benzodiazepines in Human-Urine." Clinical Chemistry **33**(6): 973-973.

Alonso-Lomillo, M. A., C. Yardimci, O. Dominguez-Renedo and M. J. Arcos-Martinez (2009). "CYP450 2B4 covalently attached to carbon and gold screen printed electrodes by diazonium salt and thiols monolayers." Analytica Chimica Acta **633**(1): 51-56.

Alvarez, M., L. G. Carrascosa, M. Moreno, A. Calle, A. Zaballos, L. M. Lechuga, C. Martinez-A and J. Tamayo (2004). "Nanomechanics of the formation of DNA self-assembled monolayers and hybridization on microcantilevers." Langmuir **20**(22): 9663-9668.

Aoyagi, S. and M. Kudo (2005). "Development of fluorescence change-based, reagent-less optic immunosensor." Biosensors & Bioelectronics **20**(8): 1680-1684.

Badcock, N. R. and D. A. Oreilly (1992). "False-Positive Emit St Ethanol Screen with Postmortem Infant Plasma." Clinical Chemistry **38**(3): 434-434.

Bagalkot, V., L. Zhang, E. Levy-Nissenbaum, S. Jon, P. W. Kantoff, R. Langer and O. C. Farokhzad (2007). "Quantum dot - Aptamer conjugates for synchronous cancer imaging, therapy, and sensing of drug delivery based on Bi-fluorescence resonance energy transfer." Nano Letters **7**(10): 3065-3070.

Baker, B. R., R. Y. Lai, M. S. Wood, E. H. Doctor, A. J. Heeger and K. W. Plaxco (2006). "An electronic, aptamer-based small-molecule sensor for the rapid, label-free detection of

cocaine in adulterated samples and biological fluids." <u>Journal of the American Chemical Society</u> **128**(10): 3138-3139.

Baker, J. E. and A. J. Jenkins (2008). "Screening for cocaine metabolite fails to detect an intoxication." <u>American Journal of Forensic Medicine and Pathology</u> **29**(2): 141-144.

Baller, M. K., H. P. Lang, J. Fritz, C. Gerber, J. K. Gimzewski, U. Drechsler, H. Rothuizen, M. Despont, P. Vettiger, F. M. Battiston, J. P. Ramseyer, P. Fornaro, E. Meyer and H. J. Guntherodt (2000). "A cantilever array-based artificial nose." <u>Ultramicroscopy</u> **82**(1-4): 1-9.

Barnes, J. R., R. J. Stephenson, M. E. Welland, C. Gerber and J. K. Gimzewski (1994). "Photothermal Spectroscopy with Femtojoule Sensitivity Using a Micromechanical Device." <u>Nature</u> **372**(6501): 79-81.

Barroso, M., M. Dias, D. N. Vieira, J. A. Queiroz and M. Lopez-Rivadulla (2008). "Development and validation of an analytical method for the simultaneous determination of cocaine and its main metabolite, benzoylecgonine, in human hair by gas chromatography/mass spectrometry." <u>Rapid Communications in Mass Spectrometry</u> **22**(20): 3320-3326.

Beijer, F. H., H. Kooijman, A. L. Spek, R. P. Sijbesma and E. W. Meijer (1998). "Self-complementarity achieved through quadruple hydrogen bonding." <u>Angewandte Chemie-International Edition</u> **37**(1-2): 75-78.

Berens, C., A. Thain and R. Schroeder (2001). "A tetracycline-binding RNA aptamer." <u>Bioorganic & Medicinal Chemistry</u> **9**(10): 2549-2556.

Berger, R., E. Delamarche, H. P. Lang, C. Gerber, J. K. Gimzewski, E. Meyer and H. J. Guntherodt (1997). "Surface stress in the self-assembly of alkanethiols on gold." <u>Science</u> **276**(5321): 2021-2024.

Biswal, S. L., D. Raorane, A. Chaiken, H. Birecki and A. Majumdar (2006). "Nanomechanical detection of DNA melting on microcantilever surfaces." <u>Analytical Chemistry</u> **78**(20): 7104-7109.

Bock, L. C., L. C. Griffin, J. A. Latham, E. H. Vermaas and J. J. Toole (1992). "Selection of Single-Stranded-DNA Molecules That Bind and Inhibit Human Thrombin." <u>Nature</u> **355**(6360): 564-566.

Bosch, M. E., A. J. R. Sanchez, F. S. Rojas and C. B. Ojeda (2007). "Recent development in optical fiber biosensors." <u>Sensors</u> **7**(6): 797-859.

Burke, D. H., D. C. Hoffman, A. Brown, M. Hansen, A. Pardi and L. Gold (1997). "RNA aptamers to the peptidyl transferase inhibitor chloramphenicol." <u>Chemistry & Biology</u> **4**(11): 833-843.

Canete, S. J. P., W. W. Yang and R. Y. Lai (2009). "Folding-based electrochemical DNA sensor fabricated by "click" chemistry." <u>Chemical Communications</u>(32): 4835-4837.

Casero, E., M. Darder, D. J. Diaz, F. Pariente, J. A. Martin-Gago, H. Abruna and E. Lorenzo (2003). "XPS and AFM characterization of oligonucleotides immobilized on gold substrates." <u>Langmuir</u> **19**(15): 6230-6235.

Castelino, K., B. Kannan and A. Majumdar (2005). "Characterization of grafting density and binding efficiency of DNA and proteins on gold surfaces." <u>Langmuir</u> **21**(5): 1956-1961.

Cekan, P., E. O. Jonsson and S. T. Sigurdsson (2009). "Folding of the cocaine aptamer studied by EPR and fluorescence spectroscopies using the bifunctional spectroscopic probe C." Nucleic Acids Research **37**(12): 3990-3995.

Chen, X. C., Y. L. Deng, Y. Lin, D. W. Pang, H. Qing, F. Qu and H. Y. Xie (2008). "Quantum dot-labeled aptamer nanoprobes specifically targeting glioma cells." Nanotechnology **19**(23).

Cheng, A. K. H., D. Sen and H. Z. Yu (2009). "Design and testing of aptamer-based electrochemical biosensors for proteins and small molecules." Bioelectrochemistry **77**(1): 1-12.

Cheng, M. M. C., G. Cuda, Y. L. Bunimovich, M. Gaspari, J. R. Heath, H. D. Hill, C. A. Mirkin, A. J. Nijdam, R. Terracciano, T. Thundat and M. Ferrari (2006). "Nanotechnologies for biomolecular detection and medical diagnostics." Current Opinion in Chemical Biology **10**(1): 11-19.

Cho, E. J., J. W. Lee and A. D. Ellington (2009). "Applications of Aptamers as Sensors." Annual Review of Analytical Chemistry **2**: 241-264.

Choi, J. H., K. H. Chen and M. S. Strano (2006). "Aptamer-capped nanocrystal quantum dots: A new method for label-free protein detection." Journal of the American Chemical Society **128**(49): 15584-15585.

Chu, T. C., J. W. Marks, L. A. Lavery, S. Faulkner, M. G. Rosenblum, A. D. Ellington and M. Levy (2006). "Aptamer : toxin conjugates that specifically target prostate tumor cells." Cancer Research **66**(12): 5989-5992.

Chu, T. C., F. Shieh, L. A. Lavery, M. Levy, R. Richards-Kortum, B. A. Korgel and A. D. Ellington (2006). "Labeling tumor cells with fluorescent nanocrystal-aptamer bioconjugates." Biosensors & Bioelectronics **21**(10): 1859-1866.

Cleveland, J. P., S. Manne, D. Bocek and P. K. Hansma (1993). "A Nondestructive Method for Determining the Spring Constant of Cantilevers for Scanning Force Microscopy." Review of Scientific Instruments **64**(2): 403-405.

Cognard, E., S. Bouchonnet and C. Staub (2006). "Validation of a gas chromatography - Ion trap tandem mass spectrometry for simultaneous analyse of cocaine and its metabolites in saliva." Journal of Pharmaceutical and Biomedical Analysis **41**(3): 925-934.

Concheiro, M., A. de Castro, O. Quintela, A. Cruz and M. Lopez-Rivadulla (2007). "Confirmation by LC-MS of drugs in oral fluid obtained from roadside testing." Forensic Science International **170**(2-3): 156-162.

Contreras, M. T., M. Gonzalez, S. Gonzalez, R. Ventura, J. L. Valverde, A. F. Hernandez, A. Pla, A. Vingut, J. Segura and R. de la Torre (2007). "Validation of a procedure for the gas chromatography-mass spectrometry analysis of cocaine and metabolites in pericardial fluid." Journal of Analytical Toxicology **31**(2): 75-80.

Contreras, M. T., A. E. Hernandez, M. Gonzalez, S. Gonzalez, R. Ventura, A. Pla, J. L. Valverde, J. Segura and R. de la Torre (2006). "Application of pericardial fluid to the analysis of morphine (heroin) and cocaine in forensic toxicology." Forensic Science International **164**(2-3): 168-171.

Copel, M., M. C. Reuter, E. Kaxiras and R. M. Tromp (1989). "Surfactants in Epitaxial-Growth." Physical Review Letters **63**(6): 632-635.

Cristoni, S., E. Basso, P. Gerthoux, P. Mocarelli, E. Gonella, M. Brambilla, S. Crotti and L. R. Bernardi (2007). "Surface-activated chemical ionization ion trap mass spectrometry for the analysis of cocaine and benzoylecgonine in hair after extraction and sample dilution." Rapid Communications in Mass Spectrometry **21**(15): 2515-2523.

Demers, L. M., C. A. Mirkin, R. C. Mucic, R. A. Reynolds, R. L. Letsinger, R. Elghanian and G. Viswanadham (2000). "A fluorescence-based method for determining the surface coverage and hybridization efficiency of thiol-capped oligonucleotides bound to gold thin films and nanoparticles." Analytical Chemistry **72**(22): 5535-5541.

Ding, P., P. Helquist and M. J. Miller (2008). "Design and synthesis of a siderophore conjugate as a potent PSMA inhibitor and potential diagnostic agent for prostate cancer." Bioorganic & Medicinal Chemistry **16**(4): 1648-1657.

Dixon, S. J., R. G. Brereton, J. F. Carter and R. Sleeman (2006). "Determination of cocaine contamination on banknotes using tandem mass spectrometry and pattern recognition." Analytica Chimica Acta **559**(1): 54-63.

Dutta, P., C. A. Tipple, N. V. Lavrik, P. G. Datskos, H. Hofstetter, O. Hofstetter and M. J. Sepaniak (2003). "Enantioselective sensors based on antibody-mediated nanomechanics." Analytical Chemistry **75**(10): 2342-2348.

Dwarakanath, S., J. G. Bruno, A. Shastry, T. Phillips, A. John, A. Kumar and L. D. Stephenson (2004). "Quantum dot-antibody and aptamer conjugates shift fluorescence upon binding bacteria." Biochemical and Biophysical Research Communications **325**(3): 739-743.

Ellington, A. D. and J. W. Szostak (1990). "Invitro Selection of Rna Molecules That Bind Specific Ligands." Nature **346**(6287): 818-822.

Ellington, A. D. and J. W. Szostak (1992). "Selection Invitro of Single-Stranded-DNA Molecules That Fold into Specific Ligand-Binding Structures." Nature **355**(6363): 850-852.

Emsley, J. (1980). "Very Strong Hydrogen-Bonding." Chemical Society Reviews **9**(1): 91-124.

Erlandsson, R., G. M. McClelland, C. M. Mate and S. Chiang (1988). "Atomic Force Microscopy Using Optical Interferometry." Journal of Vacuum Science & Technology a-Vacuum Surfaces and Films **6**(2): 266-270.

Fan, C. H., K. W. Plaxco and A. J. Heeger (2003). "Electrochemical interrogation of conformational changes as a reagentless method for the sequence-specific detection of DNA." Proceedings of the National Academy of Sciences of the United States of America **100**(16): 9134-9137.

Fang, X. H., X. J. Liu, S. Schuster and W. H. Tan (1999). "Designing a novel molecular beacon for surface-immobilized DNA hybridization studies." Journal of the American Chemical Society **121**(12): 2921-2922.

Fiorentini, V., M. Methfessel and M. Scheffler (1993). "Reconstruction Mechanism of Fcc Transition-Metal (001) Surfaces." Physical Review Letters **71**(7): 1051-1054.

Follador, M. J. D., M. Yonamine, R. L. D. Moreau and O. A. Silva (2004). "Detection of cocaine and cocaethylene in sweat by solid-phase microextraction and gas chromatography/mass spectrometry." Journal of Chromatography B-Analytical Technologies in the Biomedical and Life Sciences **811**(1): 37-40.

Freeman, R., Y. Li, R. Tel-Vered, E. Sharon, J. Elbaz and I. Willner (2009). "Self-assembly of supramolecular aptamer structures for optical or electrochemical sensing." <u>Analyst</u> **134**(4): 653-656.

Fritz, J. (2008). "Cantilever biosensors." <u>Analyst</u> **133**(7): 855-863.

Fritz, J., M. K. Baller, H. P. Lang, H. Rothuizen, P. Vettiger, E. Meyer, H. J. Guntherodt, C. Gerber and J. K. Gimzewski (2000). "Translating biomolecular recognition into nanomechanics." <u>Science</u> **288**(5464): 316-318.

Gareri, J., J. Klein and G. Koren (2006). "Drugs of abuse testing in meconium." <u>Clinica Chimica Acta</u> **366**(1-2): 101-111.

Gheorghe, A., A. van Nuijs, B. Pecceu, L. Bervoets, P. G. Jorens, R. Blust, H. Neels and A. Covaci (2008). "Analysis of cocaine and its principal metabolites in waste and surface water using solid-phase extraction and liquid chromatography-ion trap tandem mass spectrometry." <u>Analytical and Bioanalytical Chemistry</u> **391**(4): 1309-1319.

Godin, M., V. Tabard-Cossa, P. Grutter and P. Williams (2001). "Quantitative surface stress measurements using a microcantilever." <u>Applied Physics Letters</u> **79**(4): 551-553.

Godin, M., V. Tabard-Cossa, Y. Miyahara, T. Monga, P. J. Williams, L. Y. Beaulieu, R. B. Lennox and P. Grutter (2010). "Cantilever-based sensing: the origin of surface stress and optimization strategies." <u>Nanotechnology</u> **21**(7).

Godin, M., P. J. Williams, V. Tabard-Cossa, O. Laroche, L. Y. Beaulieu, R. B. Lennox and P. Grutter (2004). "Surface stress, kinetics, and structure of alkanethiol self-assembled monolayers." <u>Langmuir</u> **20**(17): 7090-7096.

Grogan, C., R. Raiteri, G. M. O'Connor, T. J. Glynn, V. Cunningham, M. Kane, M. Charlton and D. Leech (2002). "Characterisation of an antibody coated microcantilever as a potential immuno-based biosensor." Biosensors & Bioelectronics **17**(3): 201-207.

Gsell, M., P. Jakob and D. Menzel (1998). "Effect of substrate strain on adsorption." Science **280**(5364): 717-720.

Hagan, M. F., A. Majumdar and A. K. Chakraborty (2002). "Nanomechanical forces generated by surface grafted DNA." Journal of Physical Chemistry B **106**(39): 10163-10173.

Hanbury, C. M., W. G. Miller and R. B. Harris (1996). "Antibody characteristics for a continuous response fiber optic immunosensor for theophylline." Biosensors & Bioelectronics **11**(11): 1129-1138.

Hansen, K. M., H. F. Ji, G. H. Wu, R. Datar, R. Cote, A. Majumdar and T. Thundat (2001). "Cantilever-based optical deflection assay for discrimination of DNA single-nucleotide mismatches." Analytical Chemistry **73**(7): 1567-1571.

Heng, T. M. S. (1971). "Trimming of Microstrip Circuits Utilizing Microcantilever Air Gaps." Ieee Transactions on Microwave Theory and Techniques **MT19**(7): 652-&.

Hermann, T. and D. J. Patel (2000). "Biochemistry - Adaptive recognition by nucleic acid aptamers." Science **287**(5454): 820-825.

Humphris, A. D. L., J. Tamayo and M. J. Miles (2000). "Active quality factor control in liquids for force spectroscopy." Langmuir **16**(21): 7891-7894.

Ilic, B., D. Czaplewski, H. G. Craighead, P. Neuzil, C. Campagnolo and C. Batt (2000). "Mechanical resonant immunospecific biological detector." Applied Physics Letters **77**(3): 450-452.

Jagerdeo, E., M. A. Montgornery, M. Sibum, T. A. Sasaki and M. A. LeBeau (2008). "Rapid Analysis of Cocaine and Metabolites in Urine Using a Completely Automated Solid-Phase Extraction-High-Performance Liquid Chromatography-Tandem Mass Spectrometry Method." Journal of Analytical Toxicology **32**(8): 570-576.

Janshoff, A., H. J. Galla and C. Steinem (2000). "Piezoelectric mass-sensing devices as biosensors - An alternative to optical biosensors?" Angewandte Chemie-International Edition **39**(22): 4004-4032.

Jenison, R. D., S. C. Gill, A. Pardi and B. Polisky (1994). "High-Resolution Molecular Discrimination by Rna." Science **263**(5152): 1425-1429.

Ji, H. F., E. Finot, R. Dabestani, T. Thundat, G. M. Brown and P. F. Britt (2000). "A novel self-assembled monolayer (SAM) coated microcantilever for low level caesium detection." Chemical Communications(6): 457-458.

Johansen, S. S. and H. M. Bhatia (2007). "Quantitative analysis of cocaine and its metabolites in whole blood and urine by high-performance liquid chromatography coupled with tandem mass spectrometry." Journal of Chromatography B-Analytical Technologies in the Biomedical and Life Sciences **852**(1-2): 338-344.

Kaeferstein, H., J. Falk and M. A. Rothschild (2006). "Experiences in drug screening by police officers with DrugWipe (R) II and chemical-toxicological analysis of blood samples." Blutalkohol **43**(1): 1-8.

Kambhampati, D. (2004). Proteins Microarray Technology, Wiley-VCH.

Kazunori Ikebukuro, W. Y., and Koji Sode (2009). Biosensors using the aptameric enzyme subunit: The use of aptamers in the allosteric control of enzymes. Aptamers in Bioanalysis. M. Mascini, Wiley**:** 129-137.

Kergueris, M. F., M. Bourin, Y. Lenormand, C. Briand, B. Frison and C. Larousse (1983). "Digoxin Blood Assay by Immunological Methods (Emit, Elisa, Ria) - an Interaction of Serum-Proteins." Therapie **38**(1): 117-118.

Kerrigan, S. and W. H. Phillips (2001). "Comparison of ELISAs for opiates, methamphetamine, cocaine metabolite, benzodiazepines, phencyclidine, and cannabinoids in whole blood and urine." Clinical Chemistry **47**(3): 540-547.

Kim, H. C., S. K. Lee, W. B. Jeon, H. K. Lyu, S. W. Lee and S. W. Jeong (2008). "Detection of C-reactive protein on a functional poly(thiophene) self-assembled monolayer using surface plasmon resonance." Ultramicroscopy **108**(10): 1379-1383.

Kim, J., I. Y. Kim, M. S. Choi and Q. Wu (2009). "Label-free electrochemical detection of adenosine based on electron transfer from guanine bases in an adenosine-sensitive aptamer." Chemical Communications(31): 4747-4749.

Klussmann, S. (2006). The aptamer handbook: functional oligonucleotides and their applications.

Ko, S. H. and S. A. Grant (2006). "A novel FRET-based optical fiber biosensor for rapid detection of Salmonella typhimurium." Biosensors & Bioelectronics **21**(7): 1283-1290.

Kroener, L., F. Musshoff and B. Madea (2003). "Evaluation of immunochemical drug screenings of whole blood samples. A retrospective optimization of cutoff levels after confirmation-analysis on GC-MS and HPLC-DAD." Journal of Analytical Toxicology **27**(4): 205-212.

Lang, H. P., R. Berger, C. Andreoli, J. Brugger, M. Despont, P. Vettiger, C. Gerber, J. K. Gimzewski, J. P. Ramseyer, E. Meyer and H. J. Guntherodt (1998). "Sequential position

readout from arrays of micromechanical cantilever sensors." <u>Applied Physics Letters</u> **72**(3): 383-385.

Lang, H. P., R. Berger, F. Battiston, J. P. Ramseyer, E. Meyer, C. Andreoli, J. Brugger, P. Vettiger, M. Despont, T. Mezzacasa, L. Scandella, H. J. Guntherodt, C. Gerber and J. K. Gimzewski (1998). "A chemical sensor based on a micromechanical cantilever array for the identification of gases and vapors." <u>Applied Physics a-Materials Science & Processing</u> **66**: S61-S64.

Langman, L. J., M. W. Bjergum, C. L. Williamson and F. W. Crow (2009). "Sensitive Method For Detection Of Cocaine And Associated Analytes By Liquid Chromatography-Tandem Mass Spectrometry In Urine." <u>Journal of Analytical Toxicology</u> **33**(8): 447-455.

Langmuir, I. (1919). "The arrangement of electrons in atoms and molecules." <u>Journal of the American Chemical Society</u> **41**: 868-934.

Lato, S. M., A. R. Boles and A. D. Ellington (1995). "In-Vitro Selection of Rna Lectins - Using Combinatorial Chemistry to Interpret Ribozyme Evolution." <u>Chemistry & Biology</u> **2**(5): 291-303.

Lee, C. Y., G. M. Harbers, D. W. Grainger, L. J. Gamble and D. G. Castner (2007). "Fluorescence, XPS, and TOF-SIMS surface chemical state image analysis of DNA microarrays." <u>Journal of the American Chemical Society</u> **129**(30): 9429-9438.

Lee, J. O., H. M. So, E. K. Jeon, H. Chang, K. Won and Y. H. Kim (2008). "Aptamers as molecular recognition elements for electrical nanobiosensors." <u>Analytical and Bioanalytical Chemistry</u> **390**(4): 1023-1032.

Levy-Nissenbaum, E., A. F. Radovic-Moreno, A. Z. Wang, R. Langer and O. C. Farokhzad (2008). "Nanotechnology and aptamers: applications in drug delivery." Trends in Biotechnology **26**(8): 442-449.

Levy, M., S. F. Cater and A. D. Ellington (2005). "Quantum-dot aptamer beacons for the detection of proteins." Chembiochem **6**(12): 2163-2166.

Li, F., J. Zhang, X. N. Cao, L. H. Wang, D. Li, S. P. Song, B. C. Ye and C. H. Fan (2009). "Adenosine detection by using gold nanoparticles and designed aptamer sequences." Analyst **134**(7): 1355-1360.

Li, H. X. and L. Rothberg (2004). "Colorimetric detection of DNA sequences based on electrostatic interactions with unmodified gold nanoparticles." Proceedings of the National Academy of Sciences of the United States of America **101**(39): 14036-14039.

Li, H. X. and L. J. Rothberg (2004). "DNA sequence detection using selective fluorescence quenching of tagged oligonucleotide probes by gold nanoparticles." Analytical Chemistry **76**(18): 5414-5417.

Li, H. X. and L. J. Rothberg (2004). "Label-free colorimetric detection of specific sequences in genomic DNA amplified by the polymerase chain reaction." Journal of the American Chemical Society **126**(35): 10958-10961.

Lim, S. H., D. Raorane, S. Satyanarayana and A. Majumdar (2006). "Nano-chemo-mechanical sensor array platform for high-throughput chemical analysis." Sensors and Actuators B-Chemical **119**(2): 466-474.

Liu, J. W., Z. H. Cao and Y. Lu (2009). "Functional Nucleic Acid Sensors." Chemical Reviews **109**(5): 1948-1998.

Liu, Z. C., X. Zhang, N. Y. He, Z. H. Lu and Z. C. Chen (2009). "Probing DNA hybridization efficiency and single base mismatch by X-ray photoelectron spectroscopy." Colloids and Surfaces B-Biointerfaces **71**(2): 238-242.

Loopez, P., A. M. Bermejo, M. J. Tabernero, P. Fernaandez and I. Alvarez (2007). "Determination of cocaine and heroin with their respective metabolites in meconium by gas chromatography-mass spectrometry." Journal of Applied Toxicology **27**(5): 464-471.

Lopez, P., A. M. Bermejo, M. J. Tabernero, P. Fernandez and I. Alvarez (2006). "Determination of cocaine and heroin with their respective metabolites in human hair using gas chromatography-mass spectrometry." Analytical Letters **39**(11): 2307-2316.

Lopez, P., S. Martello, A. M. Bermejo, E. De Vincenzi, M. J. Tabernero and M. Chiarotti (2010). "Validation of ELISA screening and LC-MS/MS confirmation methods for cocaine in hair after simple extraction." Analytical and Bioanalytical Chemistry **397**(4): 1539-1548.

Madru, B., F. Chapuis-Hugon, E. Peyrin and V. Pichon (2009). "Determination of Cocaine in Human Plasma by Selective Solid-Phase Extraction Using an Aptamer-Based Sorbent." Analytical Chemistry **81**(16): 7081-7086.

Maehashi, K., T. Katsura, K. Kerman, Y. Takamura, K. Matsumoto and E. Tamiya (2007). "Label-free protein biosensor based on aptamer-modified carbon nanotube field-effect transistors." Analytical Chemistry **79**(2): 782-787.

Mairal, T., V. C. Ozalp, P. L. Sanchez, M. Mir, I. Katakis and C. K. O'Sullivan (2008). "Aptamers: molecular tools for analytical applications." Analytical and Bioanalytical Chemistry **390**(4): 989-1007.

Mannironi, C., A. DiNardo, P. Fruscoloni and G. P. TocchiniValentini (1997). "In vitro selection of dopamine RNA ligands." Biochemistry **36**(32): 9726-9734.

Mannironi, C., C. Scerch, P. Fruscoloni and G. P. Tocchini-Valentini (2000). "Molecular recognition of amino acids by RNA aptamers: The evolution into an L-tyrosine binder of a dopamine-binding RNA motif." Rna-a Publication of the Rna Society **6**(4): 520-527.

Maraldo, D., F. U. Garcia and R. Mutharasan (2007). "Method for quantification of a prostate cancer biomarker in urine without sample preparation." Analytical Chemistry **79**: 7683-7690.

Marie, R., J. Thaysen, C. B. V. Christensen and A. Boisen (2003). "A cantilever-based sensor for thermal cycling in buffer solution." Microelectronic Engineering **67-8**: 893-898.

Marin, S. J., L. Keith, M. Merrell and G. A. McMillin (2009). "Comparison of Drugs of Abuse Detection in Meconium by EMIT (R) II and ELISA." Journal of Analytical Toxicology **33**(3): 148-154.

Marquardt, J. D. (2008). Force interaction characterization between thrombin and DNA aptamers. Mechanical Engineering. Ames, Iowa State University. **MASTER OF SCIENCE:** 40.

Martin, Y., C. C. Williams and H. K. Wickramasinghe (1987). "Atomic Force Microscope Force Mapping and Profiling on a Sub 100-a Scale." Journal of Applied Physics **61**(10): 4723-4729.

Maurer, H. H. (2005). "Advances in analytical toxicology: the current role of liquid chromatography-mass spectrometry in drug quantification in blood and oral fluid." Analytical and Bioanalytical Chemistry **381**(1): 110-118.

McKendry, R., J. Y. Zhang, Y. Arntz, T. Strunz, M. Hegner, H. P. Lang, M. K. Baller, U. Certa, E. Meyer, H. J. Guntherodt and C. Gerber (2002). "Multiple label-free biodetection and quantitative DNA-binding assays on a nanomechanical cantilever array." Proceedings of the National Academy of Sciences of the United States of America **99**(15): 9783-9788.

McKenzie, F., K. Faulds and D. Graham (2007). "Sequence-specific DNA detection using high-affinity LNA-functionalized gold nanoparticles." Small **3**: 1866-1868.

Mead, J. A., J. Niekro and M. Staples (2003). "EMIT II plus cocaine metabolite assay with 150 ng/mL cutoff." Clinical Chemistry **49**(6): A122-A122.

Medintz, I. L., A. R. Clapp, H. Mattoussi, E. R. Goldman, B. Fisher and J. M. Mauro (2003). "Self-assembled nanoscale biosensors based on quantum dot FRET donors." Nature Materials **2**(9): 630-638.

Mertens, J., C. Rogero, M. Calleja, D. Ramos, J. A. Martin-Gago, C. Briones and J. Tamayo (2008). "Label-free detection of DNA hybridization based on hydration-induced tension in nucleic acid films." Nature Nanotechnology **3**(5): 301-307.

Meyer, G. and N. M. Amer (1988). "Novel Optical Approach to Atomic Force Microscopy." Applied Physics Letters **53**(12): 1045-1047.

Michael E. Burton, L. M. S., Jerome J. Schentag, William E. Evans (1992). Applied pharmacokinetics & pharmacodynamics: principles of therapeutic drug Lippincott Williams & Wilkins.

Michalet, X., F. F. Pinaud, L. A. Bentolila, J. M. Tsay, S. Doose, J. J. Li, G. Sundaresan, A. M. Wu, S. S. Gambhir and S. Weiss (2005). "Quantum dots for live cells, in vivo imaging, and diagnostics." Science **307**(5709): 538-544.

Min Yue, J. C. S., and Arunava Majumdar (2004). "Cantilever Arrays for Multiplexed Mechanical Analysis of Biomolecular Reactions." **1**(3): 211-220.

Mirkin, C. A., R. L. Letsinger, R. C. Mucic and J. J. Storhoff (1996). "A DNA-based method for rationally assembling nanoparticles into macroscopic materials." <u>Nature</u> **382**(6592): 607-609.

Mortier, K. A., K. E. Maudens, W. E. Lambert, K. M. Clauwaert, J. F. Van Bocxlaer, D. L. Deforce, C. H. Van Peteghem and A. P. De Leenheer (2002). "Simultaneous, quantitative determination of opiates, amphetamines, cocaine and benzoylecgonine in oral fluid by liquid chromatography quadrupole-time-of-flight mass spectrometry." <u>Journal of Chromatography B-Analytical Technologies in the Biomedical and Life Sciences</u> **779**(2): 321-330.

Moulin, A. M., S. J. O'Shea, R. A. Badley, P. Doyle and M. E. Welland (1999). "Measuring surface-induced conformational changes in proteins." <u>Langmuir</u> **15**(26): 8776-8779.

Mukhopadhyay, R., V. V. Sumbayev, M. Lorentzen, J. Kjems, P. A. Andreasen and F. Besenbacher (2005). "Cantilever sensor for nanomechanical detection of specific protein conformations." <u>Nano Letters</u> **5**(12): 2385-2388.

Nesmerak, K., M. Sticha and M. Cvancarova (2010). "HPLC/MS Analysis of Historical Pharmaceutical Preparations of Heroin and Cocaine." <u>Analytical Letters</u> **43**(16): 2572-2581.

Neves, M. A. D., O. Reinstein and P. E. Johnson "Defining a Stem Length-Dependent Binding Mechanism for the Cocaine-Binding Aptamer. A Combined NMR and Calorimetry Study." <u>Biochemistry</u> **49**(39): 8478-8487.

Neves, M. A. D., O. Reinstein and P. E. Johnson (2010). "Defining a Stem Length-Dependent Binding Mechanism for the Cocaine-Binding Aptamer. A Combined NMR and Calorimetry Study." Biochemistry **49**(39): 8478-8487.

Niemeyer, C. A. M. a. C. M. (2007). Nanobiotechnology II: more concepts and applications

Ostuni, E., R. G. Chapman, R. E. Holmlin, S. Takayama and G. M. Whitesides (2001). "A survey of structure-property relationships of surfaces that resist the adsorption of protein." Langmuir **17**(18): 5605-5620.

Ozaki, H., A. Nishihira, M. Wakabayashi, M. Kuwahara and H. Sawai (2006). "Biomolecular sensor based on fluorescence-labeled aptamer." Bioorganic & Medicinal Chemistry Letters **16**(16): 4381-4384.

Pan, C. F., M. L. Guo, Z. Nie, X. L. Xiao and S. Z. Yao (2009). "Aptamer-Based Electrochemical Sensor for Label-Free Recognition and Detection of Cancer Cells." Electroanalysis **21**(11): 1321-1326.

Pei, H., N. Lu, Y. L. Wen, S. P. Song, Y. Liu, H. Yan and C. H. Fan (2010). "A DNA Nanostructure-based Biomolecular Probe Carrier Platform for Electrochemical Biosensing." Advanced Materials **22**(42): 4754-+.

Petersen, K. E. (1979). "Micromechanical Membrane Switches on Silicon." Ibm Journal of Research and Development **23**(4): 376-385.

Potyrailo, R. A., R. C. Conrad, A. D. Ellington and G. M. Hieftje (1998). "Adapting selected nucleic acid ligands (aptamers) to biosensors." Analytical Chemistry **70**(16): 3419-3425.

Preston, K. L., M. A. Huestis, C. J. Wong, A. Umbricht, B. A. Goldberger and E. J. Cone (1999). "Monitoring cocaine use in substance-abuse-treatment patients by sweat and urine testing." Journal of Analytical Toxicology **23**(5): 313-322.

Putman, C. A. J., B. G. Degrooth, N. F. Vanhulst and J. Greve (1992). "A Detailed Analysis of the Optical Beam Deflection Technique for Use in Atomic Force Microscopy." Journal of Applied Physics **72**(1): 6-12.

Raiteri, R., H. J. Butt and M. Grattarola (2000). "Changes in surface stress at the liquid/solid interface measured with a microcantilever." Electrochimica Acta **46**(2-3): 157-163.

Raiteri, R., M. Grattarola, H. J. Butt and P. Skladal (2001). "Micromechanical cantilever-based biosensors." Sensors and Actuators B-Chemical **79**(2-3): 115-126.

Raiteri, R., G. Nelles, H. J. Butt, W. Knoll and P. Skladal (1999). "Sensing of biological substances based on the bending of microfabricated cantilevers." Sensors and Actuators B-Chemical **61**(1-3): 213-217.

Ramos, D., J. Mertens, M. Calleja and J. Tamayo (2007). "Study of the origin of bending induced by bimetallic effect on microcantilever." Sensors **7**: 1757-1765.

Rugar, D., H. J. Mamin and P. Guethner (1989). "Improved Fiber-Optic Interferometer for Atomic Force Microscopy." Applied Physics Letters **55**(25): 2588-2590.

Sader, J. E., J. W. M. Chon and P. Mulvaney (1999). "Calibration of rectangular atomic force microscope cantilevers." Review of Scientific Instruments **70**(10): 3967-3969.

Sader, J. E. and L. White (1993). "Theoretical-Analysis of the Static Deflection of Plates for Atomic-Force Microscope Applications." Journal of Applied Physics **74**(1): 1-9.

Sandros, M. G., D. Gao and D. E. Benson (2005). "A modular nanoparticle-based system for reagentless small molecule biosensing." Journal of the American Chemical Society **127**(35): 12198-12199.

Savran, C. A., T. P. Burg, J. Fritz and S. R. Manalis (2003). "Microfabricated mechanical biosensor with inherently differential readout." Applied Physics Letters **83**(8): 1659-1661.

Savran, C. A., S. M. Knudsen, A. D. Ellington and S. R. Manalis (2004). "Micromechanical detection of proteins using aptamer-based receptor molecules." Analytical Chemistry **76**(11): 3194-3198.

Schaffer, M., V. Hill and T. Cairns (2007). "Identification of cocaine-contaminated hair: Perspectives on a paper." Journal of Analytical Toxicology **31**(3): 172-174.

Scheller, F. W., U. Wollenberger, A. Warsinke and F. Lisdat (2001). "Research and development in biosensors." Current Opinion in Biotechnology **12**(1): 35-40.

Schlecht, U., A. Malave, T. M. A. Gronewold, M. Tewes and M. Lohndorf (2007). "Detection of Rev peptides with impedance-sensors - Comparison of device-geometries." Biosensors & Bioelectronics **22**(9-10): 2337-2340.

Schonenberger, C. and S. F. Alvarado (1989). "A Differential Interferometer for Force Microscopy." Review of Scientific Instruments **60**(10): 3131-3134.

Sepaniak, M., P. Datskos, N. Lavrik and C. Tipple (2002). "Microcantilever transducers: A new approach to sensor technology." Analytical Chemistry **74**(21): 568A-575A.

Services, D. o. H. a. H. (2008). Mandatory Guidelines for Federal Workplace Drug Testing Programs. S. A. a. M. H. S. Administration. **73**.

Shlyahovsky, B., D. Li, Y. Weizmann, R. Nowarski, M. Kotler and I. Willner (2007). "Spotlighting of cocaine by an autonomous aptamer-based machine." Journal of the American Chemical Society **129**(13): 3814-+.

Smith, T. (1980). "The Hydrophilic Nature of a Clean Gold Surface." Journal of Colloid and Interface Science **75**(1): 51-55.

Solanki, P. R., N. Prabhakar, M. K. Pandey and B. D. Malhotra (2008). "Self-assembled monolayer for toxicant detection using nucleic acid sensor based on surface plasmon resonance technique." Biomedical Microdevices **10**(5): 757-767.

Spiehler, V., D. S. Isenschmid, P. Matthews, P. Kemp and T. Kupiec (2003). "Performance of a microtiter plate ELISA for screening of postmortem blood for cocaine and metabolites." Journal of Analytical Toxicology **27**(8): 587-591.

Stachowiak, J. C., M. Yue, K. Castelino, A. Chakraborty and A. Majumdar (2006). "Chemomechanics of surface stresses induced by DNA hybridization." Langmuir **22**(1): 263-268.

Stephan, A. C., T. Gaulden, A. D. Brown, M. Smith, L. F. Miller and T. Thundat (2002). "Microcantilever charged-particle flux detector." Review of Scientific Instruments **73**(1): 36-41.

Stevenson, K. A., A. Mehta, P. Sachenko, K. M. Hansen and T. Thundat (2002). "Nanomechanical effect of enzymatic manipulation of DNA on microcantilever surfaces." Langmuir **18**(23): 8732-8736.

Stojanovic, M. N., P. de Prada and D. W. Landry (2001). "Aptamer-based folding fluorescent sensor for cocaine." Journal of the American Chemical Society **123**(21): 4928-4931.

Stojanovic, M. N. and D. W. Landry (2002). "Aptamer-based colorimetric probe for cocaine." Journal of the American Chemical Society **124**(33): 9678-9679.

Stoney, G. G. (1909). "The tension of metallic films deposited by electrolysis." Proceedings of the Royal Society of London: A **82**: 172-175.

Strano-Rossi, S., F. Molaioni, F. Rossi and F. Botre (2005). "Rapid screening of drugs of abuse and their metabolites by gas chromatography/mass spectrometry: application to urinalysis." Rapid Communications in Mass Spectrometry **19**(11): 1529-1535.

Tamayo, J., A. D. L. Humphris and M. J. Miles (2000). "Piconewton regime dynamic force microscopy in liquid." Applied Physics Letters **77**(4): 582-584.

Taton, T. A., C. A. Mirkin and R. L. Letsinger (2000). "Scanometric DNA array detection with nanoparticle probes." Science **289**(5485): 1757-1760.

Thaysen, J., A. D. Yalcinkaya, P. Vettiger and A. Menon (2002). "Polymer-based stress sensor with integrated readout." Journal of Physics D-Applied Physics **35**(21): 2698-2703.

Thundat, T., P. I. Oden and R. J. Warmack (1997). "Microcantilever sensors." Microscale Thermophysical Engineering **1**(3): 185-199.

Thundat, T., E. A. Wachter, S. L. Sharp and R. J. Warmack (1995). "Detection of Mercury-Vapor Using Resonating Microcantilevers." Applied Physics Letters **66**(13): 1695-1697.

Thundat, T., R. J. Warmack, G. Y. Chen and D. P. Allison (1994). "Thermal and Ambient-Induced Deflections of Scanning Force Microscope Cantilevers." Applied Physics Letters **64**(21): 2894-2896.

Torii, A., M. Sasaki, K. Hane and S. Okuma (1996). "A method for determining the spring constant of cantilevers for atomic force microscopy." Measurement Science & Technology **7**(2): 179-184.

Torres-Chavolla, E. and E. C. Alocilja (2009). "Aptasensors for detection of microbial and viral pathogens." Biosensors & Bioelectronics **24**(11): 3175-3182.

Tuerk, C. and L. Gold (1990). "Systematic Evolution of Ligands by Exponential Enrichment - Rna Ligands to Bacteriophage-T4 DNA-Polymerase." Science **249**(4968): 505-510.

Tyagi, S. and F. R. Kramer (1996). "Molecular beacons: Probes that fluoresce upon hybridization." Nature Biotechnology **14**(3): 303-308.

Uddin, A. H., P. A. E. Piunno, R. H. E. Hudson, M. J. Damha and U. J. Krull (1997). "A fiber optic biosensor for fluorimetric detection of triple-helical DNA." Nucleic Acids Research **25**(20): 4139-4146.

Ueberfeld, J. and D. R. Walt (2004). "Reversible ratiometric probe for quantitative DNA measurements." Analytical Chemistry **76**(4): 947-952.

Ullman, E. F. (1999). "Homogeneous immunoassays: Emit (R) and beyond." Journal of Clinical Ligand Assay **22**(2): 221-227.

Ulman, A. (1991). An introduction to ultrathin organic films : from Langmuir-Blodgett to self-assembly Boston : Academic Press

Valente-Campos, S., M. Yonamine, R. Moreau and O. A. Silva (2006). "Validation of a method to detect cocaine and its metabolites in nails by gas chromatography-mass spectrometry." Forensic Science International **159**(2-3): 218-222.

Velasco-Garcia, M. N. and S. Missailidis (2009). "New trends in aptamer-based electrochemical biosensors." Gene Therapy and Molecular Biology **13**(1): 1-9.

Verstraete, A. G. (2004). "Detection times of drugs of abuse in blood, urine, and oral fluid." Therapeutic Drug Monitoring **26**(2): 200-205.

Waggoner, P. S. and H. G. Craighead (2007). "Micro- and nanomechanical sensors for environmental, chemical, and biological detection." Lab on a Chip **7**: 1238-1255.

Wallace, S. T. and R. Schroeder (1998). "In vitro selection and characterization of streptomycin-binding RNAs: Recognition discrimination between antibiotics." Rna-a Publication of the Rna Society **4**(1): 112-123.

Wallis, M. G., U. Vonahsen, R. Schroeder and M. Famulok (1995). "A Novel Rna Motif for Neomycin Recognition." Chemistry & Biology **2**(8): 543-552.

Walsh, J. M., D. J. Crouch, J. P. Danaceau, L. Cangianelli, L. Liddicoat and R. Adkins (2007). "Evaluation of ten oral fluid point-of-collection drug-testing devices." Journal of Analytical Toxicology **31**(1): 44-54.

Wang, W. U., C. Chen, K. H. Lin, Y. Fang and C. M. Lieber (2005). "Label-free detection of small-molecule-protein interactions by using nanowire nanosensors." Proceedings of the National Academy of Sciences of the United States of America **102**(9): 3208-3212.

Wang, Y. and R. R. Rando (1995). "Specific Binding of Aminoglycoside Antibiotics to Rna." Chemistry & Biology **2**(5): 281-290.

Weizmann, Y., F. Patolsky, O. Lioubashevski and I. Willner (2004). "Magneto-mechanical detection of nucleic acids and telomerase activity in cancer cells." Journal of the American Chemical Society **126**(4): 1073-1080.

White, R. J., N. Phares, A. A. Lubin, Y. Xiao and K. W. Plaxco (2008). "Optimization of electrochemical aptamer-based sensors via optimization of probe packing density and surface chemistry." Langmuir **24**(18): 10513-10518.

Wilfinge.Rj, P. H. Bardell and D. S. Chhabra (1968). "Resonistor - a Frequency Selective Device Utilizing Mechanical Resonance of a Silicon Substrate." Ibm Journal of Research and Development **12**(1): 113-&.

Wilson, J. F., L. M. Tsanaclis and K. Barnett (1996). "External quality assessment of syva emit and Abbott TDx II assays for methotrexate in serum." Therapeutic Drug Monitoring **18**(6): 721-723.

Win, M. N., J. S. Klein and C. D. Smolke (2006). "Codeine-binding RNA aptamers and rapid determination of their binding constants using a direct coupling surface plasmon resonance assay." Nucleic Acids Research **34**(19): 5670-5682.

Wu, G. H., R. H. Datar, K. M. Hansen, T. Thundat, R. J. Cote and A. Majumdar (2001). "Bioassay of prostate-specific antigen (PSA) using microcantilevers." Nature Biotechnology **19**(9): 856-860.

Wu, G. H., H. F. Ji, K. Hansen, T. Thundat, R. Datar, R. Cote, M. F. Hagan, A. K. Chakraborty and A. Majumdar (2001). "Origin of nanomechanical cantilever motion generated from biomolecular interactions." Proceedings of the National Academy of Sciences of the United States of America **98**(4): 1560-1564.

Xiang, Y., A. J. Tong and Y. Lu (2009). "Abasic Site-Containing DNAzyme and Aptamer for Label-Free Fluorescent Detection of Pb2+ and Adenosine with High Sensitivity, Selectivity, and Tunable Dynamic Range." Journal of the American Chemical Society **131**(42): 15352-15357.

Xiao, Y., A. A. Lubin, A. J. Heeger and K. W. Plaxco (2005). "Label-free electronic detection of thrombin in blood serum by using an aptamer-based sensor." Angewandte Chemie-International Edition **44**(34): 5456-5459.

Yang, J. L., T. Ono and M. Esashi (2000). "Mechanical behavior of ultrathin microcantilever." Sensors and Actuators a-Physical **82**(1-3): 102-107.

Ye, K. M. and J. S. Schultz (2003). "Genetic engineering of an allosterically based glucose indicator protein for continuous glucose monitoring by fluorescence resonance energy transfer." Analytical Chemistry **75**(14): 3451-3459.

Yue, M., H. Lin, D. E. Dedrick, S. Satyanarayana, A. Majumdar, A. S. Bedekar, J. W. Jenkins and S. Sundaram (2004). "A 2-D microcantilever array for multiplexed biomolecular analysis." Journal of Microelectromechanical Systems **13**(2): 290-299.

Yue, M., J. C. Stachowiak, H. Lin, R. Datar, R. Cote and A. Majumdar (2008). "Label-free protein recognition two-dimensional array using nanomechanical sensors." Nano Letters **8**(2): 520-524.

Zhang, J., H. P. Lang, F. Huber, A. Bietsch, W. Grange, U. Certa, R. McKendry, H. J. Guntgerodt, M. Hegner and C. Gerber (2006). "Rapid and label-free nanomechanical detection of biomarker transcripts in human RNA." Nature Nanotechnology **1**(3): 214-220.

Zhang, J., S. P. Song, L. H. Wang, D. Pan and C. H. Fan (2007). "A gold nanoparticle-based chronocoulometric DNA sensor for amplified detection of DNA." Nature Protocols **2**(11): 2888-2895.

Zhang, J., L. H. Wang, D. Pan, S. P. Song, F. Y. C. Boey, H. Zhang and C. H. Fan (2008). "Visual cocaine detection with gold nanoparticles and rationally engineered aptamer structures." Small **4**(8): 1196-1200.

Zhang, Y., S. Z. Luo, Y. J. Tang, L. Yu, K. Y. Hou, J. P. Cheng, X. Q. Zeng and P. G. Wang (2006). "Carbohydrate-protein interactions by "clicked" carbohydrate self-assembled monolayers." Analytical Chemistry **78**(6): 2001-2008.

Ziegler, C. (2004). "Cantilever-based biosensors." Analytical and Bioanalytical Chemistry **379**(7-8): 946-959.

ACKNOWLEDGEMENTS

First and foremost, I would like to thank my advisor Professor Pranav Shrotriya for his guidance, help and patience during the journey of this project. Without his support, the work could not have been accomplished.

I would also like to express my gratitude and appreciation to all my committee members: Professor Abhijit Chandra, Professor Balaji Narasimhan, Professor Marit Nilsen-Hamilton and Professor Sriram Sundararajan for serving on my POS committee and providing me with all the valuable inputs for my research.

My thanks extend to all professors and colleagues in the project, particularly to Professor Marit Nilsen-Hamilton and Professor George Kraus, Dr. Lee Bendickson, Ashish Sachan, and Aaron Kempema for many useful discussions, technical and otherwise.

I would also like to thank all the lab colleagues, former and present: Dinesh Karyana-Sundaram, Kanaga Karuppiah, JaeJoong Ryu, Janice Marquardt, Xiao Ma, Yue Zhao, and Alex Avendano with whom I share and discuss a lot of professional and personal stories.

I would like to thank my family and my wife's family for their support and love. Finally, my most sincere thanks go to my beloved wife, YunJung who carried me through these years and to my little son Peter who has provided me with so much joy in so little time.

Finally, I would like to thank my God who always guides me in the right diection.